School of Architecture Urban Planning & Construction Engineering

Building and Architectural Engineering

Course of Study Architectural Engineering, Lecco

POLITECNICO MILANO 1863

Analysis and Optimization of an Energy Efficient Building in Egypt

Supervisor:

Professor Graziano Salvalai

Author:

Amr Attia

Matricola Number:

951550

Abstract

This thesis is about optimising the overall configuration of a newly constructed existing building from an architectural and energy consumption standpoint. This report demonstrates the importance of conducting energy simulation studies in the early design phase before constructing a building. Even though the selected case study building is newly built and less than two years old, the research that was conducted proves that the design should be altered to adhere to more sustainable energy consumption standards.

The importance of reaching guidelines for energy-efficient buildings in Egypt is backed up by a comprehensive urban analysis, which indicates the cities' expansions, which means new buildings will be built.

To implement sustainable building construction, building energy simulation needs to be integrated into an early design phase to control the design output and ensure the final design is coherent with the sustainable studies conducted. This means sustainable studies should be directed at the design development stage, where the architect and the energy simulation engineer work together to achieve the final design.

In the construction industry, the most used software package worldwide is Autodesk. Therefore, it is interesting to test the energy simulation engine provided by Autodesk Revit. Usually, when energy simulation is conducted for a project, a separate model is constructed with different software that the architect, engineer or designer is not working with, which delays the work process and confuses the feedback loop. Hence, if the designer and the energy simulation engineer work with the same software and have one unified model, the work process will be much more efficient and faster. This means that there will be no need to switch to a different tool for energy analysis if the architect is using Autodesk Revit for designing.

Table of Contents

List of Tables

List of Figures

1. Introduction

1.1 Thesis Relevance in Context

Over the past few years Egypt has been expanding and taking a new role in the region of the Middle East and North Africa. For example, Egypt is investing in importing new technologies for many climates friendly energies, such as, the Green Hydrogen, which can be a true green replacement for the fossil fuel's heavy applications, provided that the production cost is lower than 1.5 dollar/kg. Egypt is investing as well in the Solar Energy and Wind Energy sectors, supposedly before the year 2025, Egypt would export electricity instead of exporting only natural gas.

Nonetheless, in the building sector there is expansion happening as well, for example, the existence of New Cairo, the creation of the New Administrative Capital in Cairo, and the Alamein City in the Mediterranean. This will become more evident when reaching the urban analysis of Egypt section. One similar characteristic in these new expansions is the presence of commercial buildings and many administrative and office buildings. So, adopting the same perspective towards clean green future, the building technologies should be updated, especially since there is no clear guidelines or regulations for energy efficient buildings in the Egyptian Code, which mean a large number of these new buildings, if not all, are not adopting sustainable designs.

The chosen administrative building, to take as a reference for a case study, is located in New Cairo, which is a new urban city capital. This area is characterized by its rapid growth and development, which have led to a surge in population and economic activities. This means that New Cairo is a hub for new housing, commercial centres, offices, and schools.

1.2 Climate Change Background

For decades researchers and scientists have been studying the phenomena of climate change. After identifying the phenomena, rigorous research has been conducted to understand the causes of climate change. It took us humans quite some time to understand the complexity of this phenomena, because there is no one single root cause to all the climatic changes which resulted in increase in greenhouse gases and global warming.

There is a lot of research which discusses factors contributing to the global warming, however, all these contributions can be summarized in one aspect, which is the human behaviour and lifestyle in the modern period. We have developed technologies, and as human being we established a lifestyle that is dependent on industrialisation. This aspect nowadays touches our normal life each day, from the houses we live in, the cloths we wear, transportation we use, electronics we possess, the food we eat, and consequently the air we breathe and water we drink. In a way, we have been working against nature for so long, thinking there are no consequences. However, thus lifestyle consumes great amount of energy and materials which in return affects our world and climate.

When the phenomena of global warming was observed in the early years, the change in the climate was very subtle, but with the years passing it was being proved that there is something that changes our climate, subtly but gradually until we have reached today, where these changes are not subtle anymore, on the contrary, global warming, which is a consequence of climate change and greenhouse gases, is becoming more evident year after year. Now we have reached a point where natural disasters occur heavily each year, such as, long periods of draughts, extreme weather conditions and heat waves are becoming more intense and last longer. The four seasons are becoming more irregular each year. Earthquakes happen in regions traditionally considered to be subjected to low seismic hazard and food and water are becoming scarcer.

Now we need as human beings to work with nature instead of working against nature in hope that our impact has not reached the tipping point and the effects of climate change are still reversible.

1.3 Climate Change Futuristic Scenarios and Adaptations

In light of the escalating challenges posed by climate change, it is imperative that we consider how our built environment, specifically the urban environment and cities, can adapt to these shifting conditions. As we continue to witness the escalating impacts of global warming, it becomes clear that proactive measures are essential to mitigate further harm and to adapt according to the future situation. Architects, engineers, and urban planners must now work with the priority of designing and constructing buildings that are not only sustainable in their own right, but also resilient in the face of a changing climate.

To this end, there are several key considerations that must be taken into account. These include building with sustainable materials, implementing energy efficient designs and using passive strategies as the first line of defence. Additionally, it is crucial to consider the potential future scenarios for climate change, including projections for temperature increases and extreme weather events. By integrating these forecasts into our design and construction practices, we can ensure that our buildings are equipped to withstand the challenges that lie ahead.

Furthermore, it is essential to foster a paradigm shift in our approach to construction and urban planning. This entails not only adopting sustainable technologies and materials, but also reevaluating the way we utilize space, manage resources, and interact with our surroundings. Embracing concepts such as circular economy principles and regenerative design can play an important role in achieving a more balanced relationship between our built environment and the natural world.

As we stand at the crossroads of an ever-changing climate, our responsibility as engineers of the built environment is clear. By prioritizing sustainability, resilience, and adaptability in our building practices, we can contribute to a more sustainable and liveable future.

1.4 Built Environment – Effect of Cities

As previously stated, climate change is a very complex phenomena, therefore, it requires interdisciplinary solutions from many disciplines, in order to be able to mitigate the effects of climate change, while simultaneously adapting our lifestyle accordingly.

The construction industry can help in mitigating some of the effects of climate change. Buildings consume a tremendous amount of energy throughout their life cycle and in return they emit Green House Gases. Based on the research paper "A review on buildings energy consumption information" buildings correspond to 15% of Green House Gases and they consume from 20% to 40% of the global energy demand *(Perez-Lombard, Luis, 2007)*.

However, particularly in Egypt, the buildings energy demand is higher, it is estimated that the built environment, namely largely populated cities, uses around 70% of the energy sold, which is almost the double amount recognized globally *(William, 2021)*. It is essential to find ways to minimize the energy usage, because buildings and built-up areas massively increase each year, and Egypt is adopting the urbanization methodology and focusing in developing urban cities. This means that if new methods, or maybe as well traditional efficient approaches, are not adopted in the building urban cities, the energy demand is only going to increase year after year.

Therefore, the concept of reducing before producing is vital. If a comparison between a normal building and an energy efficient building is made, it will be evident that the energy demand of the latter building is going to be low; the reduction of energy demand can be reduced up to 1/3 of the total energy demand.

Hence, passive building design is an important aspect, which differ according to the context, location, climate, and function of the building. Passive design strategies work with the local climate in order to maintain comfortable indoor environment, which in return eliminates or reduces additional heating or cooling loads.

2. Urban Analysis

2.1 Description of Egypt

As mentioned earlier, the case study building is located in New Cairo, which is in Cairo Governorate. However, New Cairo is a part of a greater system. Therefore, it is crucial to understand the bigger system in order to be able to digest New Cairo’s urban situation.

Egypt is situated at the crossroads of Africa and the Middle East. Egypt's urban landscape is diverse, showcasing a mix of historical legacy and modern challenges. The country has over 100 million citizens, most of whom live in cities. Cairo, the capital and largest city in terms of population size and population density, is the centre of political, economic, and social life. Other important cities include Alexandria, Luxor, and Aswan, each with its own unique urban identity. These cities have been shaped by their history, geography, and economy.

Figure 1 Map of Egypt

As Fig. 1 demonstrates, Egypt is a vast country that have 27 different governorates which cover a total area of over 1,000,000 km². The Nile River runs from the southern part to the northern Mediterranean coast. As the map shows, the Nile cuts the country into eastern and western parts. It is visible that the governorate's concentrations are around the Nile as ancient Pharaonic civilizations did. For that reason, although Egypt is a vast country, only 7% of the total country's area is inhabited *(National Strategic Plan for Urban Development)*, which, again, is concentrated around the riverbanks and especially in the delta region, where the Nile River splits into two branches, namely, Domiat and Rashid branch. From the west, Egypt is neighbouring Libya, neighbouring Sudan from the south, Palestine and Saudi Arabia from the eastern side, where the Red Sea separates the latter, and finally, the Mediterranean Sea closes the Egyptian borders from the northern side. As the river splits the country into two parts, logically, the governorates should respect this geographical separation. However, this is not the case. As the map shows, many governorates, such as Banisweif, Ilmenia, Asyut, and Suhaj governorates, have territories on both riverbanks.

Governorate Area Order	***Governorate***	***Area (km²)***	***Population***	***Population % from Total %***	***Year of Data Obtained***
1	**Al Wadi Al Jadid**	440,098	234,016	0.27%	2013
2	**Red Sea**	203,685	288,233	0.33%	2006
3	**Matrouh**	166,563	573,427	0.65%	2014
4	**Aswan**	62,726	1,323,215	1.51%	2012
5	**Ilmenia**	32,279	3,686,000	4.20%	2006
6	**South Sinai**	31,272	177,900	0.20%	2013
7	**North Sinai**	27,564	419,200	0.48%	2013
8	**Asyut**	25,926	4,245,215	4.83%	2015
9	**Giza**	13,184	7,486,361	8.52%	2015
10	**Suhaj**	11,022	5,193,500	5.91%	2018
11	**Banisweif**	10,954	2,617,000	2.98%	2012
12	**Qina**	9,565	3,340,409	3.80%	2019
13	**Beherah**	9,119	5,346,253	6.09%	2013
14	**Suweis**	9,002	752,872	0.86%	2019
15	**Fayoum**	6,068	3,115,000	3.55%	2014
16	**Sharqeya**	4,911	8,000,000	9.11%	2019
17	**Kafresheikh**	3,748	3,172,753	3.61%	2015
18	**Daqahleya**	3,459	6,794,604	7.73%	2020
19	**Cairo**	3,085	9,278,441	10.56%	2015
20	**Luxor**	2,960	1,300,000	1.48%	2012
21	**Alexandria**	2,679	4,187,509	4.77%	2006
22	**Monofeya**	2,543	4,076,657	4.64%	2016
23	**Gharbeya**	1,872	4,544,438	5.17%	2013
24	**Qalyubeya**	1,001	4,340,000	4.94%	2006
25	**Port Said**	1,351	1,000,000	1.14%	2019
26	**Ismaeleya**	1,442	1,077,000	1.23%	2012
27	**Domiat**	589	1,288,406	1.47%	2015

Table 1 Governorates of Egypt

Table 1 presents the 27 governorates. The governorates are presented in the table descending from the largest governorate area until reaching the smallest governorate area. Next to each governorate, the population count is reported. The final column reports when the data on population count was obtained because, as it is apparent, the data were not reported in the same year, although all the information presented in the table is obtained from one single governmental source *(Egypt's Projects Map)*. As it is apparent, the most populated city is Cairo, with 10.56%, followed by Sharqeya and Giza, with 9.11% and 8.52%, respectively, of the total population. However, Cairo ranks as the 19th largest governorate, considering the area, while

Sharqeya ranks the 16th and Giza ranks the 9th. On the other hand, Al Wadi Al Jadid governorate, which ranks as the biggest governorate, is populated with only 0.27%. This demonstrates that the population concentration is not relevant to the governorate size, which translates, in Egypt's case, into highly congested populated regions in some areas. In contrast, other areas are almost entirely deserted.

2.1.1 Challenges

2.1.1.1 Overview

Egypt faces a lot of challenges. Unfortunately, these challenges were already present during the last 100 years at least. Some of these challenges include high rates of poverty, extreme poverty, illiteracy and unemployment. There are high social disparities between different regions in income, standard of living and services. There is a scarcity of traditional resources that can be matured, such as groundwater, oil and gas. There are extreme spatial challenges, such as population numbers, population concentration in about 7.4% of the total area, urban sprawl and erosion of agricultural lands *(National Strategic Plan for Urban Development)*. However, for the sake of the study at hand, the focus will be put on the population numbers, population concentration locations and urban sprawl. By default, these aspects are closely related to the growth rates and city developments in Egypt.

Egypt is known for its huge population number. According to the Egyptian Central Agency for Public Mobilization and Statistics, Egypt's population recorded 104,462,545 individuals in 2023 *(CAPMAS, Statistics)*.

2.1.1.2 Population & Growth Rate

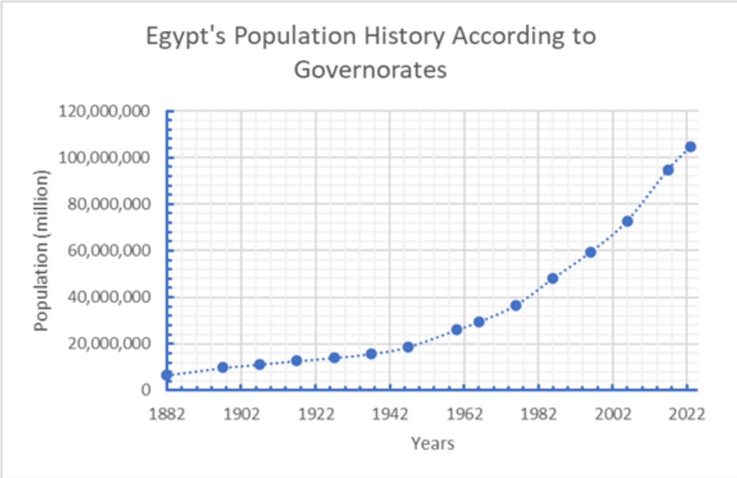

Figure 2 Egypt's Population History

Fig. 2 reveals the population count for Egypt from 1882 until 2023. It is astonishing that in less than 150 years, the population has multiplied by 16 times, starting with 6,547,985 in 1882 and reaching almost 105,000,000 individuals in 2023 *(Geonetwork)*.

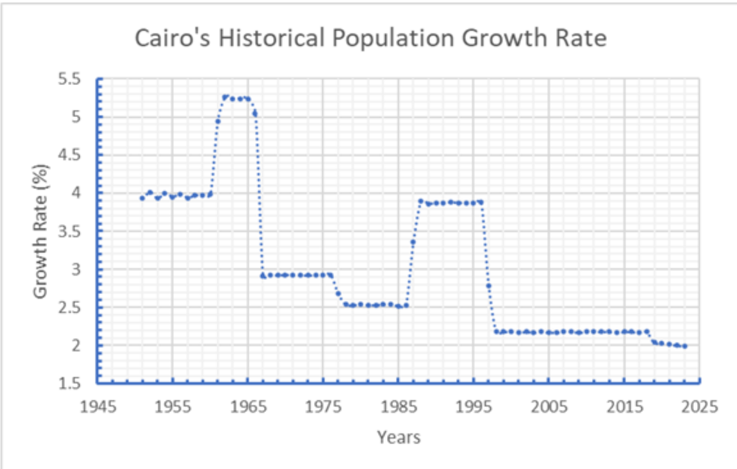

Figure 3 Cairo's Population Growth Rate History

Looking into the growth rate presented in Fig. 3, it will be understandable how Egypt reached this population count in such a short period. Fig. 3 showcases the population growth rate for Cairo as a representative sample. The growth rate is reported from 1950 until 2023. In the fifties, the rate was incredibly high, exceeding 5%. After that, the rate decreased suddenly after

1965, rose suddenly after 1985, and decreased suddenly again after 1995 until the growth rate reached 2% today *(Macrotrends)*. The sudden increase or decrease in these specific years is evident in the political and economic status of Egypt at that time. However, since this is not the focus of the study, the reasons will be neglected. Even though the rate has decreased by more than 50% compared to the growth rate in 1950, it is still a high rate because these 2% are applied to a much larger population, so the numbers will only grow exponentially. Figures 2 and 3 clearly demonstrate the problem Egypt faces when it comes to population numbers.

2.1.1.3 Urban Sprawl

Egypt had always been considered an agricultural country. Egypt did hold a prominent place in agriculture, with its origin that traces back to ancient times. The Nile River valley and delta have been the lifeline of Egypt's agriculture, allowing for a wide range of crops and upholding the economy. Agriculture still remains an important aspect of the Egyptian economy; however, its participation in driving the economy is shrinking year after year.

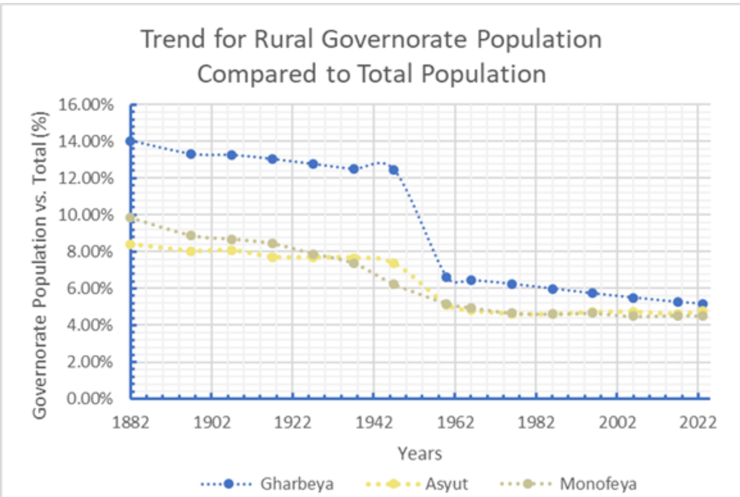

Figure 4 Rural Population Compared to Total Population

Among the problems that Egypt faces is the urban sprawl. The population seems to be centred in urban areas. This is evident when observing Fig. 4. This figure demonstrates the population compared to the total population throughout the years of 1882 until 2023 in the rural governorates, namely, Gharbeya, Asyut and Monofeya. For example, in 1882, 14% of Egypt's total population resided in the Gharbeya governorate. However, in 2023, the number of Gharbeya inhabitants is merely 5% of the total population *(Geonetwork)*.

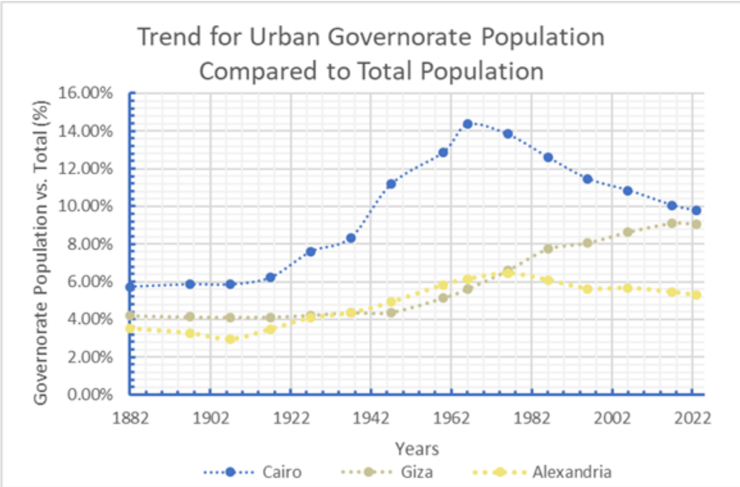

Figure 5 Urban Governorates' Population Compared to Total Population

On the other hand, Fig. 5 shows that the number population in the densest Egyptian governorates has been increasing throughout the years. The densest Governorates in Egypt are Cairo, Giza and Alexandria. Figures 4 and 5 present selected governorates to represent the phenomena of urban sprawl, where residents of rural areas tend to live in urban cities, which in turn intensifies the challenge that Egypt faces, which is population concentration in specific locations. For a more detailed representation of the population sprawl refer to Tables 34 and 35 in the Annex section.

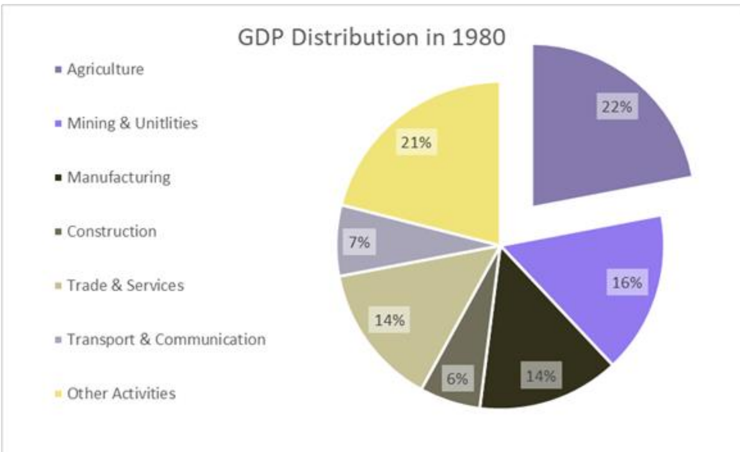

Figure 6 GDP Distribution in 1980

Fig. 6 demonstrates Egypt's GDP distribution in 1980. The GDP components in this chart consist of agriculture, mining and utilities, manufacturing, construction, trade and services, transportation and communication and finally, other activities. Until 1980, the largest driver in the Egyptian economy was agriculture, with a share of 22% *(OECD)*.

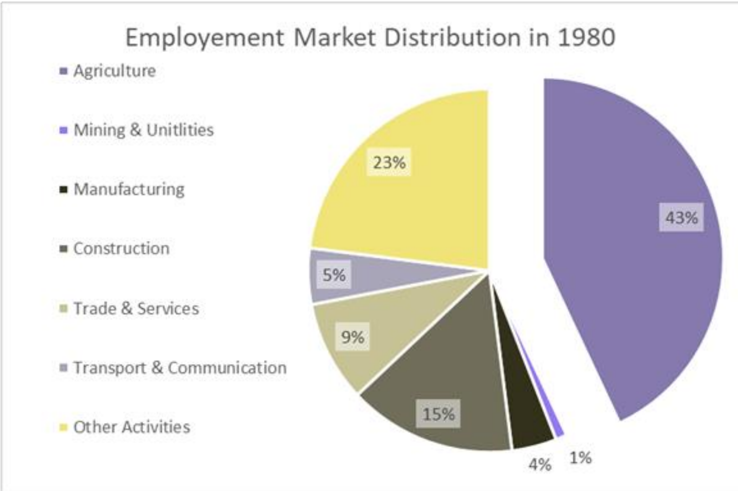

Figure 7 Employment Market Distribution in 1980

Fig. 7 shows the employment distribution in the Egyptian market in 1980. Similar to Fig. 6, the chart presents the same 7 components. The employment chart indicates that by far the largest employment force is employed in the agriculture sector, with 43% of the total workforce *(OECD)*.

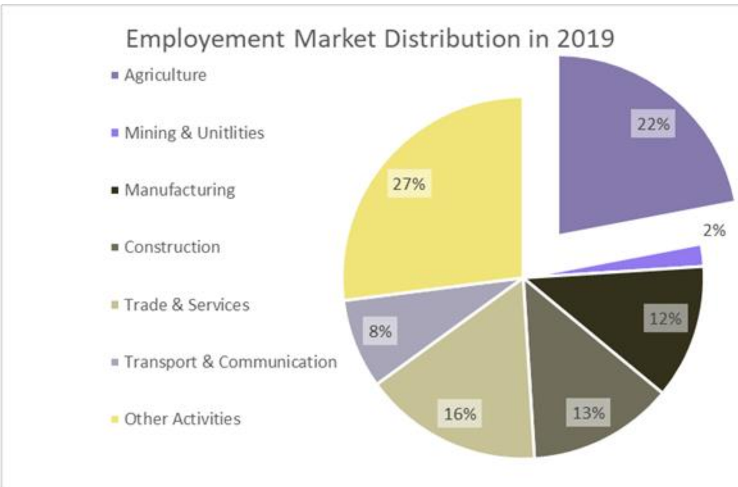

Figure 8 Employment Market Distribution in 2019

Fig. 8 displays the same information in Fig. 7 but in the year 2019. It is very evident that the employment rate in the agriculture industry dropped by almost half to 22%. This can be due to technological advancements in irrigation techniques, which require less manpower. However, Fig. 9 denies this explanation *(OECD)*.

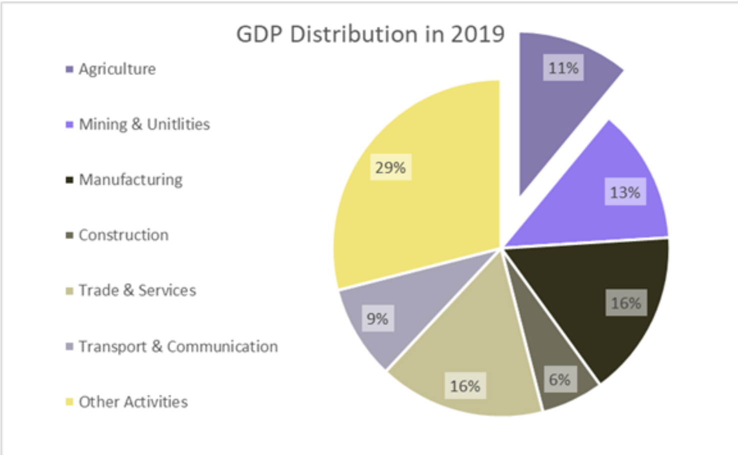

Figure 9 GDP Distribution in 2019

Fig. 9 shows that the agriculture industry's share in the total Egyptian GDP dropped in 2019 to half compared to 1980 *(OECD)*. The fast growth of Egypt's urban areas has led to a number of issues, including expanding informal communities, inadequate infrastructure and services, and difficulties in maintaining balanced urban development and administration. Understanding Egypt's urban landscape as a whole is key to seeing how cities all over the country interconnect and are affected by these issues, particularly in the Greater Cairo Metropolitan Region.

2.1.1.4 History & Futuristic Path

Egypt's Population History According to Governorates															
Governorate	***1882***	***1897***	***1907***	***1917***	***1927***	***1937***	***1947***	***1960***	***1966***	***1976***	***1986***	***1996***	***2006***	***2017***	***2023***
Cairo	374,838	570,062	654,476	790,939	1,064,567	1,312,096	2,090,654	3,348,779	4,219,853	5,074,016	6,068,695	6,800,992	7,902,085	9,539,673	10,203,693
Domiat	43,616	43,751	NR	30,984	34,907	40,332	53,631	387,962	431,596	576,326	740,365	913,555	1,097,339	1,496,765	1,610,586
Rashid	19,378	NR	NR	NR	NR	NR	NR	NR	NR	NR	NR	NR	NR	NR	NR
Port Said	21,296	NR	NR	NR	NR	NR	NR	245,318	282,977	262,760	401,172	472,335	570,603	749,371	789,241
Arish	2,936	16,991	5,897	NR	NR	NR	NR	NR	NR	NR	NR	NR	NR	NR	NR
Quṣayr	2,430	NR	NR	NR	NR	NR	NR	NR	NR	NR	NR	NR	NR	NR	NR
Beherah	372,846	631,225	798,473	892,246	976,965	1,061,596	1,244,495	1,685,679	1,978,889	2,464,445	3,338,151	3,994,297	4,747,283	6,171,613	6,830,189
Daqahleya	580,943	736,708	912,428	986,643	1,080,693	1,218,502	1,413,905	2,014,883	2,285,332	2,737,306	3,259,892	4,223,919	4,989,997	6,492,381	7,013,271
Sharqeya	437,756	749,130	879,646	955,497	1,016,912	1,120,826	1,345,829	1,819,798	2,107,971	2,617,938	3,414,308	4,281,068	5,354,041	7,163,824	7,859,068
Qalyubeya	254,507	371,465	434,575	528,581	558,876	610,157	693,908	988,055	1,211,764	1,680,837	2,515,924	3,301,244	4,251,672	5,627,420	6,103,039
Gharbeya	919,256	1,297,656	1,484,814	1,659,313	1,791,985	1,967,894	2,327,031	1,715,212	1,901,117	2,293,240	2,884,599	3,406,020	4,011,320	4,999,633	5,409,714
Asyut	550,272	782,720	903,335	981,197	1,078,600	1,205,321	1,374,454	1,329,588	1,418,164	1,697,422	2,215,679	2,802,334	3,444,967	4,383,289	5,011,815
Banisweif	194,902	314,454	372,412	452,893	508,166	561,312	612,027	859,832	927,910	1,110,132	1,442,650	1,859,214	2,291,618	3,154,100	3,561,639
Fayoum	201,516	371,006	441,583	507,617	554,040	602,122	669,696	839,163	935,281	1,141,879	1,551,214	1,989,774	2,511,027	3,596,954	4,047,387
Giza	274,815	401,634	460,080	524,352	591,391	685,331	818,158	1,336,418	1,650,381	2,416,659	3,725,420	4,784,099	6,294,319	8,632,021	9,456,137
Ilmenia	295,073	548,632	659,967	763,922	839,690	928,259	1,044,201	1,560,311	1,705,602	2,054,105	2,643,177	3,310,129	4,166,299	5,497,095	6,279,035
Isna	224,292	NR	NR	NR	NR	NR	NR	NR	NR	NR	NR	NR	NR	NR	NR
Jirja	516,075	688,011	792,971	863,234	968,383	1,118,402	1,283,468	NR	NR	NR	NR	NR	NR	NR	NR
Qina	384,026	711,457	772,492	840,317	902,170	1,017,569	1,106,302	1,351,358	1,470,812	1,709,299	2,258,926	2,442,016	3,001,681	3,164,281	3,605,518

Table 2 Egypt's Population History According to Governorates, Part1

Egypt's Population History According to Governorates Cont.															
Governorate	**1882**	**1897**	**1907**	**1917**	**1927**	**1937**	**1947**	**1960**	**1966**	**1976**	**1986**	**1996**	**2006**	**2017**	**2023**
Monofeya	643,934	864,206	970,581	1,072,636	1,105,191	1,159,701	1,165,015	1,347,953	1,458,048	1,710,849	2,221,315	2,760,431	3,270,431	4,301,601	4,707,584
Alexandria	231,396	319,766	332,246	444,617	573,063	685,736	919,024	1,516,234	1,801,056	2,362,528	2,926,859	3,339,076	4,123,869	5,163,750	5,523,511
Qanâl al-Suways	NR	50,179	61,332	91,090	NR	NR	NR	NR	NR	NR	NR	NR	NR	NR	NR
Suweis	NR	24,970	18,347	30,996	40,523	49,686	107,244	203,610	264,098	193,965	330,634	417,527	512,135	728,180	788,421
Nuba	NR	240,382	NR	NR	NR	NR	NR	NR	NR	NR	NR	NR	NR	NR	NR
Tur Sinai	NR	NR	1,510	NR	NR	NR	NR	NR	NR	NR	NR	NR	NR	NR	NR
Aswan	NR	NR	232,813	253,340	267,357	305,096	290,842	385,350	520,567	618,518	809,204	974,068	1,186,482	1,473,975	1,643,211
Asaharaa Al Gharbeya	NR	NR	NR	5,371	48,956	52,576	74,839	NR	NR	NR	NR	NR	NR	NR	NR
Asaharaa Asharqeya	NR	NR	NR	37,040	NR	NR	NR	NR	NR	NR	NR	NR	NR	NR	NR
Sinai	NR	NR	NR	5,430	15,059	18,011	37,670	49,769	63,676	9,717	NR	NR	NR	NR	NR
Red Sea	NR	NR	NR	NR	5,177	9,914	15,929	25,452	15,711	55,415	84,670	157,315	288,661	359,888	400,069
Kafresheikh	NR	NR	NR	NR	NR	NR	NR	973,019	620,495	1,407,160	1,809,221	2,223,659	2,620,208	3,362,185	3,695,336
Suhaj	NR	NR	NR	NR	NR	NR	NR	1,578,858	1,689,397	1,924,814	2,446,992	3,123,115	3,747,289	4,967,409	5,669,652
Ismaeleya	NR	NR	NR	NR	NR	NR	NR	284,115	344,789	353,975	545,259	714,828	953,006	1,303,993	1,442,402
Al Wadi Al Jadid	NR	NR	NR	NR	NR	NR	NR	33,932	28,763	85,175	113,405	141,774	187,263	241,247	265,003
Matrouh	NR	NR	NR	NR	NR	NR	NR	103,453	60,502	112,547	161,163	212,001	323,404	425,624	538,546
North Sinai	NR	NR	NR	NR	NR	NR	NR	NR	NR	NR	170,835	252,160	343,681	450,328	504,201
South Sinai	NR	NR	NR	NR	NR	NR	NR	NR	NR	NR	28,929	54,826	150,005	102,018	115,611
Luxor	NR	NR	NR	NR	NR	NR	NR	NR	NR	NR	NR	361,138	457,286	1,250,209	1,388,666
Total	6,547,985	9,736,302	11,191,885	12,720,172	14,024,598	15,732,376	18,690,269	25,986,061	29,396,717	36,673,003	48,110,644	59,314,910	72,799,977	94,800,844	104,464,568

Table 3 Egypt's Population History According to Governorates, Part2

Tables 2 and 3 present a detailed count of Egypt’s population starting from 1882 until 2023 for all governorates (*Geonetwork*). These two tables are actually one, where Table 3 is a sequel to Table 2 with the rest of the governorates. The greyed governorates in the tables are the governorates that no longer exist in the administrative sense. Obtaining data to conduct an urban analysis in Egypt is not an easy task, firstly, because the data rarely exist. If the data exist, only some are released to be shared with the public. Even when the data are obtained, it's not easy to understand them, at least not at first glance. Tables 2 and 3 exhibit the phenomena of difficulty in understanding the obtained data.

The demographic data changes a lot in the administrative sense. However, the numbers tell a story, and when understood, one can appreciate the importance of these data. For example, Tur Sinai was the area that was inhabited in Sinai that we know today in 1907. Around 1917, Tur Sinai became Sinai, with a much larger population. The population kept multiplying until it reached 63,676 in 1966. In 1976, the population dropped drastically to 9,717. In light of the events that happened around that time, it is understandable because Israel occupied Sinai from 1967 until 1979. Therefore, the demographic number of Sinai in 1986, which became North and South Sinai at that time, indicates a significant surge in population of 170,835 and 28,929, respectively.

Another example is the demographic data in the year 1960. In 1952, a revolution happened in Egypt. One of the many consequences of the revolution is that new governorates were established and new cities were planned, such as Kafresheikh, Suhaj, Ismaeleya, Al Wadi Al Jadid and Matrouh. The same thing happened with the data of the year 1986, which was after the Egyptian-Israeli war; two new governorates, North and South Sinai, were established.

These data demonstrate that after big political events in Egypt, city planning and urban demography change. In 2011, a revolution happened in Egypt, and as an expected consequence, city planning and urban demography will change as well.

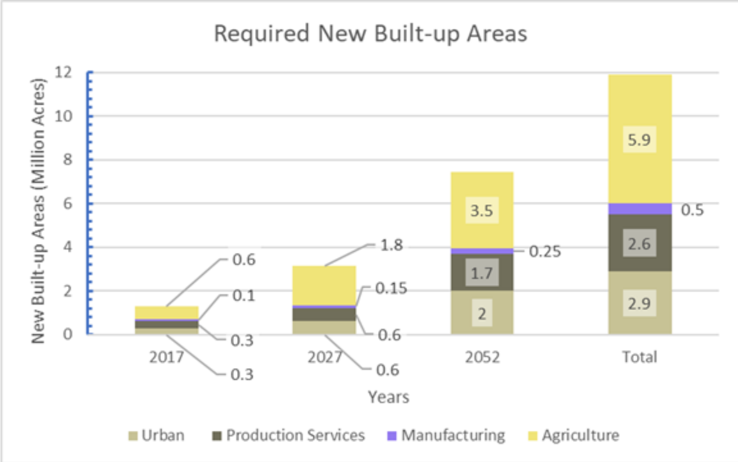

Figure 10 Required New Built-up Areas

Fig. 10 demonstrates that the government's plan for the future requires newly built inhabited lands in Egypt to accommodate the high population numbers. The numbers in this chart are divided into four categories, namely, urban land, production services, manufacturing areas and agricultural land. The newly required built-up areas are reflected in the number of million acres. In the year 2017, the aim was to reclaim and build new areas with a total of 1.3 million acres, which is equivalent to 5261 km². In the year 2027, new areas of 12,748 km² are planned to be built, excluding the 5261 km² that was supposedly reached in 2017, and finally, the ultimate goal is to have built new areas of 30,149 km² between the years 2027 and 2052 *(National Strategic Plan for Urban Development)*. These newly built areas over the years would amount to a total of 12 million acres (48562 km²), which would make the Egyptian inhabited area 11% of its total area compared to only 7% today. According to the Ministry of Housing for National Projects Egypt plans to build 45 new cities to accommodate for the future population, according to projected population growth and different scenarios.

2.1.1.4 Data Limitations

- The file that was used to obtain data for year 1986 in to create Table 2 and 3 had the name of the year 1986. However, inside the file itself is written it is fir year 1991. It was concluded to use it for the year 1986 because it made more sense with the previous historical trends.

- It should be noted that some of the information presented in the Table 2 and 3 was remedied before creating the table. For example, the Gharbeya governorate is reported to be 462,683 km², as Fig. 11 shows. However, this did not make sense because the total area of the country is just over 1,000,000 km², as mentioned before. So, when assuming that the area of Gharbeya is presented in the wrong units, everything made sense. The number of 462,683 should have the acres units instead of km², and when converted into the units of km², the area of Gharbeya will be 1,872 km². This is not the only remedied information in this table. Another piece of information that is wrongly stated in the official source is the population count of the Shuaj governorate. It was reported that 519,350 people reside in Suhaj, as Fig. 12 demonstrates, where, in fact, the actual population is 5,193,500. Furthermore, some inconsistencies were discovered in the information that is gathered in Table 1; for example, Alexandria has different areas according to different sources. In this reported source (*Egypt's Projects Map*), Alexandria is 2,679 km² *(Egypt's Projects Map | Governorates | Alexandria Governorate)*, where it is reported in the same official governmental source to be 2,818 km² but in a different section. In this source *(Egypt's Projects Map | Governorates | Alexandria Governorate)*, Alexandria is ranked to be the 17th in terms of governorate areas; however, according to the areas obtained from source *(Egypt's Projects Map)*, it ranks the 21st governorate. This issue will be presented at a later stage to address the challenges in obtaining data to conduct urban analysis.

Figure 11 Wrong Numbers from Official Sources, Part 1

Figure 12 Wrong Numbers from Official Sources, Part 2

- It should be noted that Fig. 8 and 9 show that the share of Construction in the Egyptian economy is 13% with a workforce of 6%. From my personal judgment, these figures are highly inaccurate because, basically, since 2013, the construction industry has been booming in Egypt, where new cities, roads and infrastructure are being built.

2.2 Description of Greater Cairo Metropolitan Region

2.2.1 Overview

In Egypt, around 43% of its population lives in urban areas, with over half of the urban citizens, 56%, residing in the Greater Cairo Metropolitan Region *(GCMR)* and Alexandria Governorates. GCMR, the largest metropolitan area in Africa, is a major economic powerhouse with over 22 million inhabitants *(World Urbanization Prospects)*, making up nearly 20% of Egypt's total population. However, the number of citizens in GCMR is estimated to be over 26 million citizens informally. It is projected that by the year 2050, GCMR will have between 30 and 35 million citizens *(Macrotrends)*. Since 2011, Egypt has seen a significant increase in informal and unsafe settlements, with an estimated 1,171 such areas nationwide, accommodating approximately 15 million people *(Urbanization in Egypt: Building Inclusive and Sustainable Cities)*.

Egypt's cities have grown rapidly in recent decades while planning, roads, and other essential services have fallen behind. This has caused significant problems for the vast, crowded cities that are dealing with this phenomenon. Inadequate systems for managing public land and housing rules that are too strict force poor people to live in dangerous areas that haven't been planned. This not only makes the already insufficient infrastructure worse but also puts a lot of strain on services like transportation and public works.

GCMR serves as the economic hub of Egypt, with a diverse economy encompassing industries such as finance, manufacturing, tourism, and services. The city hosts the headquarters of many Egyptian corporations, government agencies, and international organizations. Additionally, GCMR's strategic location along the Nile River and its proximity to major transportation routes contribute to its economic importance.

GCMR is an area with a rich history spanning over millennia. It was present during the Pharaonic era. However, it was founded in the shape that is present today in the 10th century AD and served as the capital of various Egyptian dynasties, including the Fatimid, Ayyubid, and Mamluk periods. The city is renowned for its ancient monuments, including the Pyramids of Giza, the Sphinx, and the Cairo Citadel.

2.2.2 Population Development

As declared earlier, GCMR is densely populated, with millions of residents living within the city and its surrounding metropolitan area. The population density is particularly high in the historic core and along the banks of the Nile River, where urban development is concentrated. GCMR comprises the Cairo Governorate and the urban areas of Giza and Qalyobiya Governorates.

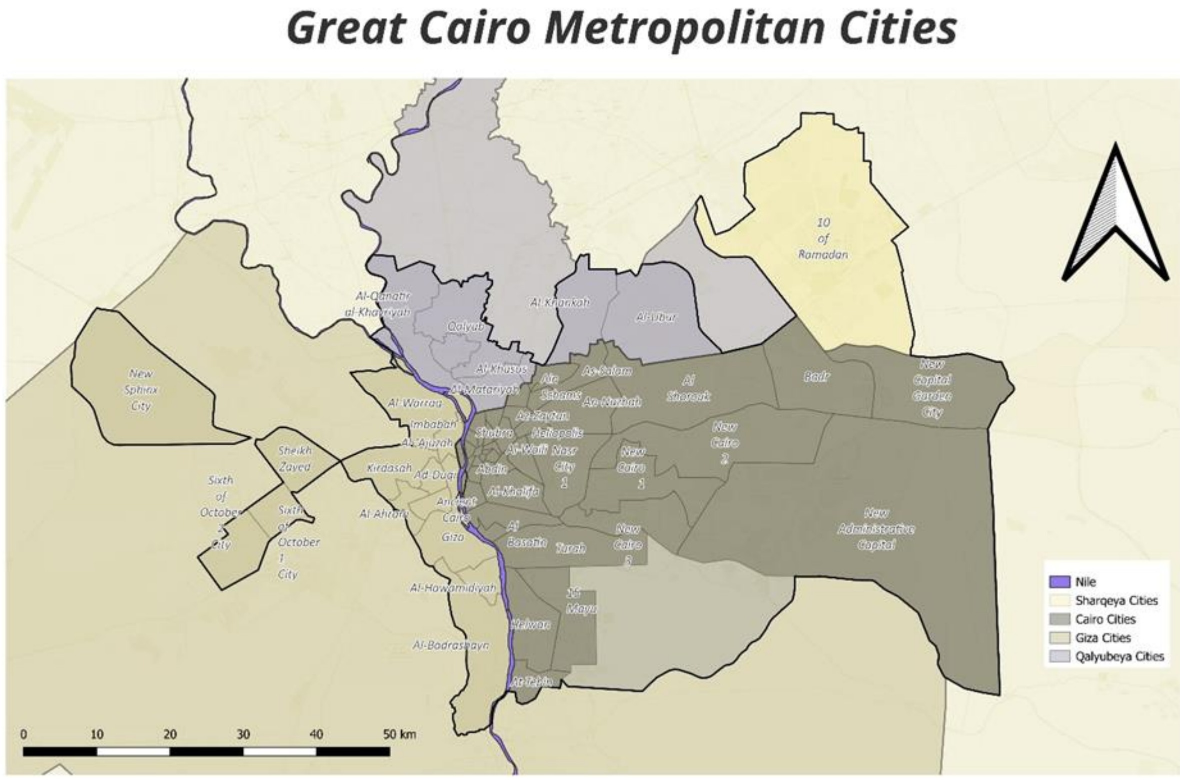

Figure 13 Great Cairo Metropolitan Area Cities

The GCMR kept developing throughout the years until it reached its shape today, which is demonstrated in Fig. 13. As the map demonstrates, some cities that lie within the Giza governorate in the west and Qalyubeya governorate in the north are within the boundaries of the GCMR, as well as 10th of Ramadan city which lies in the Sharqeya governorate. On the other hand, all cities that lie within the Cairo governorate are considered automatically to be in GCMR.

GCMR is concentrated around the river banks. Therefore, with the fast population growth, expansions for new district cities were created every few years. The logic was to move further away from the riverbanks towards the west and east. However, the result of these expansions was that there was no specific characteristic that unified all the districts in Cairo. All the districts seem to be unplanned, or better said, planned independently without taking into account the greater urban context; hence, the districts are satellite cities within the big city, for example, New Sphinx City, 10 of Ramadan City and the New Administrative Capital shown in Fig. 13 are all considered satellite cities.

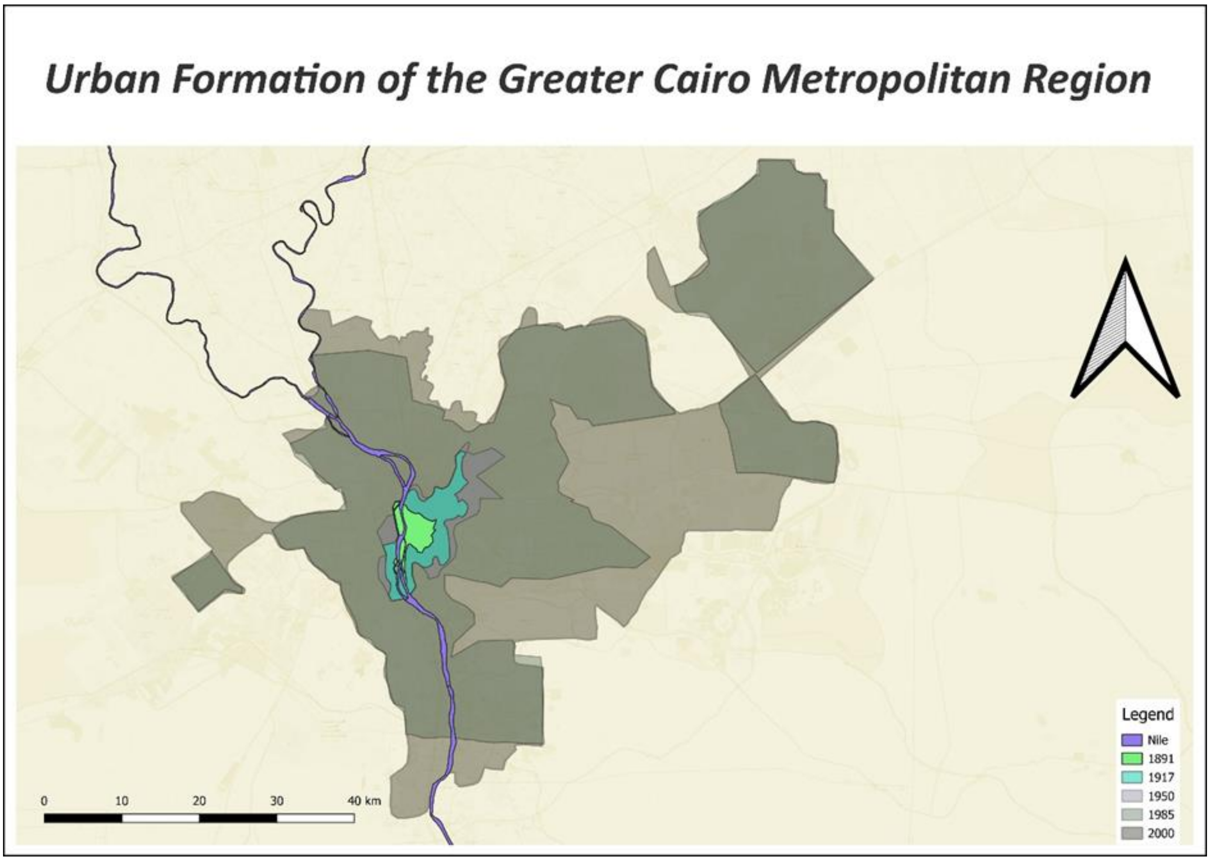

Figure 14 Urban Formation of Great Cairo Metropolitan Region

Fig. 14 demonstrates the urban formation of GCMR from 1891 until 2000. This map neglects the agricultural areas within GCMR since the focus is on urban transformation. The map shows that the urban transformation started with a very small density around the delta region of the Nile River in 1891. After that, the urban transformation kept increasing throughout the years until the year 2000, when the GCMR multiplied many times *(Updating the Urban Structuring Project for Cairo in Light of Regional Changes, Edme-François, Grand, Great Britain, Lane-Poole, Egyptian General Authority for Survey)*.

It is apparent, according to Fig. 14, that the concept of creating satellite cities is not a new occurrence. Actually, it has been systematically being applied since 1960, when a new satellite city was being created, where deserted areas surround it. In between these satellite cities, there is only a highway road connecting the city with its surrounding neighbourhoods. For some satellite cities, the connecting highway roads attract further urban development and encourage urban sprawl towards these specific locations. For other satellite cities, their condition is totally opposite, where they remain totally isolated for 47 years, as of the case of the 10th of Ramadan City. The multitude of satellite cities becomes very obvious in the years 1985 and 2000, according to Fig. 14.

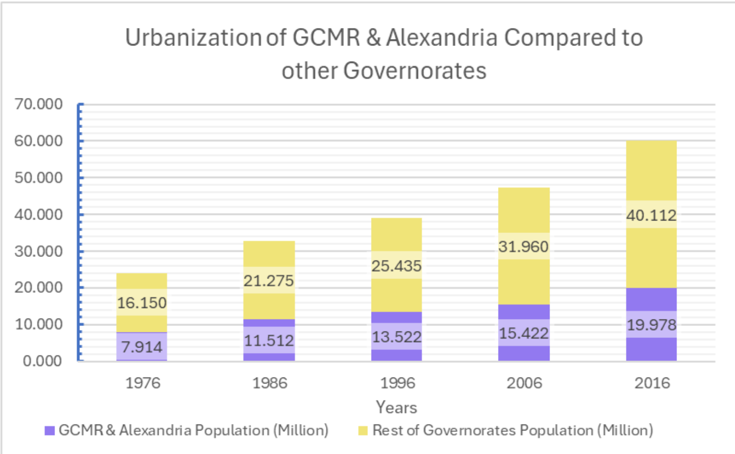

Figure 15 Urbanization of Greta Cairo Metropolitan Region & Alexandria Compared to other Governorates

GCMR is densely populated, and it has always been challenging to accommodate built-up areas, which correspond to such growth and urban sprawl. Fig. 15clearly proves that the condition of GCMR has become more complicated over the years. In the lower part of the bar chart graph, the urban population numbers are depicted for GCMR and for Alexandria. Alexandria is the second largest and densest metropolitan governorate in Egypt. Above the population values of GCMR and Alexandria, the urban population of the rest of the governorates in Egypt is reported. It is astonishing that GCMR, combined with Alexandria governorate, inhabit such a huge urban population. Cairo is the 19th biggest governorate in terms of area, with some numbered cities from the Giza and Qalyubeya governorates and Alexandria, the 21st biggest governorate in terms of area, withholding 33% of the total urban population from 27 governorates.

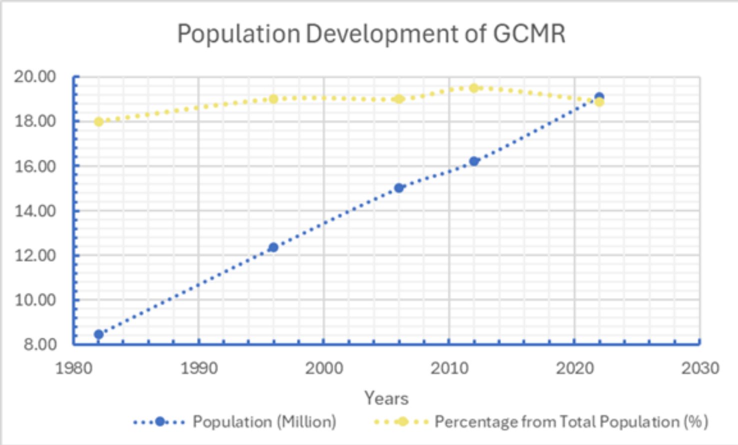

Figure 16 Population Development of Great Cairo Metropolitan Region Compared to Total Population

Taking Alexandria out of the equation, GCMR still comprises almost 20 % of the country's total population, as Fig. 16 demonstrates.

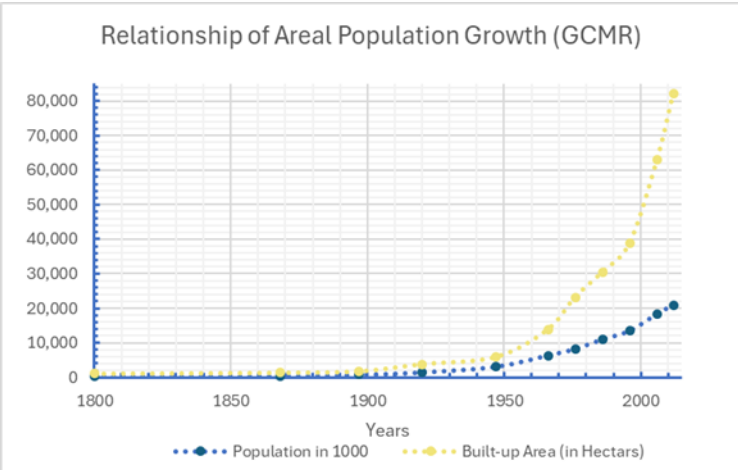

Figure 17 Relationship of Areal Population Growth History of Great Cairo Metropolitan Region

Fig. 17 showcases a correlation between the build-up area and the population growth over the years for GCMR from 1800 until 2012. It is apparent that efforts are being made to accommodate the population growth.

2.2.3 Solutions & Futuristic Adaptation

As a result to the population concentration in a limited built-up area, many problems occur, for instance traffic congestions. Cairo faces significant challenges related to traffic congestion and inadequate transportation infrastructure. The city's streets are often congested with vehicles, leading to long commuting times and air pollution. In the past few years, major infrastructure projects have taken place to address the traffic congestion problems. This is evident from the data provided by the Egyptian State Information Service, which states that Egypt has built 935 new bridges, 7000 new main roads and 13 new road axes between 2014 and 2023 *(Egypt Built 935 Bridges)*.

This drastic change solved the congestion problems in Cairo. However, it created new problems. It became extremely difficult and sometimes even dangerous to simply cross a road from one side to another. Keep in mind that many of the new roads and bridges are built in densely populated neighbourhoods. Some neighbourhoods, as a consequence to implementing drastic solution measure, only have highways to navigate through the streets. As Fig. 18 displays, the new bridge, which is located in Cairo, is built in a densely populated area, where only 50cm of thin air divides the residential building from the 4-lane bridge *(El Shamaa)*.

Figure 18 Example for Wrong Bridges Planning

The new infrastructure projects solved the congestion problems, but they came at the cost of destroying greeneries to make way for the new roads and to extend the existing ones *(Staff,* *MEO)*, as Fig. 19 demonstrates. This made the city a city for cars, where, as a resident, it is very difficult, time and energy consuming to go around without a car.

Figure 19 Example of Dredging Greenery in order to Build Roads

Egypt aims to change the urban structuring for Cairo in light of regional changes; it aims to increase its inhabited and built-up areas by 11% *(National Strategic Plan for Urban Development)*. Some sources would even state that the desired increased built-up area in Egypt would reach 14% of its total area in the year 2050 *(Updating the Urban Structuring Project for Cairo in Light of Regional Changes)*. Fig. 20 demonstrates the overall plan to develop GCMR by 2050. The Regional Ring Road would be the boundary of the metropolitan city. Within the metropolitan boundary, the city would be divided into six points of the proposed urban restructuring, namely, New Cities West Cairo, Rural Areas North Cairo, New Cities East Cairo, Rural Areas South Cairo, Urban Cluster West the Nile and finally Urban Cluster East Cairo, which is in the heart of the metropolitan city. The existing GCMR is presented with white boundaries. Many cities within these white boundaries are either still totally not inhabited, such as the New Administrative Capital or partially inhabited, such as New Cairo, which proposes that the 2050 plan is very ambitious, not only because of the sheer size of new required built-up area of GCMR, but because same approach is being applied throughout the whole country, establishing new huge vast cities.

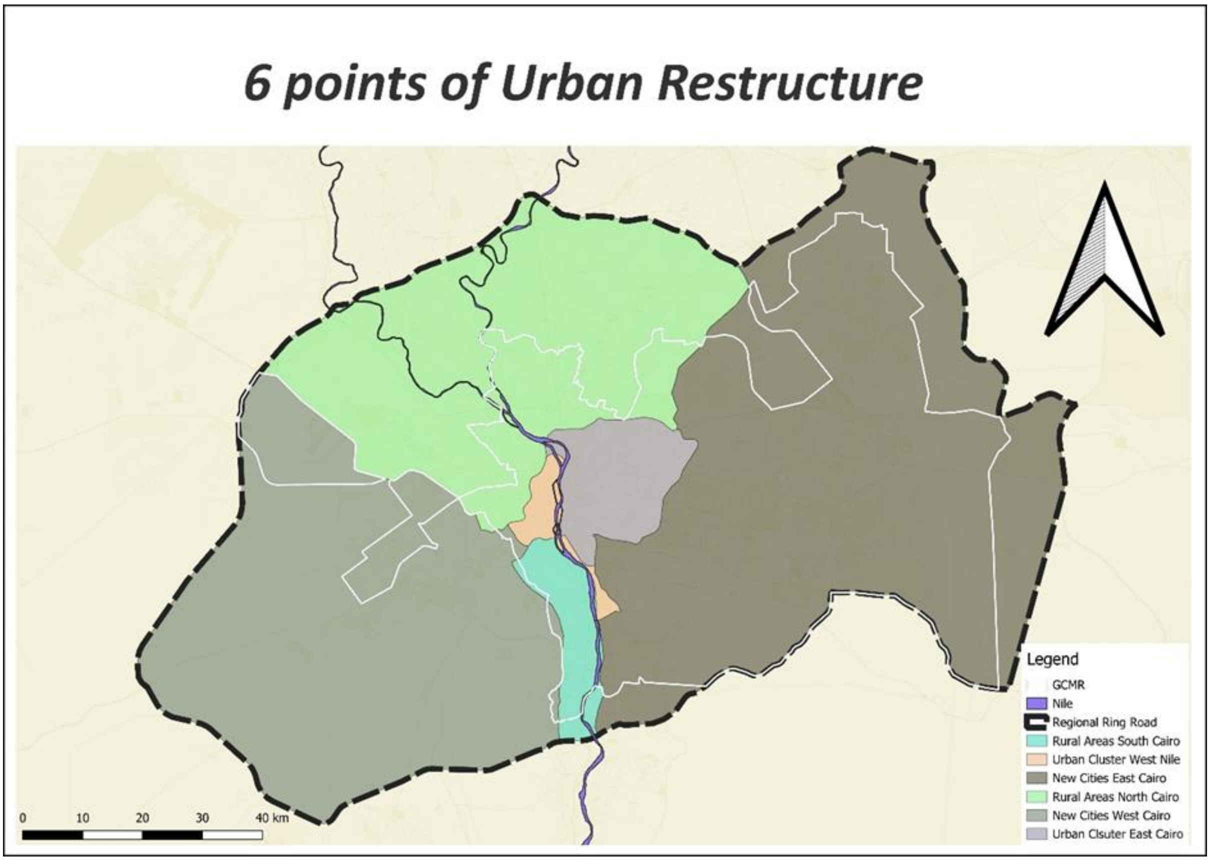

Figure 20 Futuristic Plan of Great Cairo Metropolitan Region

2.2.4 Data Limitation

- In order to create Fig. 14, various sources were used. Please note that the map is inexact as a result of using different sources. However, it suffices to show the urban transformation trend of GCMR. The sources that were used to create this map are governmental official sources, academic sources from the "Rare Books and Special Collection Digital Library" section *(The American University in Cairo)*.
- Earlier, it was stated that only three governorates are included in this region, as all found sources dealing with the subject indicate even governmental sources. However, city 10 of Ramadan, which lies on the north-western side, belongs to the Sharqeya governorate.
- Two different governmental sources report different desirable goals for the built-up area in 2050. One source state 11% *(National Strategic Plan for Urban Development)*, while the other states 14% *(Updating the Urban Structuring Project for Cairo in Light of Regional Changes)*.

- The population number in 2022 for GCMR is 19,000,000 individuals, according to governmental sources. However, according to the UN, the population reports a population of over 22,000,000 in 2022, according to the Egyptian Central Agency for Public Mobilization and Statistics (CAPMAS) *(Macrotrends)*.

2.3 Description of Cairo

2.3.1 Cairo Explained in Data

As indicated in earlier sections, GCMR consists of the Cairo governorate and urban cities in Giza and Qalyubeya governorates and the 10th of Ramadan city. Going through sources, governmental, academic and NGO data, it became evident that it is highly difficult to distinguish between Greater Cairo Metropolitan Region and Cairo governorate. According to the UN, the population in Cairo exceeded 22 million inhabitants in 2022. However, this number reflects the population of GCMR and not Cairo Governorate because, according to the CAPMAS, Cairo inhabits over 10 million people as of 2024 *(CAPMAS)*.

City	Area (km^2)	Establishment Year	Population (2017)	Population Absorption Capacity
New Administrative Capital	688	2015	0	6,500,000
6th of October & Sheikh Zayed	1354.1	2017	380,084	7,649,000 (2050)
New Sphinx City	312	2018	0	1,300,000
October Gardens	169	1979	28,885	3,000,000 (2050)
15 Mayu	75	1978	93,574	98,200 (2032)

Table 4 Selected Major Urban Projects in Cairo

Table 4 demonstrates some of the major projects that have been implemented and are currently being implemented in Cairo. Some of these presented projects are relatively old, such as 15 Mayu City and October Gardens City, which were established before 1980. Others are very new projects, such as New Sphinx City, which was established in 2018. Next to each city, its population is reported for the year 2017. Some cities already have residents, and others do not. However, the table reports the absorption capacity expected by the government. The table demonstrates that it is expected that these mega projects will lower the population density near the river banks in the future because all these cities are established far away from the Nile Delta region.

The data in Table 4 were obtained from a governmental document *(Updating the Urban Structuring Project for Cairo in Light of Regional Changes)*, under a section called when translated into “Updating the urban structuring project for Cairo in light of regional changes”. The table presents information for 5 cities in Cairo. However, according to the current governorates’ distribution, only two cities are in Cairo governorate, namely the New Administrative Capital and 15 Mayu City. The other 3 reported cities are in Giza governorate, even though this is a section of Cairo, as the translated section indicates.

Furthermore, adding to the confusion, Fig. 92 in the Annex presents the Cairo Governorate, as Fig. 93 in the Annex does as well. Both Figures are obtained from governmental sources. Fig. 92 is obtained from the Ministry of Housing *(Urban structuring of Cairo city sectors)*, Utilities and Urban Development, while Fig. 93 is obtained from the Official Portal of Cairo Governorates *(Cairo Governorate Areas)*. Although both figures map Cairo Governorate, both maps are different from each other. It seems that Fig. 93 is more inclusive than Fig. 92 because it includes the new urban cities in Cairo. However, both maps fail to report some urban cities in the governorate; for example, the New Administrative Capital is missing in both maps.

As it has been demonstrated, it is confusing and almost impossible to differentiate between the data that are related to GCMR and data for Cairo Governorate. However, it seems that in the future, GCMR will become Cairo Governorate because this way, it will be easier and more efficient to govern this metropolitan city, if only from the administrative aspect at least. Furthermore, this would multiply the size of the current Cairo Governorate, which would make sense because it is the most populated and densest region in whole Egypt.

2.3.2 Data Limitation

- Table 4 reported 5 urban cities; the second is the 6th of October and Sheikh Zayed. In the original document, data for the second city were not reported. This second city is, in fact, two separate urban cities. In the original document, it was stated next to these two cities, where they were presented as one, that "Presidential Decree No. 77 for the year 2017 has been issued to annex some areas as expansions to 6th of October City" (please note that this a translation from the original Arabic document). Therefore, a conclusion has been made, which is presented in Table 5.

City	Area (km^2)	Establishment Year	Population (2017)	Population Absorption Capacity
6th of October	655.6	1979	289,385	3,000,000 (2030)
Sheikh Zayed	42.1	1995	90,699	675,000 (2030)
New 6th of October	656.4	2016	0	3,974,000 (2050)
6th of October & Sheikh Zayed	1354.1	2017	380,084	7,649,000 (2050)

Table 5 6th of October City & Sheikh Zayed City Numbers Breakdown

As Table 5 demonstrates, the New 6th of October City was established in 2016. New 6th of October City lies within close proximity to 6th of October City. Furthermore, the presidential decree was released in 2017, one year after the establishment of New 6th of October City. Therefore, it is assumed that this new city is the new extension. Obtaining the breakdown values for these 3 separate cities allowed to complete the missing data.

2.4 Description of New Cairo

2.4.1 Overview

New Cairo is a rapidly developing satellite city located to the east of Cairo. It was established 2000 to alleviate the congestion and overpopulation of central Cairo, New Cairo has emerged as a modern urban centre characterized by residential neighbourhoods, commercial zones, educational institutions, and recreational facilities.

The area is characterized by wide landscaped streets and modern infrastructure, attracting middle- to high-income residents seeking a more spacious and modern living environment.

Residential compounds and gated communities are common, offering amenities such as parks, shopping centers, and recreational facilities within close proximity to residential areas.

New Cairo is also home to several prestigious universities and international schools, making it a hub for educational opportunities. Additionally, the area hosts a growing number of corporate offices, business parks, and commercial centers, contributing to its status as an emerging economic center within the Cairo metropolitan area.

2.4.2 Population Distribution in Light of Cairo & Egypt Shadows

Although New Cairo was established in 2000, construction activities are still heavily happening in the city. It is planned that by the year 2030 New Cairo will be 347 km² big. In 2006 New Cairo inhabited 116,678 individuals, and in 2017, it inhabited 297,387 individuals. However, it is planned to have a population capacity of 6,000,000 by the year 20230 *(Updating the Urban Structuring Project for Cairo in Light of Regional Changes)*.

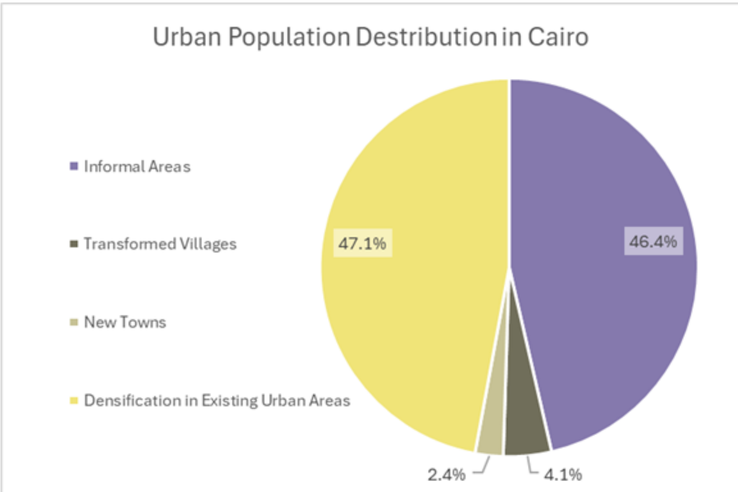

Figure 21 Urban Population Distribution in Cairo

Fig. 21 demonstrates the population distribution in GCMR until 2006. Even though, the graph is not for New Cairo, which is in GCMR, it sheds some light on important aspects that are applicable to New Cairo and most of the new urban cities in Egypt.

The chart is divided into 4 parts, namely informal areas, transformed villages, new towns and existing urban areas. As discussed previously, GCMR hosts many informal settlements which lack proper planning and infrastructure. Throughout the years, some villages were transformed into cities due to the urban sprawl. New towns are referred to the new urban cities and there is the existing urban cluster around the Nile.

When observing the graph it becomes clear that the impact of new cities on the urban redistribution is limited, which recorded absorbing only 2.4% from the total urban population in GCMR, whereas, the transformed villages reports almost the double absorption capacity with 4.1%. The rest of the population distribution is divided between the existing urban core cluster, with 47.1% and informal settelemts with 46.4%.

In the general description of New Cairo, it was eloboirated that the city is built for the middle and upper class, as of many, if not most, of the new urban cities. Ironically, 29% of the Egyptian population is calssified to be below the poverty line in 2019. Unfortunately, this percentage is increasing, because in 2023 it was estimated that more than 33% of the Egyptian population fall below the poverty line, as Dr. Al Leithy, CAPMAS advisor, stated *(CAPMAS Advisor: 33.3% of Egypt's population will be below the poverty line during 2023)*. According to the World Health Organization below the poverty line is defined as "the proportion of the population living below the international poverty line is the percentage living on less than US$ 1.90 a day" *(Population below the International Poverty Line)*. However, this metric is extremely outdated, because it was released in 2011.

Referring to Fig. 21, it makes absolute sense that the new urban cities do not attract the desired numbers of population, because simply 1/3 of the population falls below the poverty line, that is excluding the percentage of individuals who are classified to be at the poverty line. Moving to the new urban cities is expensive, and it doesn't meet the normal Egyptian citizen needs and requirements. Therefore, although New Cairo was established in 2000, until 2017 it inhabited less than 300,000 individuals compared to its actual absorption capacity which will reach 6,000,000 in 2023.

2.4 Conclusion

As the urban analysis shows, the historical trend and near future of Egypt in general and Cairo in specific exhibit almost a certain possibility of constructing new buildings. The number of new buildings that are being constructed in Egypt compared to retrofitting projects is not comparable since building retrofitting is an absolute rarity. Therefore, energy-efficient building studies and simulations must be conducted to ensure sustainability and carbon neutrality. The chosen case study, which is an administrative building, is a newly constructed building less than two years old. It was built without doing any kind of energy analysis. The results of that building's performance will be shown in a later chapter, which proves the importance of energy studies. Taking the energy efficiency aspect at early design stages into account would result in building a sustainable structure, with very limited modifications in the overall architectural design. However, in order to reach these modifications, the first step is to analyse the climate of the located building, since energy efficient building design strategies are altered in accordance with the climate conditions.

3. Weather Analysis

3.1 Geographical Description of Egypt

Egypt is located at the northeastern corner of Africa. It bordered by the Mediterranean Sea to the north and the vast Sahara Desert to the west and south and the Red sea at the east. Due to Egypt's location, it experiences climates that ranges from arid deserts to Mediterranean coastal climates.

Figure 22 Satellite image for the map of Egypt (GoogleEarth)

The most prevailing geographic characteristic of Egypt is the desert as Fig. 22 demonstrate. In fact, without the presence of the Nile River, Egypt would be a complete desert. Egypt is divided into sections, Southern Egypt, and Northern Egypt. Southern Egypt's landscape contains low mountains desert. Northern Egypt has wide valleys in close proximity to the Nile, while the east and west are deserted *(Hamid, Mohammed, 2022)*. This fact dictates the climatic characteristic in Egypt.

3.2 Climate – Egypt

Egypt falls within the hot arid climatic zone, encompassing the vast Sahara Desert in North Africa. The only exception to this arid region is the narrow linear valley, as stated before.

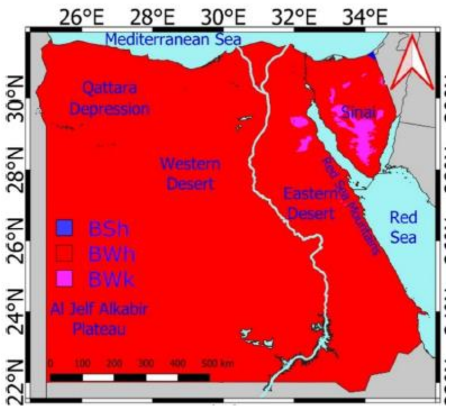

Figure 23 Köppen-Geiger climate classification map of Egypt (Britannica)

As Fig. 23 depicts, Egypt lies between 24°E-36°E and 22°N-32°N, which is zone BWh. BWh stems from Köppen classification, which accordingly implies that Egypt experiences high temperatures throughout the year, especially in the summer months, where temperatures in some areas exceed 40 °C *(Britannica)*. This means that this climatic zone is marked by its hot, arid, and deserted conditions. According to Köppen classification, the desert climate is characterized by extremely low precipitation. Egypt relies heavily on the Nile River for water, and most of the country's landscape experiences arid or hyper-arid conditions. According to Köppen classification, the subcategory BWh is characterized by even hotter temperatures compared to general desert cliate. Egypt's desert, similar to the Sahara Desert, often falls into this category.

In Köppen climate classification system, the code "BWh" stands for a specific climate category. Each letter and combination in Köppen system represents a set of climate characteristics. following the breakdown for "BWh":

- B, this letter indicates the main climate group, which is arid or desert climates. In these climates, precipitation is generally scarce.

- W, the second letter describes the second most significant climate characteristic. In the case of "BWh," the "W" stands for desert climate. Desert climates are characterized by a lack of significant rainfall.
- H, the third letter, when present, indicates the temperature of the warmest month. In the case of "BWh," the "h" signifies a hot desert climate, where the temperature of the warmest month exceeds 18°C (64.4°F).

So, "BWh" specifically represents a hot desert climate in the Köppen climate classification system. This classification is often applied to regions with extremely low precipitation and high temperatures throughout the year.

The majority of Egypt is covered by deserts, including the Eastern Desert and the Libyan Desert, however, the Red Sea and the Mediterranean Sea influence the climate along the coastal areas. The Nile River plays a crucial role in Egypt's climate. It does not only provide water for irrigation, but it moderates temperatures in the surrounding areas as well.

The topography of Egypt contributes to variations in climate, for instance, the highlands in the south can experience slightly different climatic conditions compared to the lower-lying areas.

3.3 Climate – Cairo

Earlier the climate of Egypt was discussed. However, the reference case study, which will be presented on a later stage, is located in Cairo. Therefore, the focus will be shifted towards Cairo. Concerning the climate data, they are raw average data obtained from observations made in Cairo International Airport from year 1980 until 2016. This means that the data are outdated, because in the recent years the maximum temperatures increased noticeably in comparison with 2016. However, these data will suffice to observe the general climatic conditions.

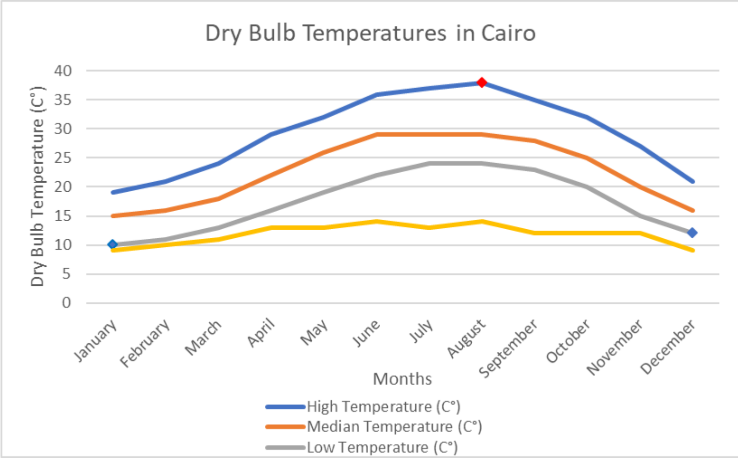

Figure 24 Average monthly dry bub temperatures in Cairo (Weather Spark)

Fig. 24 demonstrates the average temperatures for each month of the year. One can obtain many readings from the temperature graph, namely they are, maximum monthly temperature, minimum monthly temperature, median monthly temperature and the diurnal monthly temperature. According to the graph as well, the highest temperature almost reaches 40 C° in August, whereas the lowest temperature is reached in January reporting 10 C°. All these readings are vital for assessing envelope's thermal characteristics of the building.

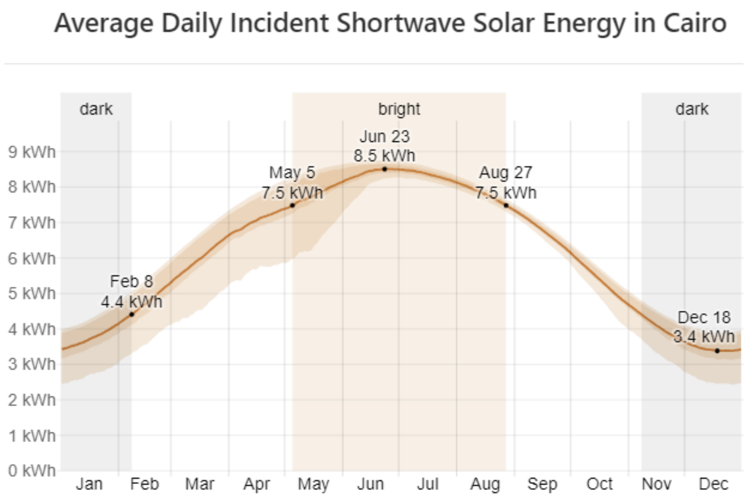

Figure 25 Average daily incident shortwave solar energy in Cairo (Weather Spark)

Fig. 25 depicts the incident solar energy around the year. The graph proves again that building's envelope in Cairo will experience high thermal stresses. However, the graph indicates as well that it is promising to utilize the use of photovoltaic panels as means of active strategy, since the peak incident solar energy reaches 8.5 kWh. This will for sure reduce the building's total energy dependency on fossil fuels sources.

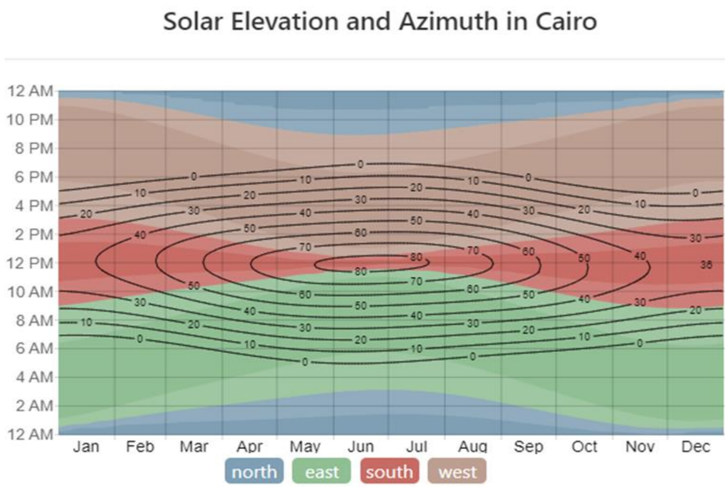

Figure 26 Solar elevation and azimuth angle in Cairo, (Weather Spark)

In order to maximize the production of electricity from PV-panels, the location and orientation of the panels should be distributed in accordance with the sun's position, which will allow for maximum exposure to sunlight over a course of a day throughout the year. Fig. 26 illustrates the different azimuth angles in relation to different orientations. Azimuth angle expresses the position of the sun relative to the horizontal plane with reference to a fixed point, which means that maximum production from a pv-panel will be obtained if it is perpendicular to the azimuth angle in given orientation. in Therefore, understanding the Azimuth Angle graph is vital.

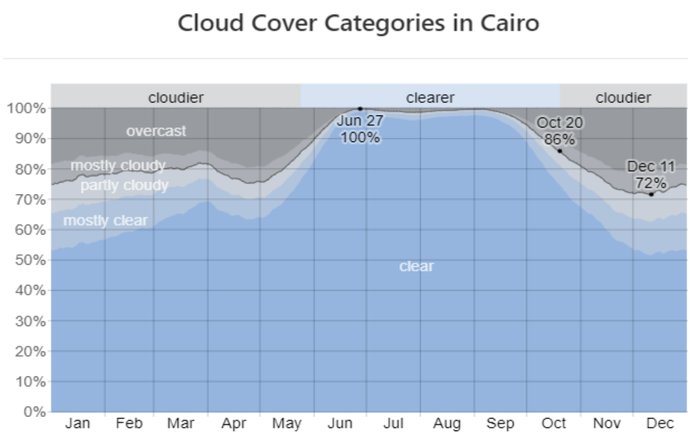

Figure 27 Cloud coverage in Cairo (Weather Spark)

Cairo’s sky is mostly clear throughout the year, especially during the months from June until October, the sky is almost completely transparent, as Fig. 27 shows. If anything, this indicates that solar radiation reaches the earth’s surface, and hence, the building’s envelope, without any obstruction. This indicates that shading is a very important design parameter in buildings for protection against overheating and maintaining internal thermal comfort.

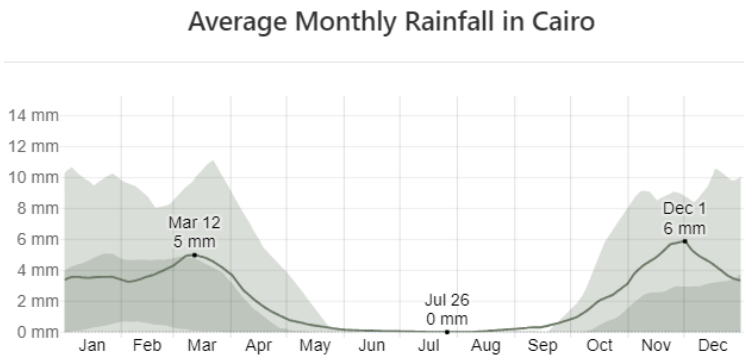

Figure 28 Average monthly rainfall in Cairo (Weather Spark)

In Cairo, as demonstrated in Fig. 28, rain is a rare phenomenon, where it rains less than 2.5 mm per year on average. By default, this indicates that the precipitation is very low as, particularly because Cairo is located in a hot climate. Rare rainfall indicates that there will be no cooling effect for the ambient air temperature.

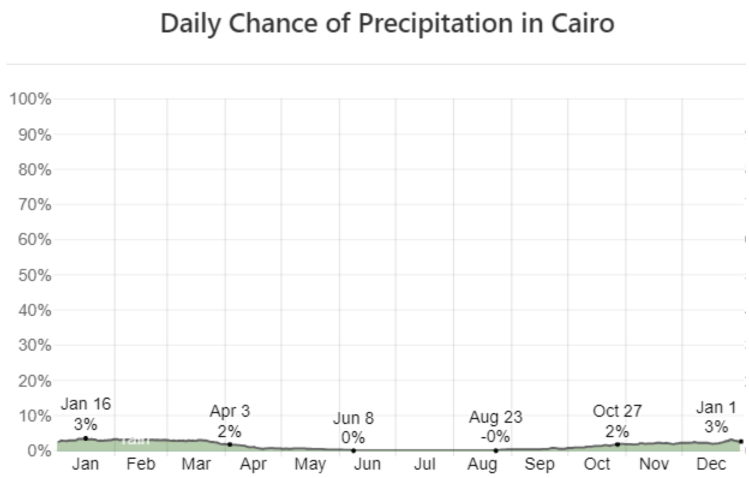

Figure 29 Daily chance of precipitation in Cairo (Weather Spark)

According to Fig. 29, there is almost no precipitation in Cairo. The almost non-existent precipitation levels means that even if it rains, water will evaporate rapidly, which again will not leave a chance for any cooling effect. These two characteristics lead to another effect which occurs frequently, sandstorms. The frequency of sandstorms in Cairo adds to the challenges of maintaining the indoor quality.

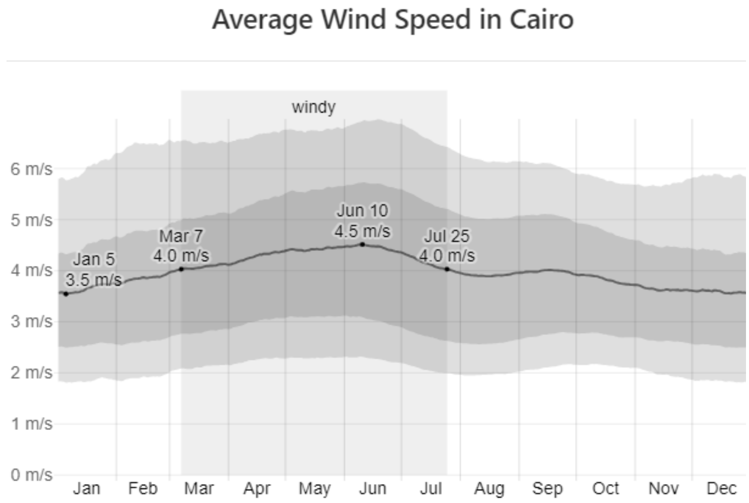

Figure 30 Average Wind Speed in Cairo (Weather Spark)

Fig. 30 depicts the average wind speed in Cairo, which is not considered to be fast, with maximum wind speed of 4.5 m/s. This suggests that utilizing wind power as an energy source generator is not efficient. However, this wind will assist the building to cool down, especially if the night flushing is applied in the building. In order to maximize the wind cooling effect, understating the wind direction will be very helpful to design envelope openings accordingly.

All the aforementioned characteristics, which are, Cairo having clear sky, high temperatures, high diurnal temperatures, negligible precipitation, moderate wind speed and high solar radiation, create an extremely challenging environment, demanding cautious and expert strategies for adaptation building adaptation.

4. Literature Review on Building's Components and Technologies for Low Energy Buildings

After stating the facts about the climatic characteristic of the location at hand, it is vital to discuss the previous studies conducted on the subject, otherwise, any research will start from ground zero. This way we will be able to build on the previous people work.

4.1 Building's Envelope

The building envelope is one of the most crucial components when it comes to energy building consumption. Some researchers estimate the envelope's impact to account for up to 50% of the total heat gain in a building in a hot climate. The building envelope refers to all elements of the building which are separating the inner environment from the external environment. These elements are external walls, external doors, windows, and roof. All these elements are affecting the building's energy performance differently, however, the degree in which an element affects the building differs according to context and aspect ratio. For example, usually walls are a predominant element of that envelope component. Nonetheless, if the building is not high enough, and the floor area is large, then the roof would have a greater impact on the building, simply because the roof would have covered more area *(Sadineni, Suresh, 2011)*.

A building's energy consumption is primarily dominated by the characteristics of its envelope because heating or colling is usually needed to maintain acceptable thermal comfort inside a building. Thermal comfort is "that condition of mind which expresses satisfaction with the thermal environment" *(ANSI/ASHRAE Standard 55-2010)*. This means that if the external environment is not satisfactory, either too hot or too cold, and it infiltrates the building, thermal comfort will not be achieved, and hence it will be compensated with mechanical measures, especially in non-residential buildings, to make the internal space comfortable for occupants.

4.1.1Heat Transfer through Envelope

There are three aspects of heat gain through the building envelope that must be taken into account, which are conduction through opaque surfaces, conduction through glass and solar radiation through glass *(Yang, Lui, 2007)*. When determining the overall heat gain of a building envelope and the accompanying cooling need, solar heat gain typically plays the major role in hot climates. Equation 1, which is the general formula for rate of heat transfer explains why the envelope is the first line of defence against external conditions.

$$Q = U * A * \Delta T \ (W)$$

Equation 1 Heat Transfer

Q stands for the rate of heat transfer through a wall at a particular time (W), U stands for the thermal transmittance of the wall (W/m^2K), A stands for the overall subject area (m^2) and ΔT is the temperature difference between the two environment, namely internal and external environment. The equation is better explained through the demonstration in Fig. 31.

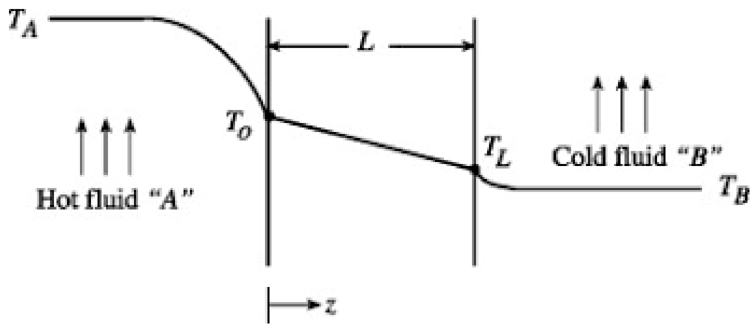

Figure 31 Temperature profile depicting heat transfer behaviour through a wall (Transfer rate in terms of bulk fluid properties)

Fig. 31 demonstrates the temperature profiles between two environments separated by a medium that has thickness L. Assuming that Ta is the external hot air temperature means Tb is the internal cold temperature. In a building in a hot climate, one would like to maintain the colder internal temperature, however, according to the presented temperature profile, temperature dissipates from hot to colder atmosphere temperature. The only medium separating the two environments is the wall, and with its characteristics, predominantly the thermal transmittance, which is affected by the material and the thickness, it determines the rate of heat transfer. This means the smaller the thermal transmittance the less heat transfer it allows to infiltrate, which means external walls with low values of thermal transmittance reduce the cooling and heating load of the building. Ino order to elaborate this principle, a practical example, which is the base case's external wall that will be presented later on, will be demonstrated. Equation 2 defines the heat transfer density, which is a function of the temperature difference between 2 environments and the thermal transmittance that is separating the 2 environments. Please note that the thermal transfer density is in fact the thermal transfer that is explained in Equation 1 but it is per unit area.

In Equation 2 Te stands for external environment, where Ti strands for the internal temperature, with the value of 40 C° and 26 C° respectively. h1 and h2 are the heat transfer coefficient for each surface side, for the sake of this example they are both estimated to be 8 W/m²K. th is the thickness for each layer and λ is the thermal conductivity for the corresponding layer. Rtot is the total thermal resistance, which is the reciprocal for the thermal transmittance, Utot. The wall in this example consists of 4 different layers. Starting from the external side, the first layer is plaster, with thickness of 0.02 m and λ of 0.51 W/mK, the second is mineral wool insulation layer with a thickness of 0.05 m and a λ of 0.035 W/mK. The following layer is Cementous brick wall with thickness of 0.23 m and a λ of 1.3 W/mK. The last layer from the internal side is another layer of plaster with the same thickness and λ.

$$q = \frac{Te-Ti}{Rtot} = Utot(Te - Ti) \text{ (W/m}^2\text{)}$$

Equation 2 Heat transfer density

$$q = \frac{Te - Ti}{\frac{1}{h1} + \sum\frac{th}{\lambda} + \frac{1}{h2}} = \frac{40 - 26}{\frac{1}{8} + \frac{0.02}{0.51} + \frac{0.23}{1.3} + \frac{0.05}{0.035} + \frac{0.02}{0.51} + \frac{1}{8}}$$

Equation 3 Heat transfer density practical example

$$q = 7.2\, W/m^2$$

Equation 4 Heat transfer density

According to Equation 3 and 4, the total heat transfer density through the opaque wall is 7.2 W/m², which is considered high transfer density. This means the heat is transferred from the outside, which is warmer, to the inside with this value through each squared meter. The external temperature is uncontrollable, and the internal temperature is kept within a certain threshold to maintain thermal comfort. The only parameter that can be utilized to control the heat transfer from inside to outside is the thermal transmittance, as Equation 2 indicates.

Equations 5 to 9 calculate the surface temperatures at different wall layer, which highlights the importance of having sufficient thermal insulation.

$$T1 = 40 - 7.2 \times \frac{1}{8} = 39.1\ C°$$

Equation 5 Heat transfer density

$$T2 = 40 - 7.2 \times \left(\frac{1}{8} + \frac{0.02}{0.51}\right) = 38.8\ C°$$

Equation 6 Heat transfer density

$$T3 = 40 - 7.2 \times \left(\frac{1}{8} + \frac{0.02}{0.51} + \frac{0.05}{0.035}\right) = 28.5\ C°$$

Equation 7 Heat transfer density

$$T4 = 40 - 7.2 \times \left(\frac{1}{8} + \frac{0.02}{0.51} + \frac{0.05}{0.035} + \frac{0.23}{1.3}\right) = 28.2\ C°$$

Equation 8 Heat transfer density

$$T5 = 40 - 7.2 \times \left(\frac{1}{8} + \frac{0.02}{0.51} + \frac{0.05}{0.035} + \frac{0.23}{1.3} + \frac{0.02}{0.51}\right) = 27.2\ C°$$

Equation 9 Heat transfer density

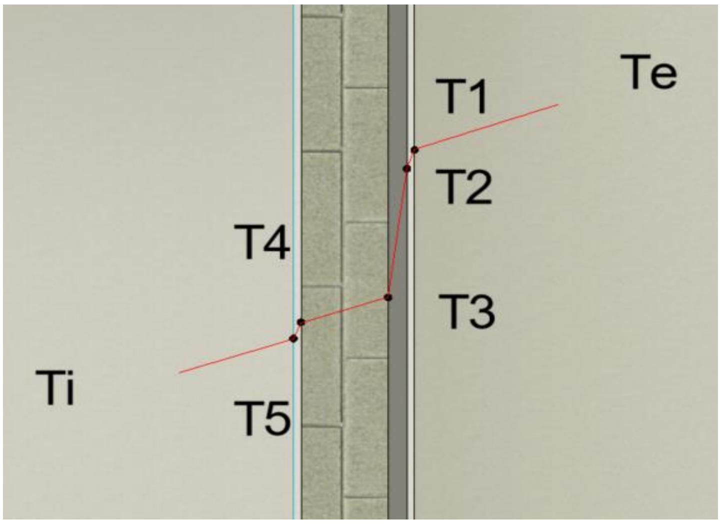

Figure 32 Heat transfer profile through opaque wall

As Fig. 32 portraits, the temperature profile is increased from the inside to the outside, however, the greatest rate of transfer happens at the insulation layer, the difference between T2 and T3 is more than 10 C°, this allows for the heat that reaches the cement brick is relatively cooled down, however if this insulation layer is thinner or it was placed on the inside, the wall temperature would be higher which would affect the internal temperature as well.

In order to maintain the thermal comfort inside the building, the energy rates should balance out. The simplest method which depicts this balance is the energy rate balance of a controlled volume (Cerutti, Emiliano Adam, 2022). The following formula depicts the energy rate balance behaviour.

$$Q_T + Q_V + Q_I + Q_S + Q_P + Q_E + Q_{HVAC} = 0$$

Q_T stands for transmission heat loss or gain, which is related to the heat flow through the building's envelope. Q_V stands for the ventilation heat loss or gain, which is related to openings in the envelope allowing for air movement. Q_I stands for the infiltration heat loss or gain, which every building has, no matter how tight the building is there will be always present uncontrolled air infiltration through the building's envelope. Q_S stands for solar gain, which goes through the building's glazed envelope. Q_P stands for heat gain due to occupants. Q_E stands for heat gain due to equipment and finally Q_{HVAC} stands for heating or cooling mechanical power. All these gains and losses should balance out according to the above presented equation. All these parameters are important, however, the last three parameters, Q_P, Q_E and Q_{HVAC} are especially important for office building designing compared to a non-residential building, because an office will have higher loads stemming from many occupants, many equipment and machine loads will be present, such as, monitors and printers, and usually an office will be mechanically ventilated.

The aim for designing an energy efficient building is to reduce the impact of the loads as much as possible. Q_T should be minimized in order to isolate the effects of the harsh external environment from the internal environment and this is mainly related to the thermal transmittance parameter. The building should be ventilated when needed, for example, to remove the excess heat. Q_S should be controlled to reduce the impact heat transmitted from solar gains and Q_{HVAC} should be optimized to achieve thermal comfort with least energy possible. All these parameters influence each other; therefore, a holistic approach should be adopted.

4.2 Glazed Envelope

In modern building architecture, the use of glass for the building envelope is being implemented at a large scale. One can clearly observe these phenomena in the presentation of commercial buildings. At the same time, fenestration technologies have seen significant advances, these include, but not limited to solar glass control, insulating glass units, low emissivity glass coatings, switchable reflective glazing, evacuated glazing, aerogels, and gas cavity fills along with improvements in the frame components.

The fenestration of the envelope is more complex compared to the opaque external walls because they not only allow for heat transmission, but they also allow for solar radiation to enter the internal space and heat the space. Therefore, in cooling dominated climates windows are responsible for unwanted solar heat gains. Key parameters of envelope's glazed components are solar heat gain coefficient (SHGC) and visual light transmittance (VLT). "SHGC is the fraction of radiation admitted through a window […] either transmitted directly and/or absorbed, and subsequently released as heat inside a home" *(U.S. Department of*

Energy). This means, just similar to thermal transmittance, that the lower the SHGC the less solar heat is transmitted into space. On the other hand, VLT is the amount of light in the visible portion of the spectrum that passes through a glazing material, therefore, having high VLT values would offset the internal gains transmitted due to internal lighting. The paradox is that in order to achieve low SHGC coatings and tints are applied, which greatly affects the cooling loads, however, this means that VLT is usually reduced *(Wand, Julian, et al, 2016)*. Studies have shown that low emissivity glass double glazing windows with 13mm air fill with low SHGC report better thermal performance in hot climate zones, with energy savings up to 15% *(He, Qiong, et al, 2019)*.

4.3 Strategies for Enhancing Building Energy Performance

The ratio of windows in relation to the external walls should be controlled, as stated before, because windows allow for solar heat gain to enter the building, which is a dominant aspect that rules buildings in hot climate. However, the total non-existence of glazed envelopes is not a solution as well. The largest portion of energy consumption in a hot climate in a building is air conditioning, followed by internal artificial lighting. This means if the approach is to reduce the window to wall ratio (WWR) absolutely, it will require in turn huge consumption of internal artificial lighting, to compensate for the absence of natural lighting. Therefore, external shading devices are an important aspect in energy conservation measures for a building in a hot climate. Shading allows for natural light to enter the building, while reducing the glare phenomena and preventing direct solar radiation to infiltrate through the glazed envelope and consequently reducing heat gain due to solar radiation. Designing a building with proper external shading can reduce the indoor cooling loads by up to 30% *(Shahdan, et al., 2018)*.

However, to analyse external shading effect on building's total energy consumption, it is imperative to have a thorough understanding of the physical properties of the devices, as different building orientations call for different kinds of shading devices to provide efficient shade. Basically, there are three main shading categories, namely, horizontal shading, vertical shadings and egg-crate shadings. Egg-crate shading is principally horizontal and vertical shading system combined in one. Studies have shown that egg-crate shadings have a positive impact in decreasing energy consumption when placed in the southern and western façade.

Horizontal shadings have as well positive impact when placed in the western and eastern façade, however, horizontal shadings in these facades will have more positive effect in energy consumption if they are slanted downwards *(Chua, Klan Jon, and Slaw Klang Chou, 2010)*.

Furthermore, another strategy which enhances building energy behaviour in a hot arid climate is the ventilated façade skin. Ventilated façade skin is believed to increase the thermal performance of a building. There are two types of ventilated façade, one is mechanically ventilated and the other is naturally ventilated, which means the latter basically is applying the stack effect through the cavity wall. Studies have shown that a cavity wall has indeed a positive effect on the building's energy performance. It has been observed that there is a correlation between energy demand decrease and the width of the air gap between both skin layers, however, cavity increase over 0.15 m offers minimal and negligible energy savings, which means 0.15 m cavity can be taken as the limit for this cavity.

In climates with great amount of solar radiation roofs become an important factor, because roofs are highly susceptible to solar radiation, therefore roofs account in this case for a lot of heat gain. There are many studies conducted on roof technologies, however, there are two interesting ones which can be effective to protect the building from heat and solar radiation. The first technology is the ventilated roofs. Ventilated roofs mean that essentially in the upper floor, there will be 2 slabs instead of just one, where an air gap is created between the two slabs. This air gap would allow for air movement, just similar to the ventilated façade system and it will diminish the heat transfer across the roof into the building. The second technology is called solar reflective roofs. The main characteristic of these roofs it that they have high solar reflectance and high infrared emittance properties. These two properties affect the thermal performance of the roof greatly. These properties can be simply applied with specific coatings that have high emissivity and high solar reflectivity. Tests have revealed that solar reflective roofs have the ability to reduce the cooling loads by 5% to 40%.

Additionally, a very efficient method to release a building's thermal stresses in a hot arid climate is night ventilation, also referred to as night flushing. These thermal stresses are a consequence of high thermal mass material properties. High thermal mass materials, such as concrete and bricks, absorb, store and later release this accumulated heat into the interior.

Night flushing means allowing the circulation of the night cooler air to infiltrate the interior spaces of the building. By applying night flushing, the thermal mass of the building, which stored heat during the day due to solar and internal gains, will cool down. Subsequently, this will result in reduction of HVAC system cooling loads. At the same time, night ventilation prepares the building for the next day, now the thermal mass has emptied its stored heat, and it will be able to absorb and store heat on the following day.

If the stored heat is not released, it will have many negative implications on the building and its occupants. The building and the solar radiation each have a heating cycle. The buildings cycle follows the solar cycle, but with a shifted degree. The solar gains, following the sun path during the day, increase incrementally starting from sun rise, until the radiation, hence, the ambient air temperature reaches the peak in midday, and then decline incrementally until sun set. The building starts heating up after sunrise, and this is the shifted aspect. The building, or specifically the thermal mass of the building heats up and continues to heat even after solar radiation have reached the peak during the day. This means that the thermal mass will continue to heat even after the heat from solar radiation has diminished. Now, each day this cycle happens, however, if the thermal mass is not cooled down each day, before the sun rise, the thermal mass will start heating up and storing energy at a higher baseline degree each day, which will result that each day the building will have higher stored temperatures compared to the previous day. Consequently, this heat will affect the thermal comfort of the occupants and the building may represent an oven for its occupants, putting the building and its ventilation system into more stresses and more energy consumption.

4.4 Traditional Effective Vernacular Architecture

There are always new technologies discovered which enhance the thermal performance and energy efficiency of a building. However, energy efficient building principles are present since old times, one can see this in the old structures of any area. Each country has its traditional building style, which is dictated by the climate of the country or the region, therefore, the strategies applied in old buildings differ according to the region.

Figure 33 Mashrabeya

Figure 34 Sheesh

Egypt has its own traditional building style as well, which was influenced by tradition and its climate, such as, the courtyard, a covered out outdoor sitting area at the ground level, open wooded lattice window screens called Mashrabeya, see Fig. 34 and venetian blinds called sheesh, see Fig. 33. Mashrabeya and sheesh both allow for natural ventilation while providing shading and protection from direct solar radiation. The sheesh in its function acts like a tight horizontal shading element, were these elements are tilted with a 60 degree angle downwards towards the external side. This way, the sheesh blocks the direct solar radiation while allowing the cool air flow to enter through the openings and limitting the hot air flow to enter the protected internal space. The Mashrabeya acts like external shading ellement and a buffer zone at the same time, because the mashrabeya is constructed in the external limits of the building, which creates extra space but at the same time it is a buffer zone, which is between the mashrabeya itself and the external wall which is laying behind. In the Egyptian varnicular architecture, an element called shukhshekha is usually present on the buildings as well. Shukhshekha is basically a vented lantern that is placed over the main hall in the upper floor, which allows for the hot air to escape outside the building. This way air circulation is guaranteed inside the building, whiule constantly emitting hot air to the external environmenent. In addition to the shukhshekha, the taka is a populare vernicular element in the Egyptian architecture. Taka is basically a small window opening that is placed on the upper level of the wall. This way, it is further promoted for the hot air inside the building to flow to the outside, since the hot air is lighter than the colder air, and therefore, the hot air would be accumilated on the upper level of the room. All these are traditional building characteristics in Egypt. These design strategies are sufficient to guarantee energy efficient buildings *(Mady, Mohamed, 2010)*, however, nowadays, where buildings are larger and many of the building materials are different from the old local materials, like mud, which was used in Egypt many years ago, there is more challenge to combine new technologies with old effective principles in order to achieve a truly efficient commercial building.

5. Method of Works

The methodology and sequence of works of this thesis in presented in the below graph. The first step was choosing a building as a base reference to carry out an energy analysis as Fig. 35 demonstrates. The second step is building the 3-D geometrical model, then the thermal properties of the envelope, space vetntilation paramters and the climatic data will be applied to the model. Subsequently, the 3-D model will be ready to carry out energy and daylight simulation on Revit. Thirdly, after finishing the 3-D model different parameters will be analyzed to achieve optimum results. The simulations will be carried out using Revit Insight and Revit Built-in function tools. The first set of simuations will test the model and the tools, after that calibration will be applied to the model to achieve more reliable results in the optimizztion process. Finally, optimized parameters will be reached and optimized model will be built, whoch will be compared with the base case reference model to verify the optimized paramters.

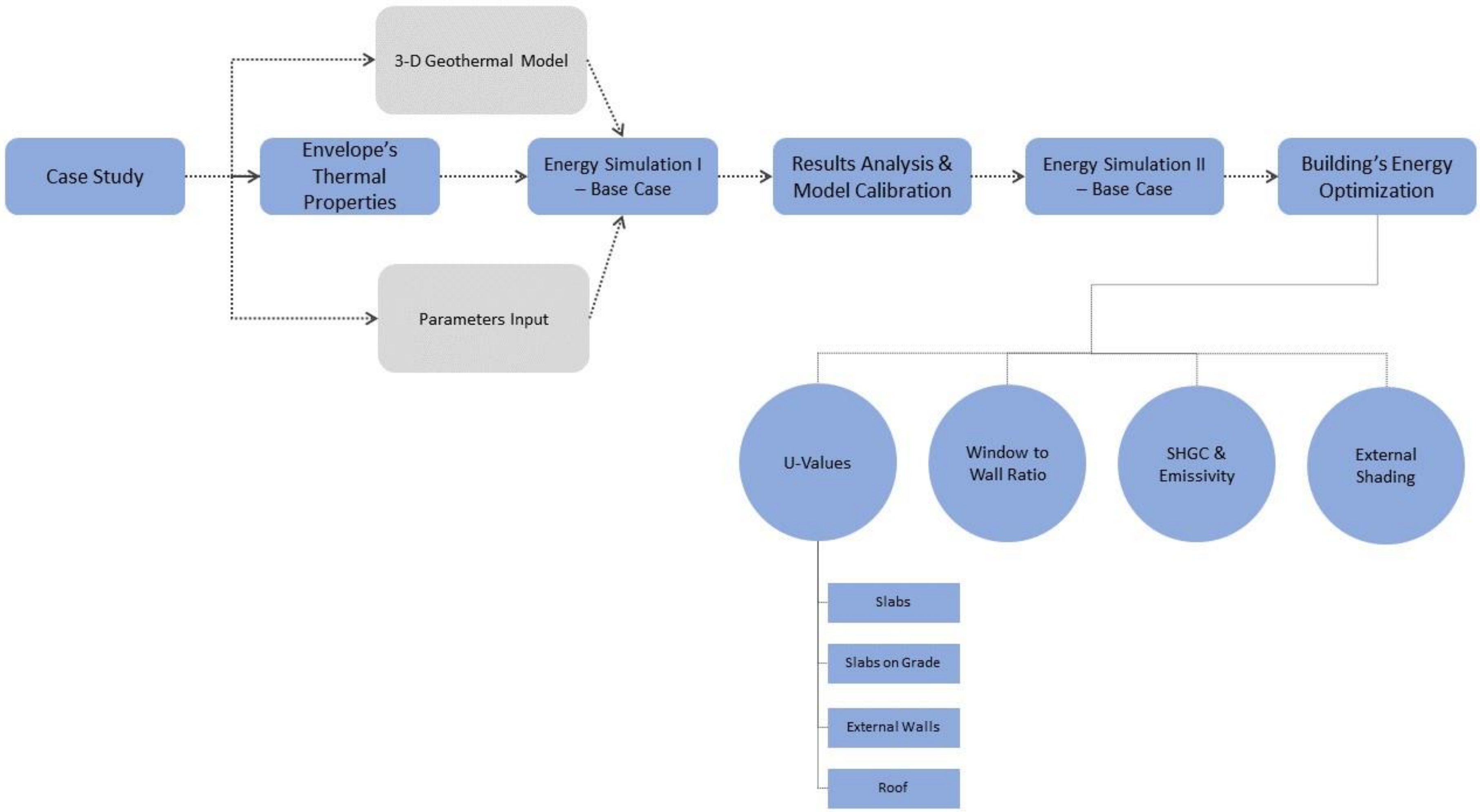

Figure 35 Workflow chart

6. Case Study

6.1 Case Study Presentation

The study carried out concerns a realistic architectural project located in Egypt. The chosen building is designed by the architect Hisham Bahaa Eldin. The building is an office and a commercial building located in one of the new neighbourhoods in Cairo, which is called New Cairo, as indicated in Fig. 36. This neighbourhood, New Cairo, is in the east side of Cairo. As Fig. 36 demonstrates, the location is in a deserted terrain, which characterizes the conditions governed there.

Figure 36 Office building location in Cairo (Google Earth)

The building is already constructed, as shown in Fig. 37. This photo was taken in August 2023. The building was supposed to be operating in year 2022, however, it is still not operating until this year. The building has a built-up clear area, excluding external walls, of about 9600 m².

Figure 37 Photo of the real built administrative building in Cairo

The building is neighbored from all directions accept from the northern direction. However, the geometry of the building creates an inner court.

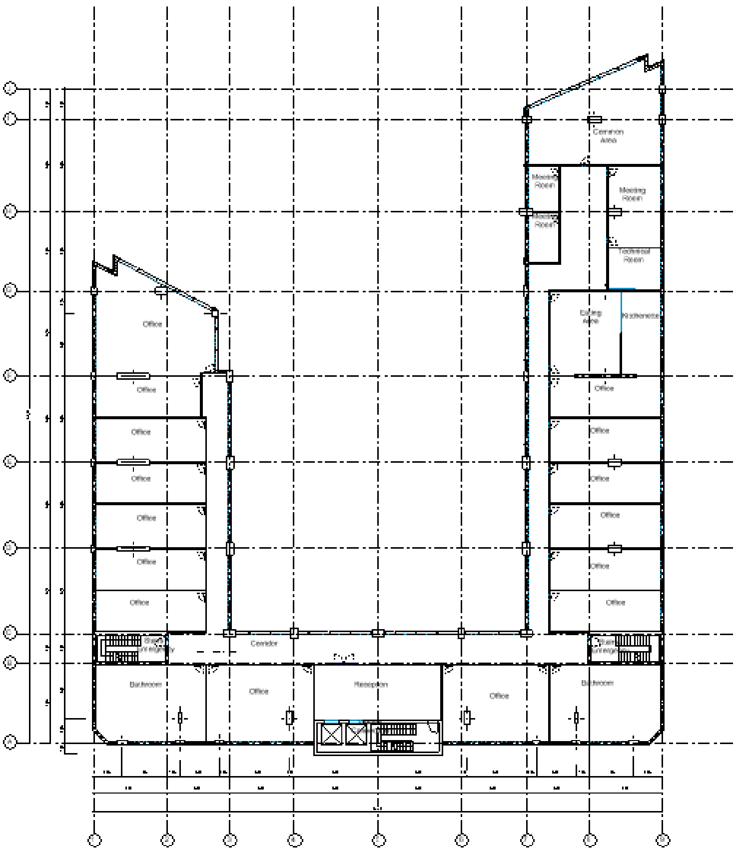

Figure 38 Floor plan, fourth floor

This building is designed to accommodate 54 offices, 20 meeting rooms, 5 kitchenettes, 5 eating areas, 5 receptions, 2 lobbies, 9 cafes, 15 bathrooms, 8 corridors and 19 vertical connections (Elevator/Stair) as Table 6 demonstrates. The Building is about 27,037 m³, where the maximum hight of the floor reaches 3.95 m and the average window to wall ratio along all facades is 65%.

Facility	Area	Floor
Bathroom 1	54.00	Ground Floor
Bathroom 2	76.00	Ground Floor
Bathroom 3	5.00	Ground Floor
Bathroom 4	24.00	Ground Floor
Bathroom 5	74.00	First Floor
Bathroom 6	74.00	First Floor
Bathroom 7	74.00	Second Floor
Bathroom 8	74.00	Second Floor
Bathroom 9	74.00	Third Floor
Bathroom 10	74.00	Third Floor
Bathroom 11	74.00	Fourth Floor
Bathroom 12	74.00	Fourth Floor
Bathroom 13	74.00	Fifth Floor
Bathroom 14	74.00	Fifth Floor
Bathroom 15	13.00	Sixth Floor
Café 1	93.00	Ground Floor
Café 2	102.00	Ground Floor
Café 3	99.00	Ground Floor
Café 4	73.00	Ground Floor
Café 5	140.00	Ground Floor
Café 6	142.00	Ground Floor
Café 7	73.00	Ground Floor
Café 8	99.00	Ground Floor
Café 9	101.00	Ground Floor
Common Area 1	95.30	First Floor
Common Area 2	95.30	Second Floor
Common Area 3	95.30	Third Floor
Common Area 4	95.30	Fourth Floor
Common Area 5	95.30	First Floor
Corridor 1	25.00	Ground Floor
Corridor 2	25.00	Ground Floor
Corridor 3	268	First Floor
Corridor 4	268.00	Second Floor
Corridor 5	268.00	Third Floor
Corridor 6	268.00	Fourth Floor

Corridor 7	268.00	Fifth Floor
Corridor 8	28.00	Sixth Floor
Eating Room 1	52	First Floor
Eating Room 2	52.00	Second Floor
Eating Room 3	52.00	Third Floor
Eating Room 4	52.00	Fourth Floor
Eating Room 5	52.00	Fifth Floor
Kitchenette 1	25	First Floor
Kitchenette 2	25	Second Floor
Kitchenette 3	25	Third Floor
Kitchenette 4	25	Third Floor
Kitchenette 5	25	Fifth Floor
Lobby 1	259.00	Ground Floor
Lobby 2	114.00	Ground Floor
Meeting Room 1	13.00	Ground Floor
Meeting Room 2	11.00	Ground Floor
Meeting Room 3	20.00	Ground Floor
Meeting Room 4	35.50	First Floor
Meeting Room 5	14.00	First Floor
Meeting Room 6	14.00	First Floor
Meeting Room 7	35.50	Second Floor
Meeting Room 8	14.00	Second Floor
Meeting Room 9	14.00	Second Floor
Meeting Room 10	35.50	Third Floor
Meeting Room 11	14.00	Third Floor
Meeting Room 12	14.00	Third Floor
Meeting Room 13	35.50	Fourth Floor
Meeting Room 14	14.00	Fourth Floor
Meeting Room 15	14.00	Fourth Floor
Meeting Room 16	35.50	Fifth Floor
Meeting Room 17	14.00	Fifth Floor
Meeting Room 18	14.00	Fifth Floor
Meeting Room 19	41.00	Sixth Floor
Meeting Room 20	41.00	Sixth Floor
Office 1	84.00	First Floor
Office 2	83.00	First Floor
Office 3	83.00	First Floor
Office 4	83.00	First Floor
Office 5	81.00	First Floor
Office 6	82.00	First Floor
Office 7	82.00	First Floor
Office 8	195.00	First Floor
Office 9	84.00	Second Floor
Office 10	83.00	Second Floor

Office 11	83.00	Second Floor
Office 12	83.00	Second Floor
Office 13	81.00	Second Floor
Office 14	82.00	Second Floor
Office 15	82.00	Second Floor
Office 16	195.00	Second Floor
Office 17	84.00	Third Floor
Office 18	83.00	Third Floor
Office 19	83.00	Third Floor
Office 20	83.00	Third Floor
Office 21	81.00	Third Floor
Office 22	82.00	Third Floor
Office 23	82.00	Third Floor
Office 24	195.00	Third Floor
Office 25	42.00	Fourth Floor
Office 26	41.00	Fourth Floor
Office 27	41.00	Fourth Floor
Office 28	41.00	Fourth Floor
Office 29	41.00	Fourth Floor
Office 30	41.00	Fourth Floor
Office 31	83.00	Fourth Floor
Office 32	81.00	Fourth Floor
Office 33	41.00	Fourth Floor
Office 34	41.00	Fourth Floor
Office 35	41.00	Fourth Floor
Office 36	41.00	Fourth Floor
Office 37	41.00	Fourth Floor
Office 38	41.00	Fourth Floor
Office 39	92.00	Fourth Floor
Office 40	42.00	Fifth Floor
Office 41	41.00	Fifth Floor
Office 42	41.00	Fifth Floor
Office 43	41.00	Fifth Floor
Office 44	41.00	Fifth Floor
Office 45	41.00	Fifth Floor
Office 46	83.00	Fifth Floor
Office 47	81.00	Fifth Floor
Office 48	41.00	Fifth Floor
Office 49	41.00	Fifth Floor
Office 50	41.00	Fifth Floor
Office 51	41.00	Fifth Floor
Office 52	41.00	Fifth Floor
Office 53	41.00	Fifth Floor
Office 54	92.00	Fifth Floor

Reception 1	55.00	First Floor
Reception 2	55.00	Second Floor
Reception 3	55.00	Third Floor
Reception 4	55.00	Fourth Floor
Reception 5	55.00	Fifth Floor
Vertical Connection 1	30.00	Ground Floor
Vertical Connection 2	30.00	First Floor
Vertical Connection 3	30.00	First Floor
Vertical Connection 4	30.00	Second Floor
Vertical Connection 5	30.00	Second Floor
Vertical Connection 6	30.00	Third Floor
Vertical Connection 7	30.00	Third Floor
Vertical Connection 8	30.00	Fourth Floor
Vertical Connection 9	30.00	Fourth Floor
Vertical Connection 10	30.00	Fifth Floor
Vertical Connection 11	30.00	Fifth Floor
Vertical Connection 12	30.00	Sixth Floor
Vertical Connection 13	30.00	First Floor
Vertical Connection 14	30.00	Second Floor
Vertical Connection 15	30.00	Third Floor
Vertical Connection 16	30.00	Fourth Floor
Vertical Connection 17	30.00	Fifth Floor
Vertical Connection 18	30.00	Ground Floor
Vertical Connection 19	30.00	Ground Floor

Table 6 Areas of all rooms in the entire project

All the rooms and functions are dispersed on 7 different levels. As Fig. 39 demonstrates, the building is divided into two parts. The first part is the ground floor which consists of mainly cafes and is separated from the upper floor. Starting from the first floor, each floor encompasses offices, two bathrooms, one eating area, one kitchenette, one common area, one reception and one great corridor that connects the whole floor area. As Fig. 39 demonstrates as well, the number of office spaces is increased when you go up in upper levels resulting in smaller floor area for offices. There are 3 vertical connections in each floor to accommodate the huge number of people inside the building, except for the last floor which has only one vertical access, because the floor area in the last floor is relatively limited compared to the other floors.

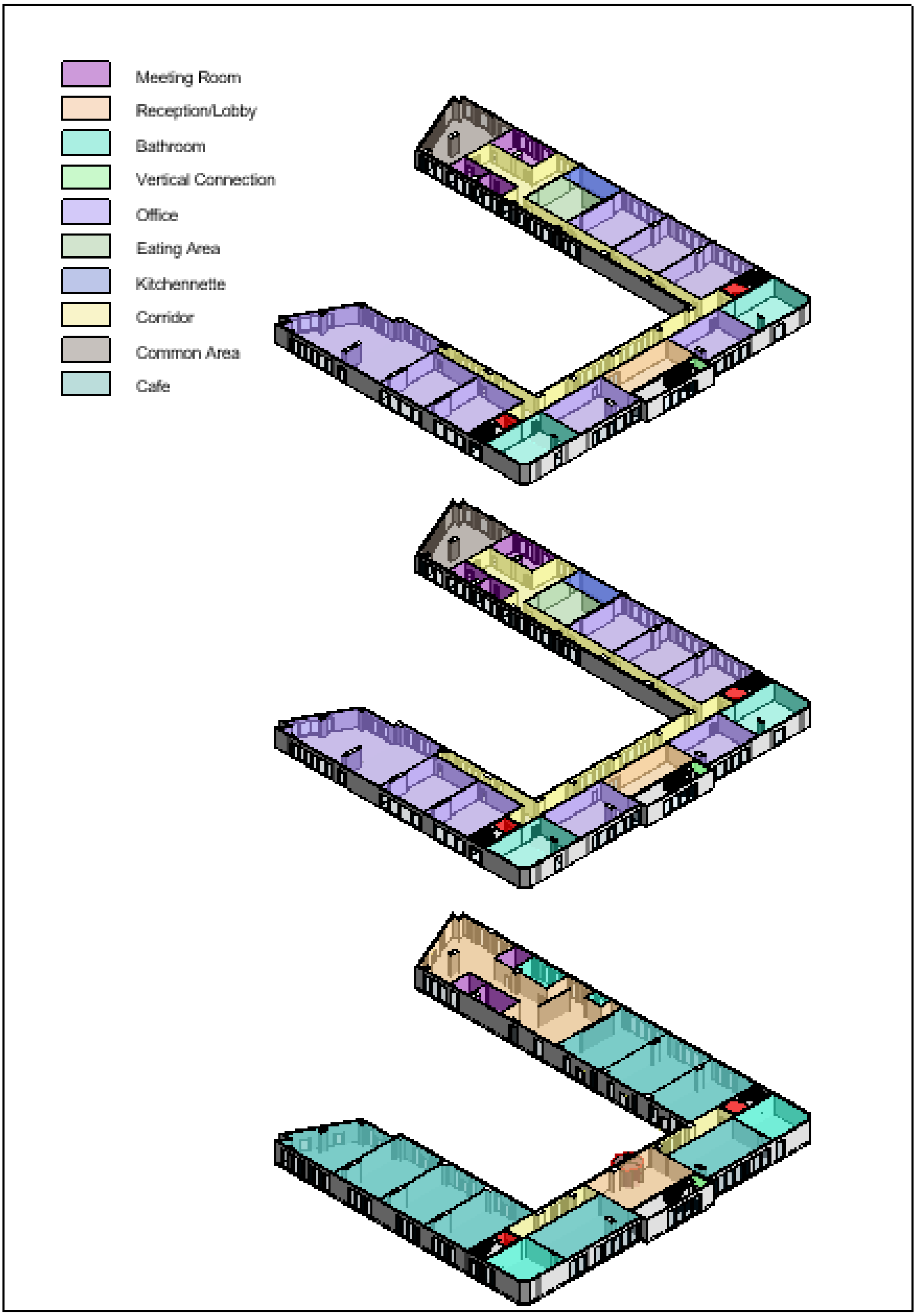

Figure 39 Axonometric view for Ground, First & Second floor

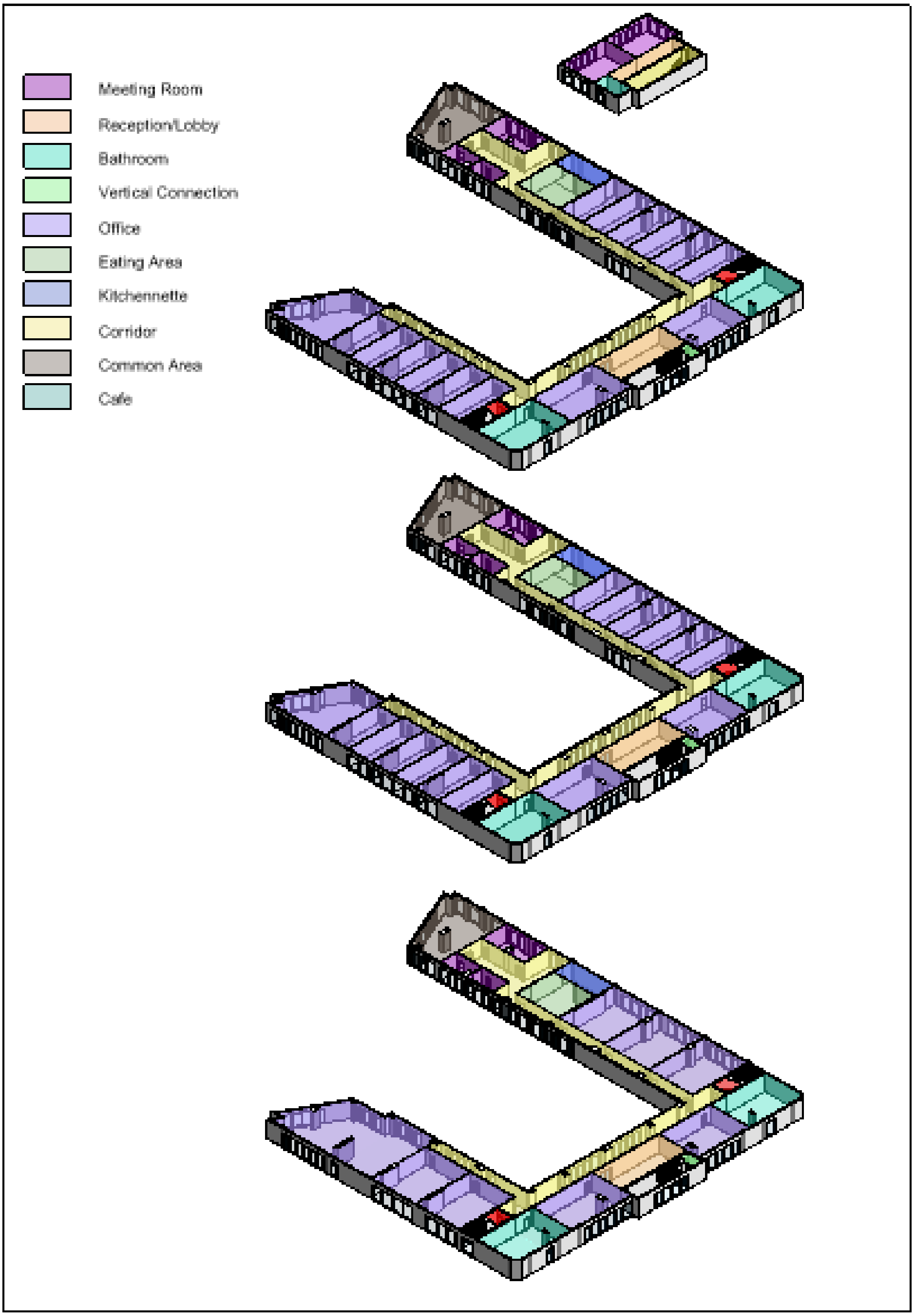

Figure 40 Axonometric view for the Third, Fourth, Fifth & Sixth floors

The different quantities of the building's components are presented in Table 7. The obvious and remarkable quantity reading from this table is the area of glazed walls compared to opaque walls. The windows to walls ratio (WWR) reports more than 65%. Which means that the glazed components exceed the area of opaque external walls. This puts the system of the building into extreme conditions because the building is located in a hot and arid climate, with a predominant glazed envelope. According to studies, this high amount of glazed envelope will be responsible for a large amount of cooling loads and consequently incredible amount of energy will be consumed.

Surface Type	Area (m2)
Curtain Wall & Glazed Components	4063
External Walls	2124
Interior Floor	8009
Interior Walls	6129
Slab on Grade	1562
Roof	1599
Total Surface Area	23486
W/W ratio	65.67%

Table 7 Quantities of the building's components

6.2 Case Study Application

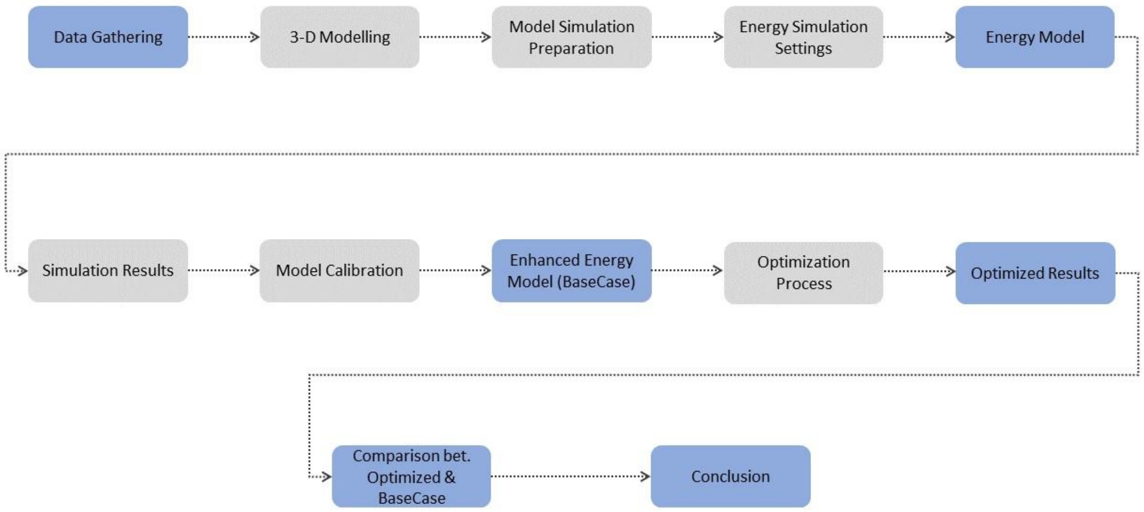

Figure 41 Methodology application scheme, 1

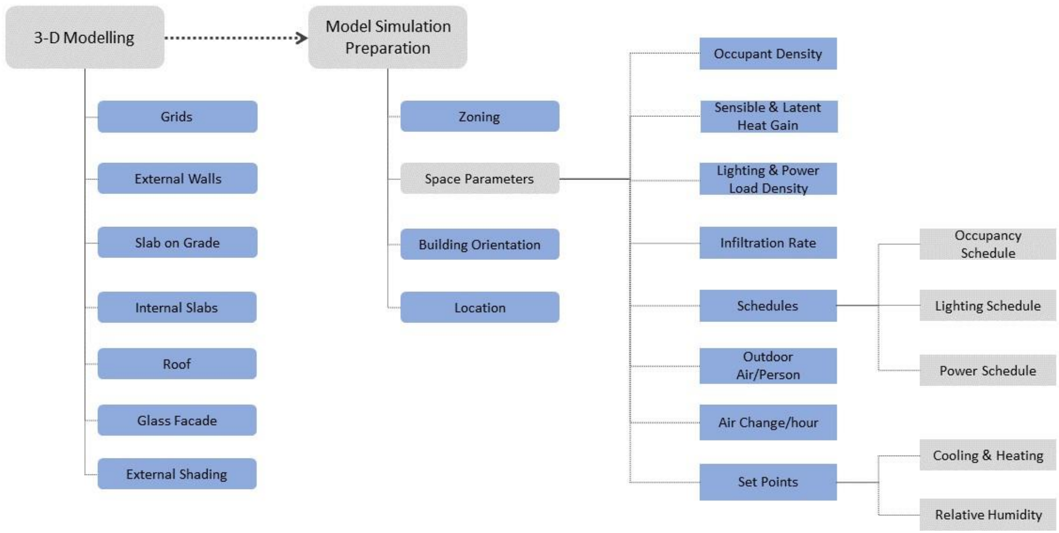

Figure 42 Methodology application scheme, 2

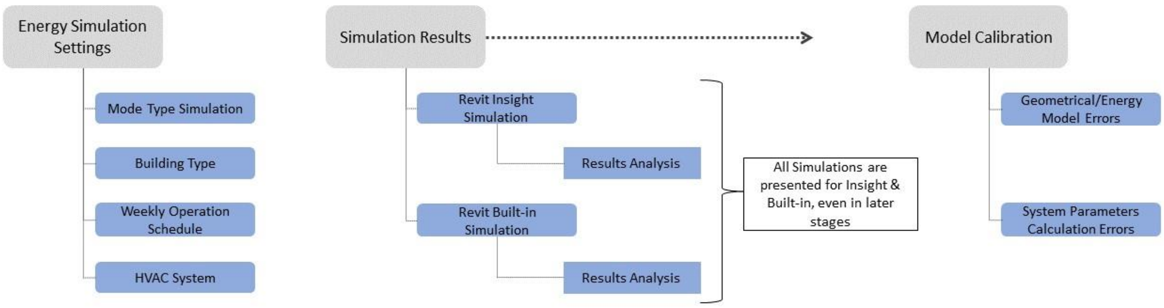

Figure 43 Methodology application scheme, 3

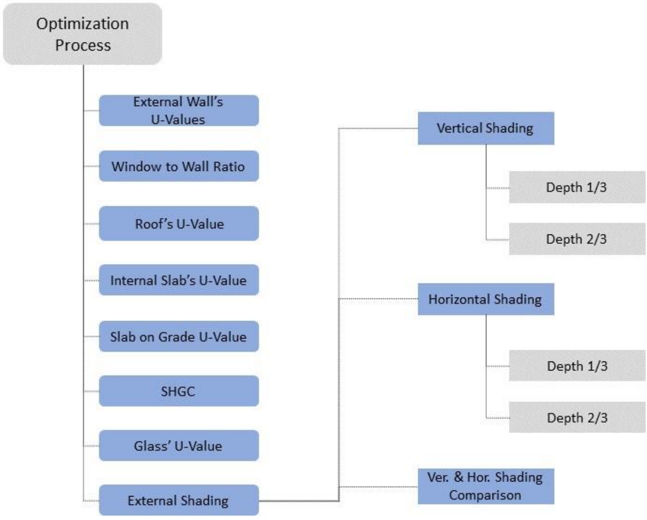

Figure 44 Methodology application scheme, 4

6.2.1 3-D Model

Before going forward with the case study application, it should be noted there are no official Egyptian guidelines in the Egyptian code to guide for energy efficient commercial building design, therefore, ASHRAE standards, are used in this case study for comparison and for determining some parameters such as, ventilation and internal gains recommendations, which will be discussed at a later stage. However, the first comparison was made between the envelope characteristics and ASHRAE Standards 90.1. According to the classifications in Table 8 Cairo lies in Zone 2B, which is a hot and dry region.

Location	Zone	Zone Characteristics
Miami	1A	very hot, humid
Houston	2A	hot, humid
Phoenix	2B	hot, dry
El Paso	3B	warm, dry
San Francisco	3C	warm, marine
Baltimore	4A	mild, humid
Albuquerque	4B	mild, dry
Salem	4C	mild, marine
Chicago	5A	cold, humid
Boise	5B	cold, dry
Burlington	6A	cold, humid
Helena	6B	cold, dry
Duluth	7	very cold
Fairbanks	8	subarctic

Table 8 ASHRAE climatic classifications (ANSI/ASHRAE Standard 90.1-2007)

In this section steps are discussed in order to build the 3-D model in Revit 2021 for the case study representation. Once the 3-D model is built, another set of steps must be applied to prepare the model for energy simulations.

Step 1: Placing the grids and levels in order to use it as a reference for constructing the envelope and internal spaces.

Step 2: The external walls were constructed, using customized wall family in Revit that reflect the desired thermal parameters. As Table 9 demonstrates the external wall composition has a value of 0.6 W/m²K for its thermal transmittance. It is worth noting that this value is within the threshold suggested by ASHRAE 90.1, see Table 36 in Annex section.

External Wall						
Nº	***Layers***	***Thickness (m)***	***Thermal Conductivity [λ] (W/mK)***	***Specific Heat Capacity [C] (J/gxC°)***	***Gross Density [ρ] (kg/m3)***	***Thermal Resistance [R] (m2K/W)***
Internal						
1	***Paint***	0.00003	-	-	-	-
2	***Plaster***	0.02	0.51	0.96	1120	0.039
3	***Cement Bricks***	0.23	1.3	0.84	1800	0.18
4	***Glass Wool (Mineral Wool)***	0.05	0.035	1.47	23	1.4
5	***Plaster***	0.02	0.51	0.96	1120	0.039
External						
Results						
Thickness Total (m)		0.32003				
Thermal Transmittance [U] (W/m2K)		0.6031				

Table 9 External walls, base case, thermal properties

Step 3: Salb on grade is constructed using customized slab family in Revit that reflect the desired thermal parameters. As Table 10 demonstrates the slab on grade composition has a value of 0.79 W/m²K for its thermal transmittance.

Slab on Grade						
Nº	***Layers***	***Thickness (m)***	***Thermal Conductivity [λ] (W/mK)***	***Specific Heat Capacity [C] (J/gxC°)***	***Gross Density [ρ] (kg/m3)***	***Thermal Resistance [R] (m2K/W)***
1	***Cement Screed***	0.02	1.046	0.657	2300	0.019
2	***Sand***	0.05	0.335	0.1	1600	0.15
3	***Rigid Insulation - EPS***	0.03	0.035	1.47	23	0.857
4	***RC-Concrete***	0.25	1.046	0.657	2300	0.239
Results						
Thickness Total (m)		0.35				
Thermal Transmittance [U] (W/m2K)		0.7905				

Table 10 Slab on Grade, base case, thermal properties

Step 4: Intermediate/internal slabs are constructed using customized slab family in Revit that reflect the desired thermal parameters. As Table 11 demonstrates the internal slabs composition have a value of 1.83 W/m²K for its thermal transmittance. It is worth noting that this value is greater than the threshold suggested by ASHRAE 90.1 which is 0.6 W/m²K, ASHRAE 90.1, see Table 36 in Annex section.

Internal Slab						
Nº	***Layers***	***Thickness (m)***	***Thermal Conductivity [λ] (W/mK)***	***Specific Heat Capacity [C] (J/gxC°)***	***Gross Density [ρ] (kg/m3)***	***Thermal Resistance [R] (m2K/W)***
1	***Cement Screed***	0.02	1.046	0.657	2300	0.01912
2	***Sand***	0.08	0.335	0.1	1600	0.24
3	***RC-Concrete***	0.3	1.046	0.657	2300	0.287
Results						
Thickness Total (m)			0.4			
Thermal Transmittance [U] (W/m2K)			1.8311			

Table 11 Internal slabs, base case, thermal properties

Step 5: Roofs are constructed using customized slab family in Revit that reflect the desired thermal parameters. In this model there is more than one roof, because there is the roof of the 6th floor and parts of the 5th floor have a roof as well. As Table 12 demonstrates the roofs composition have a value of 0.3 W/m²K for its thermal transmittance. It is worth noting that this value is greater than the threshold suggested by ASHRAE 90.1, see Table 36 in Annex section.

Roof						
Nº	***Layers***	***Thickness (m)***	***Thermal Conductivity [λ] (W/mK)***	***Specific Heat Capacity [C] (J/gxC°)***	***Gross Density [ρ] (kg/m3)***	***Thermal Resistance [R] (m2K/W)***
1	***Cement Screed***	0.03	1.046	0.657	2300	0.0287
2	***Sand***	0.05	0.335	0.1	1600	0.15
3	***EPDM Membrane***	0.003	0.138	2.09	930	0.00002
4	***Rigid Insulation - EPS***	0.1	0.035	1.47	23	2.86
5	***RC - Concrete***	0.3	1.046	0.657	2300	0.287
Results						
Thickness Total (m)			0.483			
Thermal Transmittance [U] (W/m2K)			0.3007			

Table 12 Roof, base case, thermal properties

Step 6: The glass panels of the curtain wall system are constructed using customized curtain wall family in Revit that reflect the desired analytical parameters. As Table 13 demonstrates the glass panels have value 0.9 for visual light transmittance, 0.15 m²K/W for thermal resistance, 86% for the solar heat gain coefficient and a value of 1.83 W/m²K for its thermal transmittance. It is worth noting that thermal transmittance and SHGC values are greater than the threshold suggested by ASHRAE 90.1 which are 4.26 W/m²K and 0.25 respectively, see Table 36 in Annex section.

Glass Panel Properties	
Visual Transmittance	0.9
Thermal Resistance [R] (m2K/W)	0.15
Solar Heat Gain Coefficient	0.86
Thermal Transmittance [U] (W/m2K)	6.7

Table 13 Glass panels, base case, thermal properties

Step 7: In this step the internal partitions were constructed using already available wall family in Revit. As Table 14 demonstrates the internal wall composition having a value of 8 W/m²K for its thermal transmittance.

Internal Partition						
Nº	***Layers***	***Thickness (m)***	***Thermal Conductivity [λ] (W/mK)***	***Specific Heat Capacity [C] (J/gxC°)***	***Gross Density [ρ] (kg/m3)***	***Thermal Resistance [R] (m2K/W)***
1	***Plaster***	0.0125	0.51	0.96	1120	0.0245
2	***Sand***	0.075	0.65	0.84	1100	0.1154
3	***Plaster***	0.0125	0.51	0.96	1120	0.0245
Results						
Thickness Total (m)			0.1			
Thermal Transmittance [U] (W/m2K)			6.0827			

Table 14 Internal partitions, base case, thermal properties

Step 8: In this step the external shadings were placed in location according to real project.

After completing all these 8 steps, see Fig. 45, the model is ready to be prepared to perform energy simulation.

Figure 45 Completed 3-D geometrical model

6.2.2 Building Simulation: Methodology

After building the 3-D model, it is necessary to determine some parameters related to the ventilation rates in breathing zones. ASHRAE Standard 62.1, see Table 38 in Annex, was used as guidance for calculating these values, for instance, outdoor airflow due to individuals inside the building, outdoor airflow in relation to the area and occupation density. These calculated parameters will be used to verify Revit's calculations at a later step. In the following, steps are demonstrated to prepare the 3-D model for energy simulation and to conduct simulation.

Step 1: Creating zones by defining spaces through the "Analyze" tab as indicated in Fig. 46. These zones are separated by each room's function. After that, it should be checked that the boundaries of the space are correctly defined, as shown in Fig. 47. The boundaries are specified between two internal partitions and the top of slab and the bottom of slab. Fig. 47 shows the plenum height is ignored, which means it will be considered in the energy simulation. Not specifying the plenum is due to simplifying the model, however, in reality, the plenum height is not taken within the volumes for heating and cooling.

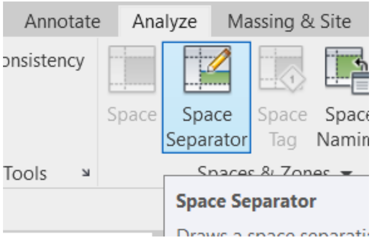

Figure 46 Zoning through spaces in Revit

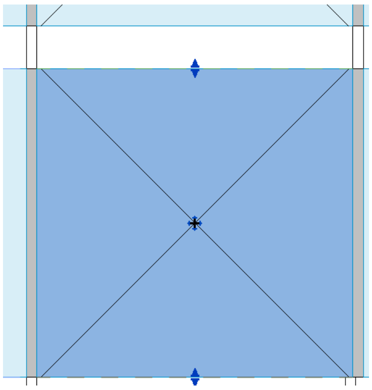

Figure 47 Zones Boundaries

Step 2: Mechanical parameters are defined at this step. When selecting the created zone space, it is possible to define the space type parameters according to the desired standards and values. First, the selected space is defined as "Occupiable", which defines the whole zone as occupied disregarding the plenum, as mentioned in Step 1. Then the desired "Condition Type" is selected, which is in this case chosen for ventilating, for heating and for cooling. After that, by clicking on the "Space Type", as indicated in Fig. 48, another window will open, as indicated in Fig. 49, which is an example of the applied parameters in offices zones. In this new window, the desired space parameters are set, in this thesis project ASHRAE Standards 62.1-2019 are applied. The "Area per Person" in Revit is related to the "Occupant Density" in ASHRAE.

Energy Analysis	
Zone	Default
Plenum	☐
Occupiable	☑
Condition Type	Heated and cooled
Space Type	AA_Office - Enclosed
Construction Type	<Building>
People	Edit...
Electrical Loads	Edit...
Outdoor Air Information	From Space Type
Outdoor Air per Person	2.50 L/s
Outdoor Air per Area	0.30 L/(s·m²)
Air Changes per Hour	0.000000
Outdoor Air Method	by People and by Area
Calculated Heating Load	1156.95 W

Figure 48 Energy configurations, Revit

Parameter	Value
Energy Analysis	
Area per Person	20.000 m²
Sensible Heat Gain per person	64.00 W
Latent Heat Gain per person	16.00 W
Lighting Load Density	11.00 W/m²
Power Load Density	16.00 W/m²
Infiltration Airflow per area	0.19 L/(s·m²)
Plenum Lighting Contribution	20.0000%
Occupancy Schedule	AA_Office
Lighting Schedule	AA_Office
Power Schedule	AA_Office
Outdoor Air per Person	2.50 L/s
Outdoor Air per Area	0.30 L/(s·m²)
Air Changes per Hour	0.000000
Outdoor Air Method	by People and by Area
Heating Set Point	21.11 °C
Cooling Set Point	26.00 °C
Humidification Set Point	0.0000%
Dehumidification Set Point	70.0000%

Figure 49 Energy simulations parameters

Area Function	Occupant Density AHSRAE	Area per Person (m^2) REVIT
Café	0.7	2
Breakrooms	0.5	2
Corridor	-	-
Eating Area	0.7	1.43
Kitchenette	0.2	5
Lobby	0.1	10
Office	0.05	20
Meeting Room	0.25	4
Reception	0.3	3.3
Stairs	-	-
WC	-	-

Table 15 ASHRAE 55-2010 conversion to Revit

Table 15 demonstrates the conversions applied from ASHRAE concerning occupant density and then set inside the different spaces in REVIT. It should be noted that some occupant densities were not associated directly with certain function types in ASHRAE 62.1 - 2019, because the space type "office" only has the following subcategories, which could be used for the simulations, namely, Breakrooms, that correspond to common areas, main entry lobbies, office areas and reception areas, as Table 38 in Annex demonstrate. This means that the rest of the spaces which exist in the project had to be estimated. Eating areas are estimated to have the same parameters as restaurant dining rooms under food and beverages services, as Table 38 in Annex demonstrates. Kitchenettes are estimated to have the same parameters as kitchen under food and beverages services, as Table 38 demonstrates, which is an overestimation because kitchenettes in office buildings are not used for cooking. Meeting rooms were compared with breakrooms, but the occupant density was divided by a factor of 2 to account for the space needed for desks, tables, and meeting room's appliances, which are not present in a breakroom. Finally, corridors, bathrooms and stairs have to occupant densities, as Table 38 demonstrates, which makes sense, because they are merely a transitional area or in the case of bathroom, one does not reside in.

Step 3: The following parameters to set are the sensible and latent heat gain per person, as Fig. 49 shows. ASHRAE Standard 55-2010, see Table 39 in Annex section, was used as guidance for obtaining these parameters. According to Table 39, different metabolic rates, in W/m², are reported for different office activities. The metabolic rates range from 55 W/m² to 120 W/m². An average value of 80 W/m² is used, which is a filing standing office activity. This value was chosen as well because it characterizes middle ground activities in the office, ranging from sitting, typing, and walking and for simplicity, the same metabolic rates are set for all zones in the building. These values are references for simulations, because in reality, these parameters are different for each individual and the temperature setting will have an impact on these metabolic rates.

However, in Revit, sensible heat gain and latent heat gain are set instead of the total metabolic rate and the rates are set in W instead of W/m². The correct way to go forward would be to calculate the number of people in the zone, multiply the metabolic rate obtained from ASHRAE 55-2010 and then divide the number of occupants by the total metabolic rate of the zone. However, for simplicity, the 80 W/m² metabolic rate were taken directly as 80 W.

The sensible heat produced by a person is primarily due to their metabolism and can be estimated based on the metabolic rate. As an approximation 80% of the metabolic rate is dedicated for sensible heat gain reporting 64 W, while 20% is dedicated for latent heat gain reporting 16 W, as Fig. 49 presents.

Step 4: Following sensible and latent heat gain determination, comes the determination of lighting load density and power load density, as Fig. 49 shows. The lighting load density is determined using the Building Area Method according to ASHRAE 90.1 – 2007. Table 37 in Annex section reports that an office has a lighting power density of 11 W/m².

Power load density for modern office environments is reflected in the range of 0.5 W/ft² to 1.5 W/ft² *(Chang, Roger, and Dury B Crawley, 2018)*,which translates into 5.4 W/m² to 16.1 W/m². Hence, to adopt the more conservative approach, 16.1 W/m² is chosen to represent the power load density.

Step 5: Infiltration rates depend on the building's components *(Gowri, K, et al, 2009)*. The infiltration rates of different components range between 0.12 cfm/ft² to 0.4 cfm/

ft², as Table 16 shows, which converts to 0.06 L/s x m² to 0.19 L/s x m². However, the base case is glass fenestration dominant, therefore, to be more conservative, the overall infiltration rate is chosen to be the maximum presented rate, which is 0.19 L/sxm².

Opaque Elements	Baseline Infiltration Rate (cfm/sf)	Baseline Infiltration Rate (L/s x m²)	Area calculation notes
Roofs	0.12	0.06	Net opaque area of roof
Above Grade Walls	0.12	0.06	Net opaque area of above grade walls
Below Grade Walls	-	-	*Not used in infiltration calculations*
Floor	0.12	0.06	Net opaque area of floor over unconditioned space
Slab	-	-	*Not used in infiltration calculations*
Opaque Doors	0.40	0.19	Area of opaque doors
Loading Dock Doors	0.40	0.19	Area of door, applicable only for warehouses
Fenestration Elements			
Swinging or Revolving Glass Doors	1.00	0.47	Area of swinging or revolving glass doors
Vestibule	1.00	0.47	Area of door
Sliding Glass Doors	0.40	0.19	Area of sliding glass doors
Windows	0.40	0.19	Area of windows
Skylights	0.40	0.19	Area of skylights

Table 16 Infiltration rate according to envelope elements (Gowri, K, et al, 2009)

Step 6: In this step, the plenum lighting contribution is set at 20%.

Step 7: In this step, operating schedules are defined. By clicking on the "Occupancy Schedule", see Fig. 49, another window will open to define the desired schedule. Defining occupancy schedules are a very subjective matter, depending on the nature of the office and working culture, plus it will never be completely true. However, and estimation was conducted for different rooms and spaces, taking into account the general office behavior in Egypt, a general contractor office, and general café's operating hours. The occupancy schedules are defined as follows:

Fig. 50 demonstrates the estimated customers' traffic of a regular café. Night life in Egypt is very popular, therefore cafes usually are open until 2 o'clock, with less costumers traffic. In the next morning costumers arrive as well, with small traffic starting from 6 o'clock until 9 o'clock. After that the cafes start filling up with customers until 14 o'clock, this is the first half of the day. The second busy half starts at 18 o'clock and continues until 23 o'clock. It should be noted that the cafes in the ground are separated from the rest of the building, which serves as offices.

Fig. 51 demonstrates the estimated occupant's behavior in an office in Egypt. From 6 o'clock workers start progressively arriving at the office. At 9 o'clock most workers are already present. Between 11 and 12 o'clock, they have their lunch break. After that work continues normally until 18 o'clock, then workers start to leave the building. However, there are always people remaining in the office due to submissions and deadlines, until approximately 22 o'clock.

Fig. 52 demonstrates the estimated meeting rooms behavior in an office, which reaches its peak between the hours of 11 and 12 o'clock. This is because the busiest time in an office is right before lunchtime and after lunchtime, which is at 15 and 16 o'clock.

Fig. 53 demonstrates the estimated occupancy for an eating area in an office, which indicates that the busiest occupancy happens during lunch time between 13 and 14 o'clock. In the early morning people might have breakfast and in the late afternoon they might have a snack, especially if those individuals are working late at night.

Fig. 54 demonstrates the kitchenette's occupancy behavior. It is similar to the eating area occupancy schedule because both are related. However, traffic in the kitchenette starts earlier, because workers go there for tea and coffee as well, which starts in the early morning.

As for the lobbies and reception areas, its behavior is shown in Fig. 55, if guests or visitors or subcontractors in the case of a general contractor office, are coming, they will come a little but later after the office's opening hours, therefore, the traffic in these areas start at 8 o'clock and it remains almost constant until closing time.

Fig. 56 shows that the common area starts having traffic after the first two hours from the office's opening, because workers would enjoy break time. The traffic increases incrementally until before the eating break time, because after that, workers switch to eating areas and kitchenette. The occupancy increases again in the late afternoon until 19 o'clock, for the workers who stay late to rest before continuing work.

Fig. 57 demonstrates the occupancy behavior of vertical transition areas. By default, the traffic will start with the building's opening. It will remain constant throughout the day until the whole occupancy of the building is reduced in the late afternoon, it will decrease as well until the building closes.

Fig. 58 reports the corridors occupancy behavior. The behavior here is similar to the elevators and stairs' behavior, they are both linked by being a transitional space. However, the occupancy of corridors is higher and has a peak during lunch break time because workers are frequently moving around the same floor for different purposes, such as, work collaborating or going to the bathroom.

Finally, Fig. 59 shows the occupancy behavior of the bathrooms, which is constant throughout the day from opening hours until closing hours.

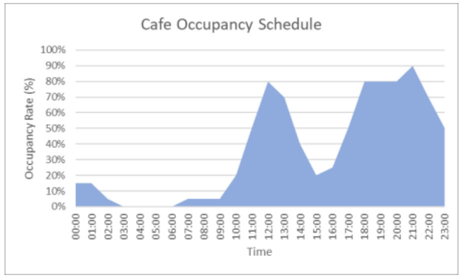

Figure 50 Café occupancy schedule

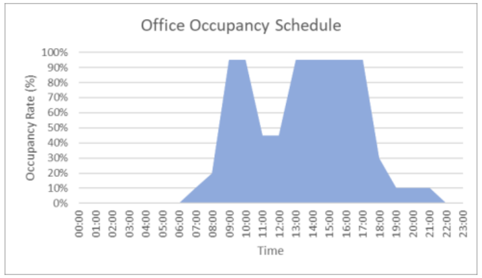

Figure 51 Office occupancy schedule

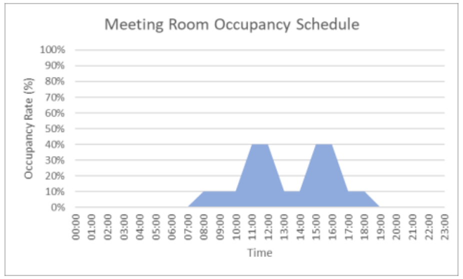

Figure 52 Meeting rooms occupancy schedule

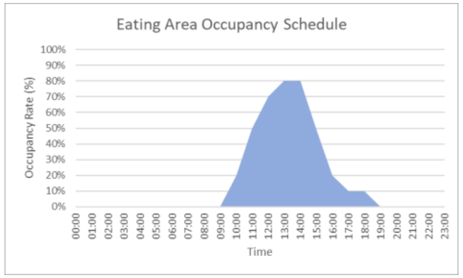

Figure 53 Eating area occupancy schedule

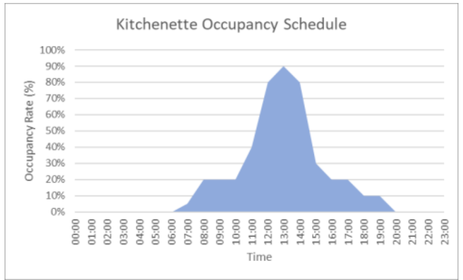

Figure 54 Kitchenette's occupancy schedule

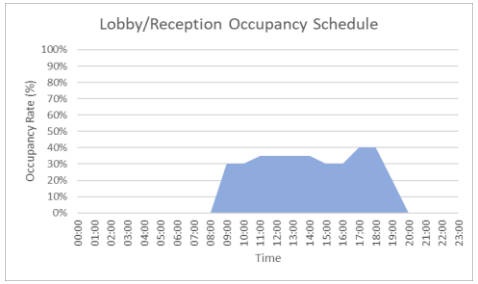

Figure 55 Lobby & reception occupancy schedule

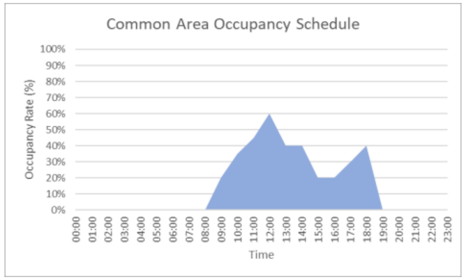

Figure 56 Common area occupancy schedule

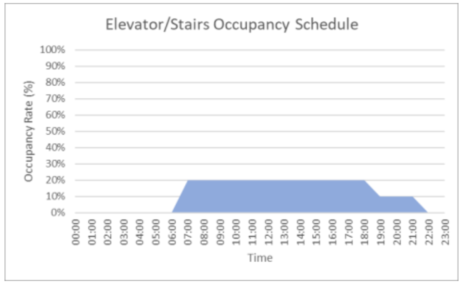

Figure 57 Vertical transition areas occupancy schedule

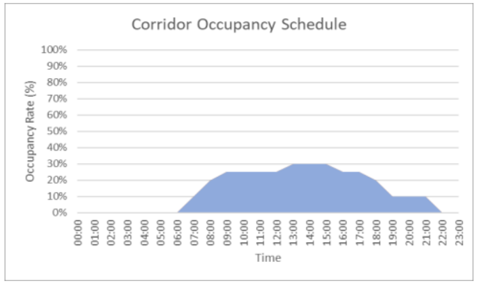

Figure 58 Corridor occupancy schedule

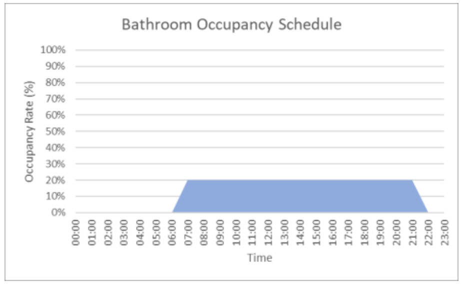

Figure 59 Bathroom occupancy schedule

Step 8: After configuring schedules occupancy schedules for the different zones, the same steps are applied to define lighting schedule and power schedule, see Fig. 49. For simplicity all three schedules, namely, occupancy, lighting and power schedules will have the same identical operating schedules, which were customized and defined in step 7.

Step 9: Next the outdoor air per person and outdoor air per area, shown in Fig. 49, are defined. These parameters are defined according to ASHRAE 62.1 – 2019, see Table 38. According to these standards, each zone has its specific air requirements. These requirements are summarized in Table 17.

Area Function	***Outdoor Air per Person (L/s)***	***Outdoor Air per Area ($L/(s*m^2)$)***
Café	3.8	0.9
Breakrooms	2.5	0.6
Corridor	-	0.3
Eating Area	3.8	0.6
Kitchenette	3.8	0.6
Lobby	2.5	0.3
Office	2.5	0.3
Meeting Room	2.5	0.3
Reception	2.5	0.3
Stairs	-	0.3
WC	-	0.3

Table 17 Summery air rates due to people & area according to ASHRAE

Step 10: Following the outdoor air areas, the air change per hour is defined according to Fig. 49. The outdoor air rate for people or area and air changes per hour are related concepts in the context of ventilation in buildings. The outdoor air rate for people or area is a specific ventilation strategy which provides a targeted measure of the amount of outdoor air supplied to a space based on the number of occupants or the floor area. On the other hand, the air change per hour provides a more holistic measure of the overall ventilation effectiveness by indicating how many times the entire volume of air in a space is replaced with outdoor air in one hour. The air change per hour accesses the systems to dilute indoor pollutants and maintain acceptable indoor air quality. According to ASHRAE Handbook 2020 for Heating, Ventilating and Air -Conditioning

Systems and Equipment *(ASHRAE Handbook, 2020)* the air change per hour for an office range between 6 and 8 times. However, as Fig. 49 demonstrates, the air change per hour parameter is not considered in the simulations, to reduce the number of parameters considered and to simplify the calculations.

Step 11: In this step, the outdoor air calculation method is chosen. The method chosen method is by people and by area, to take into consideration both parameters which affect the zone. By choosing this method as well it is made sure that the air change per hour rate is ignored, even if a value is placed for this parameter.

Step 12: Here the set point for heating and cooling is set at 21 C° and 26 C° respectively, which means that the HCAV system will be activated for heating or cooling when these thresholds are surpassed. It is assumed in this research that these setpoints guarantee internal thermal comfort.

Step 13: According to ASHRAE 55-2010 there are no established lower humidity limits for thermal comfort; consequently, Standard 55 does not specify a minimum humidity level. Therefore, for the simplicity of the simulation, the humidification set point is not considered. However, according to ASHRAE 62.1 – 2019 it is required that relative humidity levels be limited to 65% or less, hence, dehumidification setpoint for 65% is set as Fig. 49 demonstrates.

The previous steps were explaining the parameters setting up for the model in order to do energy simulations. Until now the 3-D model and setting up parameters were discussed. In the following, final steps will be explained to prepare the model for energy simulations.

Step 14: At this stage the model is oriented in the same orientation as the real building in Cairo, to ensure that the conducted simulation is as accurate as possible to reality, since this first simulation will serve as a baseline reference for the coming energy optimizations.

Step 15: In this step the model is placed in the correct location by clicking on the location inside the Analyze tab, in Energy Optimization section in Revit and then specifying the location. As Fig. 60 demonstrates, the location is set in Cairo. By specifying this location, the simulation will consider the weather data, such as monthly average temperatures and annual wind speed, obtained from Cairo International Airport, which is the closest weather station to the building's location.

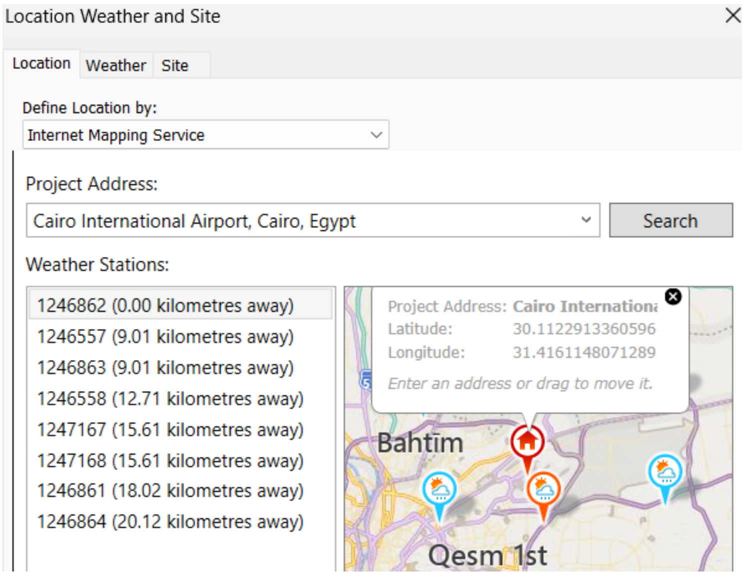

Figure 60 Location defining in Revit

Step 16: Next will be to specify the energy settings for the whole building. This is achieved by clicking on the "Energy Settings" from the "Analyze" tab in the "Energy Optimization" section. Once clicking on the "Energy Settings", a window will open as indicated in Fig. 61. The most important setting to control is the "Mode". The "Mode" is set on "Use Building Elements". There are two other options, which are, "Use Conceptual Masses" or both modes combined. The choice is using "Building Elements" because the model contains accurate theraml characteristics, which are specified in the costumized Revit families as explained from Step 2 to Step 7 in section 5.2.1.

After specifying the mode in the energy analytical model, further specifications are applied by clicking on "Other Options" under "Advanced" as Fig. 61 shows. When clicking on the "Other Options" another window will open as shown in Fig. 62. Under "Building Data" the overall general "Building Type" is selected as an "Office". After that, the "Building Operating Schedule" is chosen as "Default", which means that the building is operating 5 days per week. Following, the "HVAC System" is chosen as a central VAV HVAC system, that uses hot water for heating, chiller for cooling with a

COP 5.96 and an overal boiler's efficiency of 84.5%. Next, the "Export Category" is chosen as "Spaces", to enable Revit to recognize all the parametrs that were set from Step 2 to Step 13 in the simulation steps section. Finally, the "Conceptual Types" and "Schematic Type" under "Material Thermal Properties" are ignored, because "Detailed Elements" are checked, which means the "Use of Building Elements" are used as a refernce for the simulation, as shown in Fig. 61 and Fig. 62.

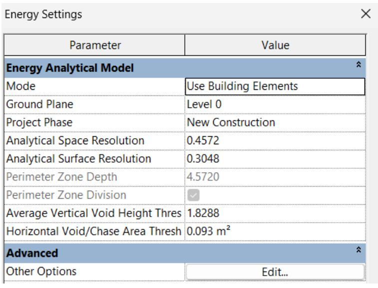

Figure 61 Energy settings defining

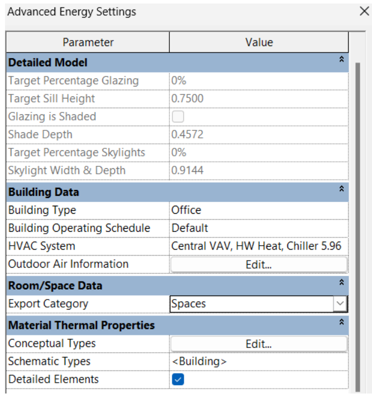

Figure 62 Advanced energy settings defining

Step 17: Now the model is almost ready to conduct energy simulation. As a final step the energy model is created by clicking "Create Energy Model" under the "Analyze" tab in the "Energy Optimization" section. Once clicking on "Create Energy Model" the energy model is created as shown in Fig. 63.

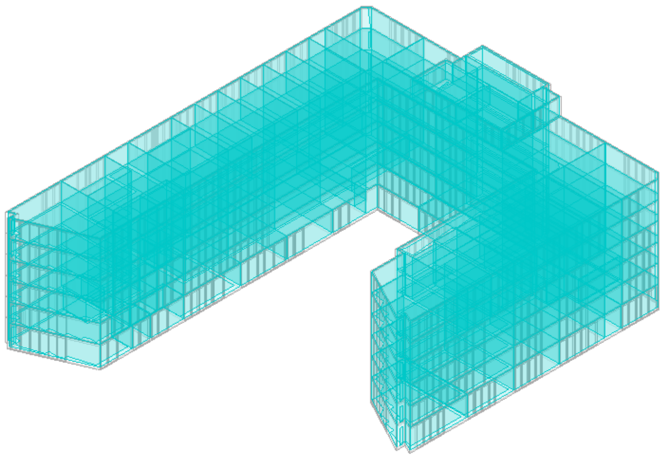

Figure 63 Energy model created in Revit

Before explaining the results in the following section, it is important to categorize the variables and parameters used in order to conduct energy simulation. There are two main categories, namely constant variables, and changeable variables, which are listed below.

Constant variables through all defined zones:

- Lighting load density
- Power load density
- Sensible heat gain per person
- Latent heat gain per person
- Infiltration airflow per area
- Plenum lighting contribution
- Air change per hours
- Outdoor air method
- Heating set point
- Cooling set point
- Humidification set point
- Dehumidification set point
- Simulation throughout the whole year

Changeable variables according to zone's function:

- Area per person, occupant density
- Occupancy schedule
- Lighting schedule
- Power schedule
- Outdoor area per person
- Outdoor area per area

7. Simulation Results

After the energy model is generated, the energy simulation is conducted with two methods with Revit. The first method is to upload the model on the cloud, by clicking on "Generate" under the "Analyze" tab in the "Optimization" section, to use Revit Insight for energy simulation. The second method is to use Revit built-in energy simulation function, by clicking on "System Analysis" and choosing "Annual Building Energy Simulation" under the "Analyze" tab in the "Optimization" section.

Results from both methods will be presented and explained, to reach a conclusion on which method to go forward with in the energy optimization process.

7.1 Revit Insight Simulation

Revit Insight is a cloud-based software tool that is designed to perform energy analysis and simulations for building designs. It allows to evaluate the energy performance and environmental impact of a building. Many metricizes are included in the simulation, such as, energy analysis to determine. It takes into account environmental metrics to calculate for example the carbon emissions. It considers the local climate conditions and performs daylight analysis. Revit Insight provides many more analysis and it gives suggestions on how to make the building more energy efficient, for example, with just one model it gives results for different energy consumption for different scenarios, such as listed in the following:

- different orientations
- different window to wall ratios (WWR)for each façade
- different external shades for each façade
- different glass type for each façade
- different wall constructions
- different roof constructions,
- different infiltration values
- different lighting efficiencies
- Different PV-Panel efficiencies
- PV-Panel payback limit
- PV-Panel surface coverage

Basically, Revit Insight needs a complete and accurate 3-D model, with all its parameters included, to be uploaded for simulations. It runs the simulations, and it gives a value for a chosen metric to be presented, in this case, the Energy Use Intensity (EUI) is used to present the results. This presented EUI value is a mean value, which mean there is a maximum and minimum value.

7.1.1 Revit Insight Simulation Results

The results of the energy simulation conducted on the 3-D model report 223 kWh/m^2/year as shown in Fig. 64. After uploading the model for simulation in Revit Insight, the EUI value is given as a mean, see Fig. 65, which means the result does not represent the actual energy consumption of the building. Therefore, before taking the result directly, opening the tabs of different parameters, and adjusting the blue ribbon at the bottom to cover only the correct parameter value is vital, see Fig. 66.

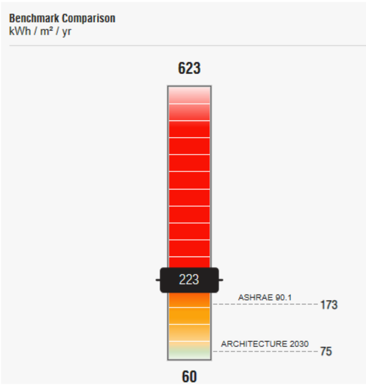

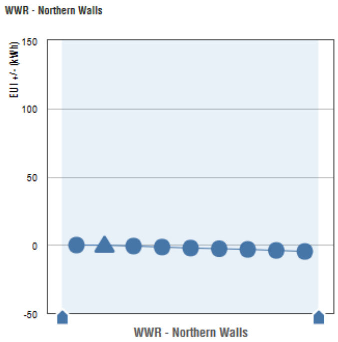

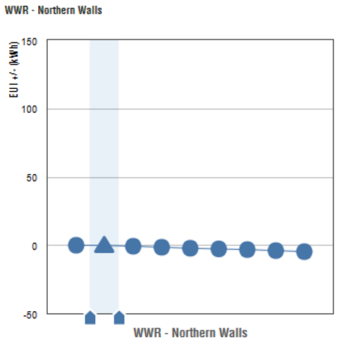

Figure 64 Simulation result *Figure 65 Mean results values* *Figure 66 Specific results values*

The EUI value is a considerably high energy consumption. This high energy demand is due to the fact that many of the building's components do not respect the thresholds for different thermal properties suggested by ASHRAE 90.1. However, it is assumed that the greatest factor explaining this high demand is the solar radiation filtration through the curtain wall, because the WWR is extremely high, and the glass properties are very low.

In order to understand better the results of the base case energy simulation, more experiments are conducted with creating 9 different models with different values for external wall's thermal transmittance. The base case has a value of 0.6 W/m²K, therefore, models with thermal transmittance from 0.1 W/m²K to 0.85 W/m²K were built and uploaded to conduct energy simulations in Revit Insight.

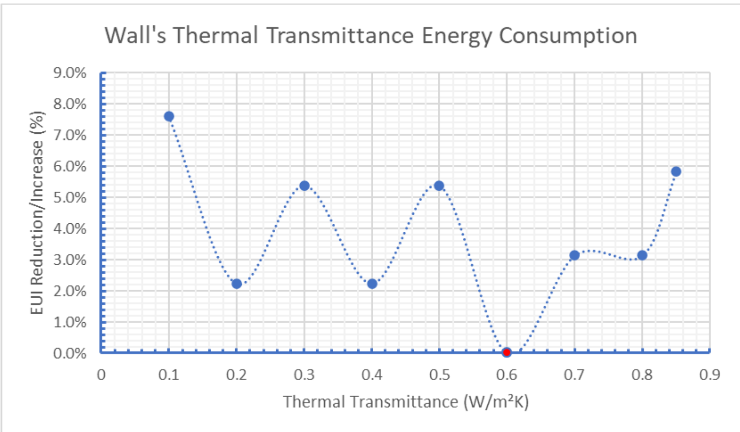

Figure 67 Energy consumption difference with different thermal transmittance values, Revit Insight

In this experimental set of simulations, the results were compared with the base case. The result of the base case is highlighted in red, as Fig. 67 demonstrates. Until this point the validity of the simulation is not concluded, however, the trend in Fig. 67 is odd, because according to the behavior in the graph, the higher the value of the thermal transmittance, the less energy it consumes. This statement is fundamentally wrong, since, as explained in the literature review section, the lower the thermal transmittance value, the less energy would the building consume, because the heat transfer from the external environment to the internal environment is reduced, in hot climates. In addition to that, the trend itself is very inconsistent, making it almost impossible to take readings from.

In order to verify the results of the 3-D model and understand the tool used better, further experiments are conducted with one 3-D model while changing the parameters in Revit Insight. The set of experiments concern the WWR parameter in this section. Fig. 66 shows the current building's results with the given WWR in the northern façade, which is 94%. Fig. 66 shows the ability of Revit Insight to simulate different parameters with the same model simply by clicking and dragging the blue ribbons in the x-axis, for example having 0% WWR. When changing the WWR in the northern façade to have a 0%, by dragging the 2 blue ribbon to 0%, it will have a reduction in EUI with the value of 5 kWh/m²/year. Adopting this technique, the behavior of the different facades is analyzed with the different WWRs.

Fig. 68 shows the results obtained by using the technique of analyzing the impact of different WWR for different facades with the same model in Revit Insight. It should be noted that each façade is analyzed separately, for example, changing the WWR for the northern façade to be 40%, while maintaining the same ratio of WWR for the other 3 facades, WWR of south façade remains 4%, west facades remain 79%, and east façade remain 75% as the original model, the base case, as Table 18 shows. Table 18 shows the energy consumption of the building with different WWRs.

Façade Orientation	Window to Wall Ratio
South	4%
North	92%
West	79%
East	75%
Total	65%

Table 18 Different WWR for different facades in base case

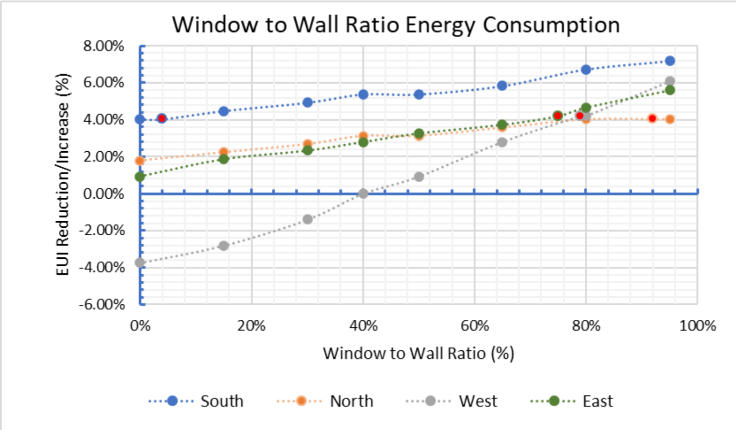

Figure 68 WWR energy consumptions for different facades, conducted with one model in Revit Insight

The general trend observed by Fig. 68 is that the lower the value of WWR, the less energy is consumed by the building, which is logical and aligned with the research conducted. It is observed that different WWR in the western façade has the most impact for energy consumption, since the difference in energy consumption between the highest and lowest WWR values is 10%.

As indicated earlier, the values in Fig. 68 are all obtained by only one single model uploaded into Revit Insight. Therefore, as an extra check for the WWR presented in Fig. 68, the 3-D model was updated to have actual different WWR, in order to upload these models and check the Values obtained by one single model. WWR values of 0% and 40% were chosen to run these set of simulations, meaning that 8 different models were created and uploaded to Revit Insight.

Façade Orientation	EUI (kWh/m²/yr) - Actual Model	EUI (kWh/m²/yr) - One Model
0% South	225	223
0% North	213	218
0%West	215	206
0%East	217	216

Table 19 EUI values obtained with several model compared with values obtained from one model, 0% WWR

Façade Orientation	EUI (kWh/m²/yr) - Actual Model	EUI (kWh/m²/yr) - One Model
40% South	227	226
40% North	218	221
40%West	216	216
40%East	222	221

Table 20 EUI values obtained with several model compared with values obtained from one model, 40% WWR

Table 19 and 20 demonstrate the values obtained for the 8 updated models, 4 different models for 0% WWR in different facades, and 4 models for 40% WWR in different facades. In these two figures the corresponding EUI values obtained from one single model, are reported for comparison.

It is evident that simulating with one model is not accurate, because when models were created that contain the actual simulated parameters, they obtained different results. Most of the actual models report higher energy consumption compared to the values obtained with one model.

Furthermore, Fig. 69 demonstrates another observation, which is that not always Revit Insight recognizes the parameters of WWR correctly. In this case, the WWR is 40%, whereas it is recognized as 54%.

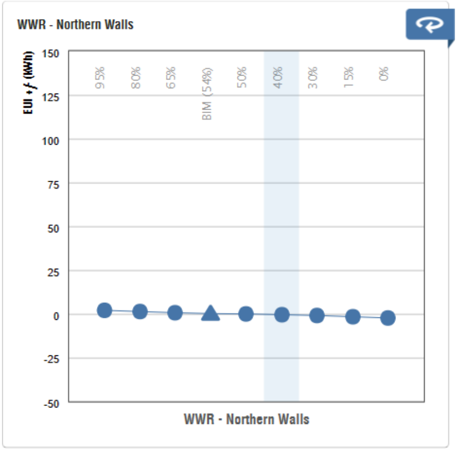

Figure 69 WWR wrongly recognized by Revit Insight

As a conclusion, until now, the model is not validated for conducting energy simulations.

7.2 Revit Built-in Energy Simulation Results

According to Autodesk Revit webpage, this is how Revit built-in energy simulation functions, "after analytical spaces are assigned, you can run a systems analysis. Revit uses a workflow to run the analysis. A workflow is a script that takes data from Revit, translates it to EnergyPlus, runs a simulation, and creates a report for design heating, cooling, and airflow." There are many differences between conducting simulations with Revit Insight and Revit built-in simulation function. With the built-in simulation function, a new model must be created when changing any parameter, the possibility of conducting all simulations with one model is not possible. Secondly, it gives results in yearly consumption, not as EUI parameter. However, the built-in energy simulation gives a breakdown for the energy consumption, which is needed to understand where the energy is being consumed, for example, with the built-in function, one can observe whether heating or cooling loads are dominant.

The Base case model reported 22283451 kWh/year, when simulated with Revit Built-in function, which is considered an extremely high energy consumption for this building, considering its total area, which does not exceed 19600 m².

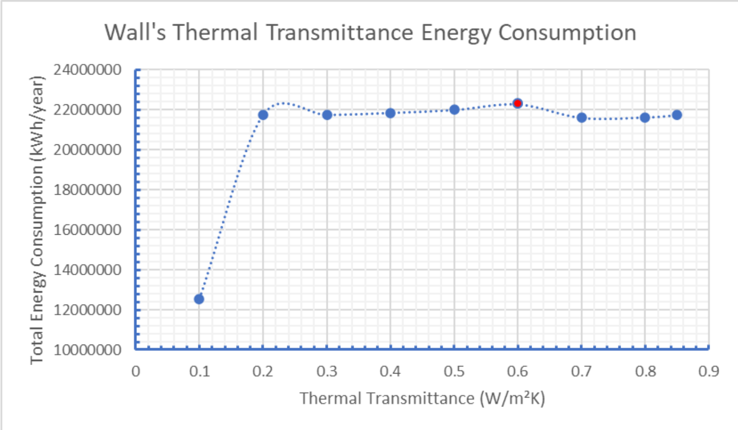

Figure 70 Energy consumption difference with different thermal transmittance values, Revit built-in function

Fig. 70 demonstrates the energy consumption due to different thermal transmittance for the external walls. As indicated before, the built-in function provides consumption values in kWh/year, therefore, the results are presented accordingly. It should be noted that these models had the original WWR for the different facades. The trend in this graph indicates that different thermal transmittance for external walls have minimal impact on the energy consumption. However, from 0.1 W/m²K to 0.6 W/m²K the energy consumption is slightly decreased, which is aligned with a building having a tighter envelope is performing better form the energy perspective.

Façade Orientation	0% WWR	40%WWR
South	18,957,103	19,446,364
North	18,806,247	18,938,650
West	17,916,375	19,039,184
East	18,683,269	18,683,269

Table 21 Energy consumption comparison between 0% WWR & 40% WWR, Revit built-in

Table 21 reports the energy consumption with 2 different WWRs. It should be noted that similar to the glazing ratios experiments conducted in the Revit Insight section, only one façade is updated to have the reported WWR while the other 3 facades maintain the original WWR, as indicated in Table 18. It is very clear in Table 21 that energy consumption increases when the WWR increases as well. The energy consumption reported by this method, Revit built-in, is extremely high.

0%WWR Energy Breakdown		
Cooling	18,460,908 kWh/Year	97.38%
Heating	15,617 kWh/year	0.08%
Int. Light	245,817 kWh/year	1.37%
Int. Equipment	234,761 kWh/year	1.25%

Table 22 0% WWR Energy breakdown

Table 22 reports the energy breakdown of the 0% WWR model. It is evident that the cooling demand is by far the dominant load responsible for the energy consumption, which exceeds 95% of the total energy demand, while heating demand is almost non-existent.

40%WWR Energy Breakdown		
Cooling	18,956,053 kWh/year	97.48%
Heating	9,750 kWh/year	0.05%
Int. Light	234,753 kWh/year	1.23%
Int. Equipment	245,808 kWh/year	1.30%

Table 23 40% WWR Energy breakdown

Table 23 reports the energy breakdown of the 40 % WWR model. The energy breakdown indicates that the energy consumptions are almost identical to Table 23, with the exception in heating, which is decreased. This makes sense, since when the WWR increases in a building in a hot climate, more solar radiation penetrates the envelope, hence, more natural heating occurs during winter and consequently less heating loads are needed.

7.3 Conclusion

Experiments were conducted with Revit Insight and Revit Built-in simulation function. It should be noted that results obtained from both simulation methods are not compared with each other at this stage, because both methods provide different types of results. Moreover, the goal at this point is to validate the model for conducting simulations. Later on, the optimization work of method will be explicitly explained.

Revit Insight reported unexpected results, in terms of the behavior and trend itself, throughout the experiments. Different thermal transmittance shows inconsistent behavior for the energy consumption, and the trend can be described that smaller, inefficient values of envelope's thermal transmittance are responsible for more energy consumption, which is not true. The values of different WWR obtained by one model in Revit Insight support the theory that more glazed components in the external envelope are responsible for more energy consumption. However, the obtained values do not correlate to the values obtained by simulations conducted on the different model, trying to validate the values obtained by one single model. Furthermore, it was observed, that there some parameters are wrongly by Revit Insight and the energy consumption values sometimes change when closing and reopening the browser.

Revit built-in function seems more reliable. The different thermal transmittance values report a behavior which is not totally wrong, because the trend can be described that smaller, efficient values of thermal transmittance are responsible for reduced energy consumption. The WWR analysis supports as well as that less glazed components in the envelope are slightly responsible for reduced energy consumption. However, it should be noted that the energy consumption reported by the built-in function is extremely high.

Until this point, it is concluded that both methods for simulation are not reliable for conducting optimization analysis for the case study building, therefore, the model will be calibrated and then the optimization analysis will continue.

7.4 3-D Model Calibration

After a thorough investigation to the 3-D Model, mechanical parameters and its associated energy model, some discrepancies were discovered. Fig. 71 displays a better representation of the energy model, and with model many geometrical discrepancies were discovered. To transform the energy model into analytical surfaces model, the "Visibility Graphics" in the energy model view is opened, and the "Analytical Model Categories" tab is chosen. After that, a list will open, in which the |Analytical Spaces" are turned off and the "Analytical Surfaces" are turned on.

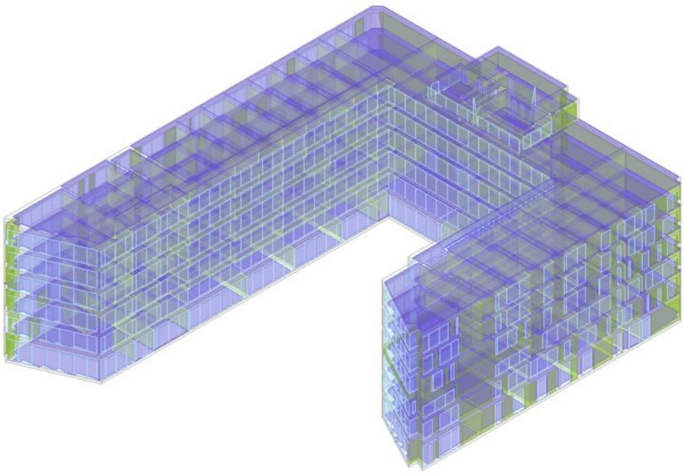

Figure 71 Analytical surfaces model

The analytical surfaces model categorizes different surface types with different colors, hence, a clear distinction between building's components is made visible.

Error 1. The first base case model that was created and used so far is correct, but only in terms of architectural model representation, for example, the external walls are supported by the underlaying slab, which is correct, but this will not be correctly translated into the energy model, because in this way the external envelope is not continues. The slab that is placed in the energy model is after all just represented as a single surface plane, ignoring the slab's thickness, which in turn creates an unjustified void in the project between different levels as Fig. 72 depicts.

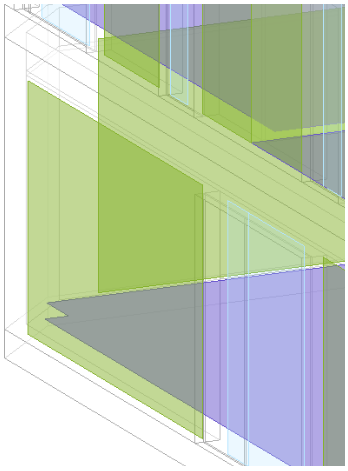

Figure 72 Analytical surfaces model showing discontinuous external walls

Error 2. Another error that was detected was the representation of curtain wall system in the energy model. The curtain wall system is imbedded in the external walls, and according to the base case many envelope parts have continuous vertical curtain wall system through different floors. However, the slab thickness and plenum hight are spandrel panels. It is difficult to split the wall into multiple layers and assign the correct construction properties that the energy model would recognize as spandrel panels, nevertheless, in reality these spandrel panels are not transparent. To simplify the model and reduce the number of parameters, the hight of the curtain wall was reduced up to the plenum height level. This is translated into having opaque wall over the curtain walls in each floor. After taking a close look on the analytical surfaces model it is discovered that the opaque wall above the curtain wall system is not recognized, as Fig. 73 indicates.

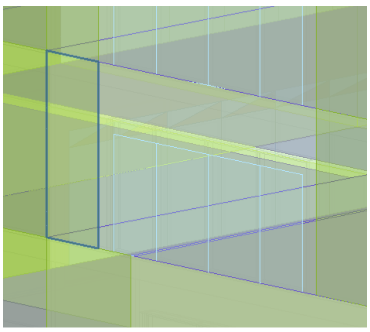

Figure 73 Analytical surfaces model only recognizes walls next to curtain walls and not wall portion above the curtain wall

Error 3. Furthermore, in the simulated model, the wall in different floors were not aligned and stacked on the same line, as Fig. 74 highlights, which means that the unstacked walls create another unjustified void through the external envelope.

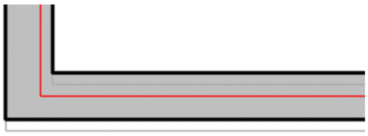

Figure 74 Underlaying external wall not stacked aligned with current floor's walls

The mechanical parameters had to be checked at this point, and one of the most important parameters to be checked is the outdoor supply air rate calculated by Revit when conducting energy simulations.

Table 24 below is an example of the calculated outdoor air supply according to ASHRAE 62.1 – 2019 only for the 6th floor, the calculations of the other floors are presented in Annex, from Table 40 to Table 45. These calculations are related to Step 2 in section 5.2.2, but here it is calculated manually.

First, calculating the outdoor supply air rate due to occupants is calculated. This is obtained by using the occupant density suggested by ASHRAE 62.1 according to space function then multiplying it by the room's area. This way the total number of occupants in the room is calculated. Next the total number of occupants will be multiplied by the outdoor air rate / person (L/s x person), to reach the desired calculated value of outdoor supplied air rate due to occupants.

Calculating the outdoor supply air due to area is calculated by multiplying the area of the room by the outdoor supply air / area (L/s*m^2). This way the total outdoor supply air due to area is calculated.

Finally, the calculated total outdoor supply air due to occupants is added to the total outdoor supply air due to area, this way the total supply air due to occupants and surface area is obtained.

Facility	Area (m^2)	Occupant Density (-)	Total Occupants	People Outdoor Air Rate/Person (L/(s*person))	Total People Outdoor Air Rate (L/s) due Occupants	Area Outdoor Air Rate/Area (L/(s*m^2))	Total Area Outdoor Air Rate (L/s) due Area	Total Outdoor Air Rate (L/s)
Meeting R.19	41.00	0.25	10.25	2.50	25.63	0.30	12.30	37.93
Meeting R.20	41.00	0.25	10.25	2.50	25.63	0.30	12.30	37.93
Corridor 8	28.00	-	-	-	-	0.30	8.40	8.40
Stairs 12	31.00	-	-	-	-	0.30	9.30	9.30
WC 15	13.00	-	-	-	-	0.30	3.90	3.90

Table 24 Calculated total outdoor air flow rate, sixth floor

Error 4. After obtaining the total outdoor air flow rate for each zone, the calculated value is compared with same parameter calculated by Revit. Fig. 75 shows the calculated mechanical parameters, which are the greyed-out values, after conducting the energy simulation with Revit built-in function. It should be noted that only the outdoor airflow is calculated when conducting energy simulations, the calculated supply airflow is calculated after generating load reports to calculate peak cooling and heating loads, which was conducted on the model in earlier stages to understand Revit tool better.

However, returning to the calculated outdoor airflow by Revit, Fig. 75 indicates a value of 202.48 L/s, whereas the manually calculated total airflow, as indicated in Table 24 for meeting room 19 is 37.93. This indicates that there are probably some parameters wrongly reported, which was done in from Step 2 to Step 13 in section 5.2.2.

Figure 75 Mechanical flow in Revit, meeting room 19

Error 5. This error is related to Error 4, because the wrongly calculated outdoor supply airflow by Revit means that the parameters, in Fig. 49, must be checked in all zones, represented in all customized spaces. When the parameters for many zones were checked, some zones had wrongly reported parameters, such as, incorrect "Area per Person", incorrect values of heat gains, incorrect "Outdoor Air per Person or per Area" and wrongly assigned "Outdoor Air Method", because some zones were specified for the outdoor calculation method to be calculated by the air change per hour method, which of course increases the total outdoor airflow rate significantly.

As a result, another model is built to rectify the detected errors translated through the architectural model, even though, this new model would not be considered correctly from the real perspective. In the new base case model, the external walls were constructed continuously from one level to another, ignoring the slab thickness, which results in a continues external envelope, as Fig. 76 shows. Furthermore, the external walls of different levels were built in an identical time through each floor to make sure they are stacked, which means that they must lie exactly on the same position, in order not to create another error.

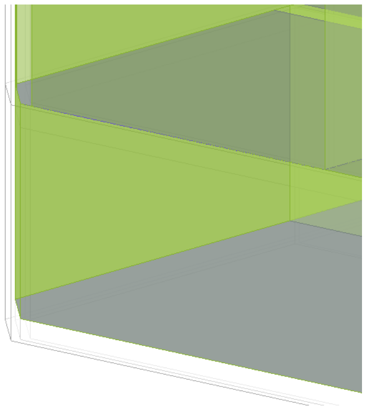

Figure 76 Analytical surfaces model showing continuous external walls

In order to rectify Error 2, the curtain wall was replaced with fixed windows, while maintaining the same glass properties. With this family replacement, the opaque component above the transparent components was recognized in the energy model, as Fig. 77 shows.

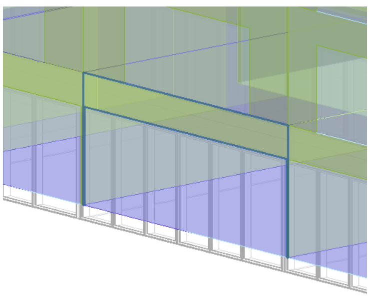

Figure 77 Analytical surfaces model recognizes walls above curtain walls

In the new model the parameters were cautiously set, the values of outdoor airflows calculated by Revit were examined. Almost all zones had nearly identical values compared to the manually calculated airflows in Table 24, for example, office 1 is calculated to have 35.7 L/s for the outdoor airflow rate, see Table 40 in Annex, while it is calculated by Revit to have 36.03 L/s, as Fig. 78 indicates. However, some zones had still higher outdoor airflow rates compared to the manually calculated ones, for example, meeting room 19 has a calculated outdoor airflow of 37.93 L/s, see Table 24, while after calibrating it is calculated by Revit to have a less value compared to the uncalibrated model, but still higher than anticipated to have a value of 63.47 L/s as Fig. 79 demonstrates.

Mechanical - Flow	
Specified Supply Airflow	160.31 L/s
Calculated Supply Airflow	160.31 L/s
Actual Supply Airflow	0.00 L/s
Return Airflow	Specified
Specified Return Airflow	0.06 L/s
Actual Return Airflow	0.00 L/s
Specified Exhaust Airflow	0.00 L/s
Actual Exhaust Airflow	0.00 L/s
Outdoor Airflow	36.03 L/s

Figure 78 Calibrated m. flow in Revit, meeting room 19

Mechanical - Flow	
Specified Supply Airflow	354.15 L/s
Calculated Supply Airflow	354.15 L/s
Actual Supply Airflow	0.00 L/s
Return Airflow	Specified
Specified Return Airflow	0.06 L/s
Actual Return Airflow	0.00 L/s
Specified Exhaust Airflow	0.00 L/s
Actual Exhaust Airflow	0.00 L/s
Outdoor Airflow	63.47 L/s

Figure 79 Calibrated m. flow in Revit, office 1

8. Optimization

In the earlier chapter the base case model was examined with Revit Insight simulation and Revit Built-in simulation tool. Some discrepancies were discovered; hence, model calibration was required. A new model is built, with all discrepancies rectified. Before proceeding with the optimization process, some key aspects should be noted.

In section 5.2.2, constant variables and changeable variables were listed at the end. In the optimization section there will be additional constant variables and changeable variables, depending on the set of simulations considered, which is related to the envelope's characteristics. Therefore, at the beginning of each set of analysis, these variables will be stated.

The new calibrated base case model reported 198 kWh/m²/year, when simulated with Revit Insight, compared to the model before calibration, which reported 223 kWh/m²/year. The same calibrated model reported 26,311,424 kWh/year as well, when simulated with Revit Built-in function compared to 22,283,451 kWh/year. It is odd that the energy consumption for the calibrated model simulated with Revit Insight reports a decrease compared with the uncalibrated model, whereas the calibrated model simulated with Revit Built-in function reports an increase. The energy consumption is still too high as well after the calibration process, this can be a result due to several factors, such as that the model does not include reflected ceiling, which means that volume being cooled and heated is actually much larger than the real volume. For example, the full hight of the ground floor is 3.95 m, the plenum usually takes around 0.5 m of this hight, but in the case of this model, it is an extra volume that is being added to the whole surface area in each floor multiplied by 0.5 m. Another reason that could be responsible for this increase in energy consumption is the use of windows instead of curtain walls, because windows have separate frames, which are responsible for excess in thermal bridges, whereas curtain walls are a complete system. The Please note that both models are the same, the simulation method is the only difference.

From this point on forward, the energy optimization will be conducted, without taking into consideration the base case model, which means for example, when simulating WWR of 50% for the northern façade, the rest of the facades will have 0% WWR, unlike the process adopted earlier. This will help in focusing on the different parameters' behaviour, which will allow for conclusion reaching, at the end, the base case model will be compared with the concluded optimum model.

Concerning the simulations that will be conducted from this point on forward with Revit Insight, will be with different models. As it was explained earlier, Revit Insight gives the opportunity to conduct different simulations for different parameters with one model, however, it was evident that the results obtained from one model are different from the results obtained by different models, even though kind of results stem from Revit Insight.

In the optimization process, results for both simulation tools will be provided in each optimization step.

8.1 Optimizing Wall’s Thermal Transmittance

To conduct energy simulations and optimization for the external walls’ thermal transmittance value, the model will have the same characteristics as demonstrated in Tables 10,11,12 and Table 14. However, it was concluded to use WWR of 0% throughout the whole building, in order to eliminate solar radiation in these set of simulations, since the focus here is on the external opaque walls.

8.1.1 Revit Insight

Fig. 80 demonstrates the energy consumption results, obtained from Revit Insight, of the calibrated model for different thermal transmittance values. The behaviour of this graph is extremely peculiar, because lowest and highest values of thermal transmittance have both the same energy consumption, which is 133 kWh/m²/year, whereas the middle values give lower energy consumption values. As indicated earlier, this behaviour is incorrect.

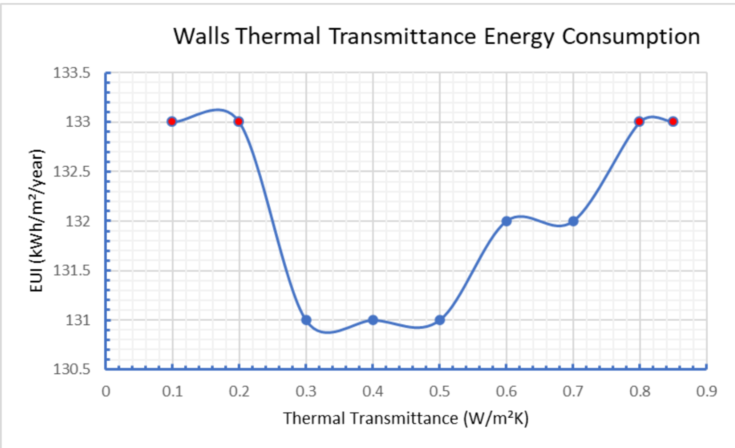

Figure 80 Energy consumption difference with different thermal transmittance values, Revit Insight, calibrated model

8.1.2 Revit Built-in Function

Fig. 81 demonstrates the energy consumption results, obtained from Revit Built-in function, of the calibrated model for different thermal transmittance values. The trend in this graph describes to a certain extent the expected behaviour for thermal transmittance values, where the model with the lowest thermal transmittance value reports the lowest energy consumption, with more than 10% difference compared to the highest consumption of the same category. At the same time the consumption progressively increases until it reaches its highest demand with the highest, highlighted with red, less efficient thermal transmittance value.

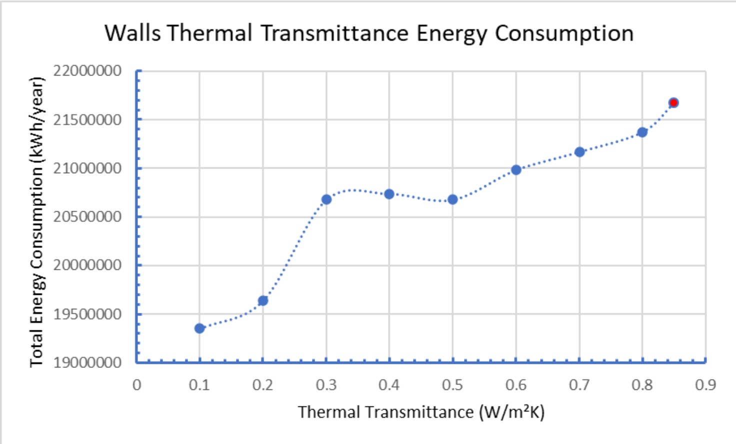

Figure 81 Energy consumption difference with different thermal transmittance values, Revit built-in function, calibrated model

8.2 Optimizing Window to Wall Ratio

In this set of analyses the WWR will be examined. The concerned 3-D model has the same characteristics as stated in Tables 9,10,11,12,13 and Table 14. The model is created in such a way that only the façade under examination has the specified WWR and the rest of the 3 facades have 0% WWR.

8.2.1 Revit Insight

Fig. 61 demonstrates the energy consumption for different WWR for the different 4 facades. As shown, all different energy consumption starts from the same value, because 0% WWR is applied for the 4 facades. In should be noted, that Revit Insight recognizes a maximum WWR of 95%. All facades report the highest energy consumption, highlighted in red, with a WWR of 95%, which is the expected behavior, especially in a hot climate, because the more transparent walls exist in the envelope the more solar radiation penetrates through the envelope, which in return the building will consume more energy for cooling to maintain internal comfort.

According to Fig. 82, the northern façade has the least impact on energy consumption for different WWR values for the building, followed by the southern façade, followed by the eastern façade while finally the western façade has the highest impact on the building.

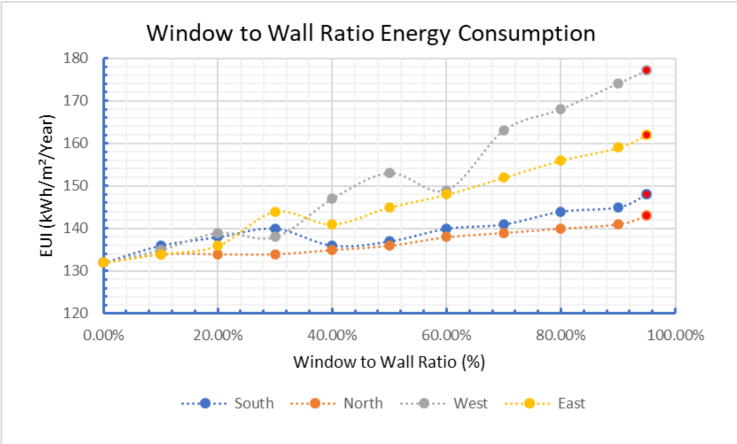

Figure 82 WWR energy consumptions for different facades, conducted with different models, Revit Insight, calibrated model

8.2.2 Revit Built-in Function

Fig. 83 demonstrates the different behavior of different WWR for the 4 facades. Similarly, to Fig. 82 energy consumptions due to different facades start from the same consumption value for 0% WWR. Similar to Fig. 82 the trend for all facades increases, while there is a drop in the energy consumption at 60% WWR for the western façade. The highest energy demand is reported at the highest WWR for all facades except for the southern façade, where it reports the highest consumption at 90% WWR. Similar to Fig. 82, the northern façade has the lowest energy impact with the different WWR. This means that the northern façade is optimal to maximize natural daylight with minimal direct sunlight exposure, because higher WWR on the northern façade from the consistent and relatively low angle sunlight.

However, unlike Fig. 82, Fig. 83 ranks the impact of the rest of the facades differently. After the northern façade in hierarchy of least energy consumption impact comes the western façade, followed by the eastern façade while the southern façade has the highest impact on energy consumption.

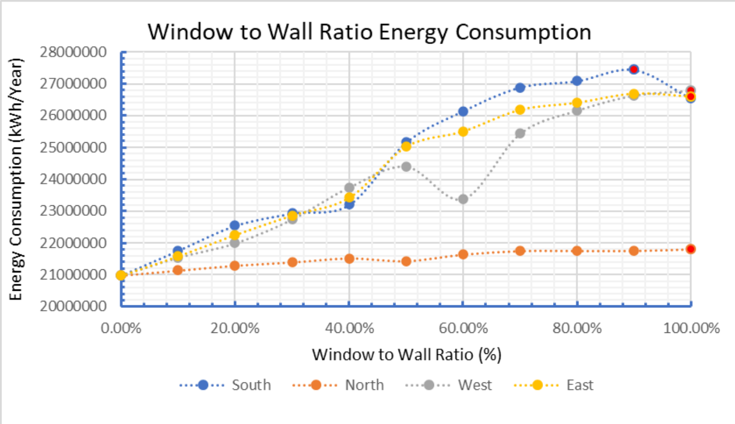

Figure 83 WWR energy consumptions for different facades, conducted with different models, Revit Built-in function, calibrated model

The southern façade of a building typically receives the most direct sunlight throughout the day, especially in the northern hemisphere. According to Fig 5. the sun is generally higher in the sky in south, 80° Azimuth Angle; therefore, the southern façade receives more intense direct solar radiation than the eastern and western façade. According to Fig. 84, the western façade receives intense afternoon solar radiation, while the eastern façade receives intense radiation in the morning. However, the bigger portion of the building lies relatively in the eastern façade, therefore, it makes sense that the eastern façade in this particular case study has more impact concerning the energy consumption.

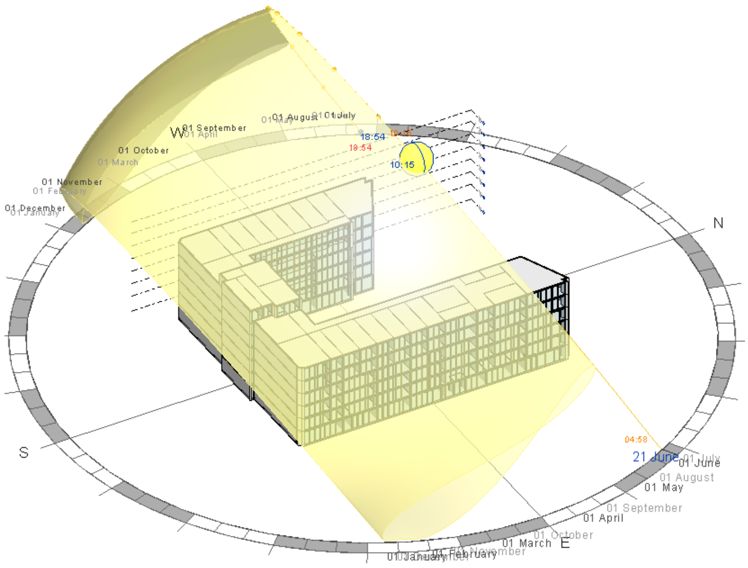

Figure 84 Sun path relative to the building

8.3. Optimizing Roof

In these set of simulations the roof is going to be analyzed from the impact of its different thermal transmittance on the overall energy consumption. The models in this analysis have the same characteristics as presented in Tables 9,10,11 and Table 14. It is concluded to exclude any transparent walls in these simulations to isolate the effect of solar radiation penetrating the envelope and to emphasis on the results of the roof.

8.3.1 Revit Insight

Fig. 85 demonstrates the energy behavior of the building with different thermal transmittance values of the roof. It should be noted that roof's thermal transmittance are simulated until 0.3 W/m²K, because the threshold suggested by ASHRAE 90.1 is 0.27 W/m²K. The behavior described in the graph is constant until thermal transmittance value 0.25 W/m²K, after that the energy consumption jumps to record 132 kWh/m²/year, highlighted in red. This trend suggests that when the thermal transmittance of the roof is more efficient, energy consumption may be reduced.

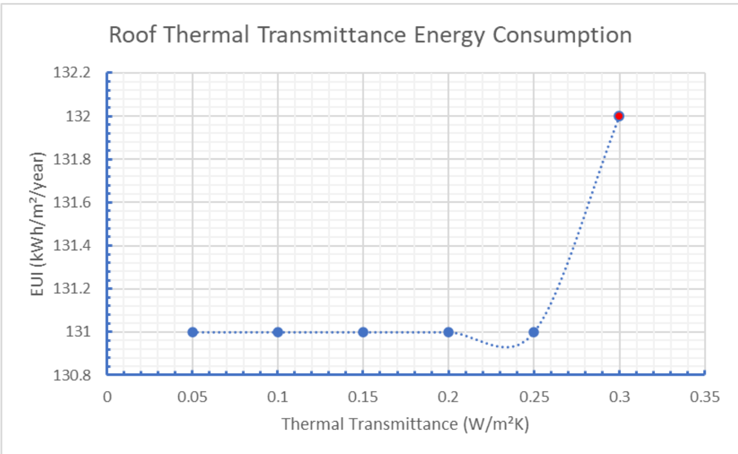

Figure 85 Energy consumption difference with roof's different thermal transmittance values, Revit Insight, calibrated model

8.3.2 Revit Built-in Function

Fig. 86 depicts the behavior of roof's different thermal transmittance concerning the energy consumption when simulated with Revit Built-in function. Unlike Fig. 85, the energy consumption is variable, where the lowest consumption is recorded with the lowest value of thermal transmittance, and it increases with the increase of thermal transmittance. This is the expected result, since the roof encloses the envelope from the top, hence, it protects it from the extreme solar radiation to enter the building, especially on the last floor. However, the highest energy consumption is recorded in at 1 W/m²K, which is not correct, because the highest energy consumption should be recorded at the highest thermal transmittance value. Furthermore, the trend describes increase with the increase of the thermal transmittance as stated before, however, the difference in energy consumption is not significant, because the difference between the highest and lowest value is less than 5%. In the conducted research earlier in this report, it was elaborated that the impact of roof is proportional according to the building's height and area. In this project's case, the roof's area is 1599 m² as indicated in Table 7 compared to external walls and transparent walls of 6187 m². Therefore, the bigger impact on energy consumption will be due to walls and glazed façade as reported in Fig. 81 and 83.

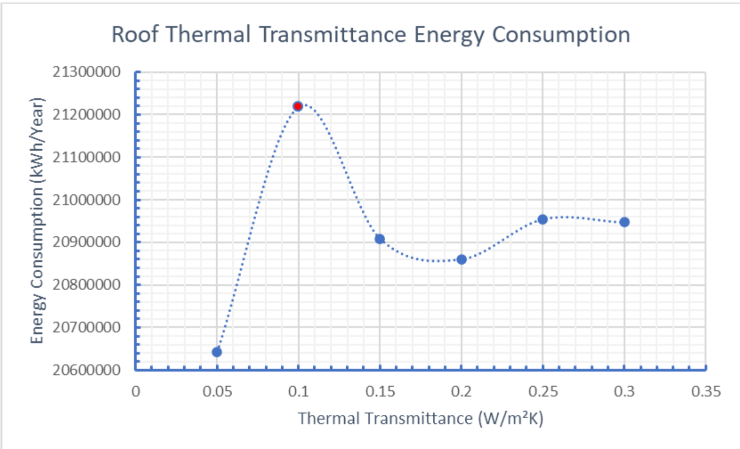

Figure 86 Energy consumption difference with roof's different thermal transmittance values, Revit Built-in function, calibrated model

8.4 Optimizing Internal Slabs

In this set of simulations, the internal slabs on each floor will be analyzed according to the different thermal transmittance. The models used in these simulations possess the same properties as demonstrated in Tables 9, 10, 12 and Table 14. It is concluded as well to eliminate the influence of glass components from these simulations.

8.4.1 Revit Insight

Fig. 87 demonstrates the results obtained from Revit Insight after simulation. It should be noted that the simulations were conducted only until thermal transmittance value 0.6 W/m²K, as suggested by ASHRAE 90.1. The graph indicates that the different thermal transmittance of the internal slabs has almost no effect on the energy consumption of the building. However, the simulations report that the highest energy consumption is reported with the lowest thermal transmittance value, which is incorrect.

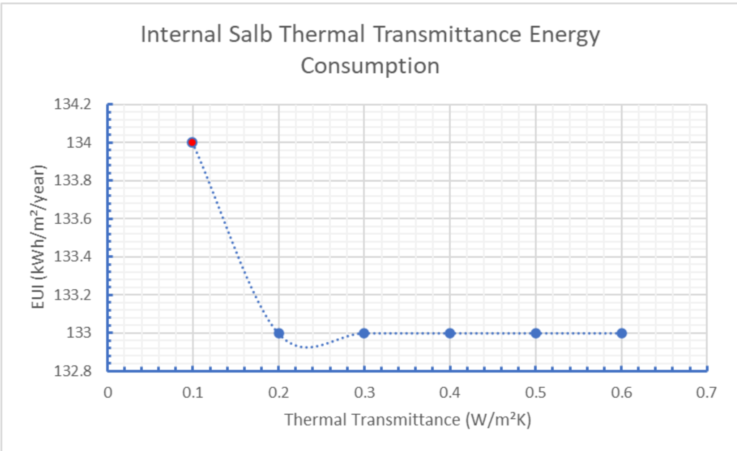

Figure 87 Energy consumption difference with internal slabs' different thermal transmittance values, Revit Insight, calibrated model

8.4.2 Revit Built-in Function

Fig. 88 demonstrates the behavior of different thermal transmittance values for the internal slabs. The lowest consumption is recorded with the lowest thermal transmittance value while the highest consumption is recorded with the highest thermal transmittance value. The trend in this graph can be described as energy consumption increases with the decrease of the thermal transmittance efficiency, which is expected. However, the graph records a drop in energy consumption with 0.4 W/m²K and 0.5 W/m²K, which is not expected. The internal slabs are an imported parameter to be considered when designing an energy efficient building. The whole building is considered as one entity, however, each floor should be tight on its own to reduce heat flow from different floors.

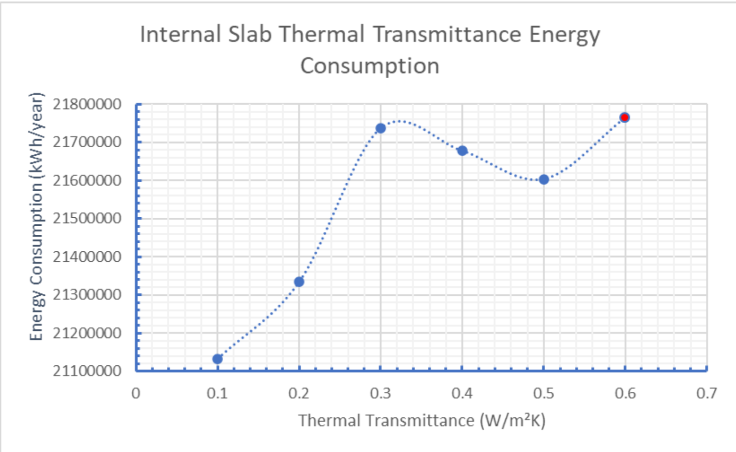

Figure 88 Energy consumption difference with internal slabs' different thermal transmittance values, Revit Built-in function, calibrated model

8.5 Optimizing Slab on Grade

In this set of simulations, the effect of different slabs on grade will be analyzed. The model used in these simulations respects the parameters indicated in Tables 9, 11, 12 and Table 14. It is concluded to exclude the glazed components from these simulations.

8.5.1 Revit Insight

Fig. 89 demonstrates the building's behavior with different slabs on grade. The trend suggests that the lower value the slab on grade has, the more energy consumption is reduced from values 0.1 W/m²K to 0.3 W/m²K, the lowest consumptions are recorded. However, from values of 0.4 W/m²K to 0.8 W/m²K the highest energy consumptions are reported. This behavior is expected, because the less efficient the thermal transmittance, the more energy is consumed by the building to maintain indoor thermal comfort.

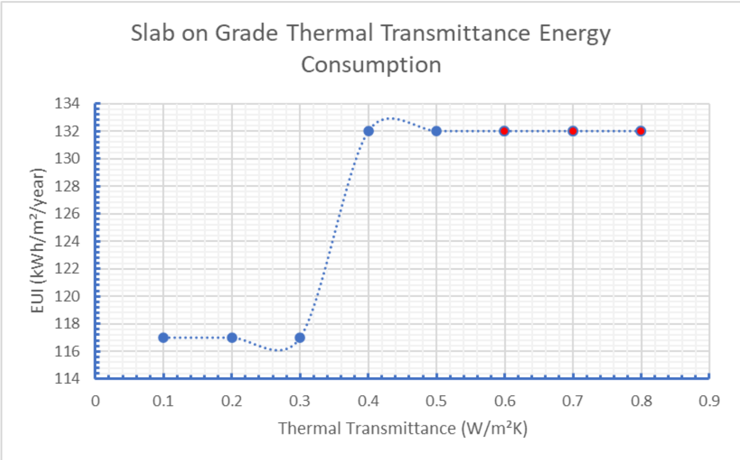

Figure 89 Energy consumption difference with slabs on grade different thermal transmittance values, Revit Insight, calibrated model

8.5.2 Revit Built-in Function

Fig. 90 demonstrates the building's behavior with different slabs on grade when simulations are conducted with Revit Built-in function. The trend in this figure is almost identical to the trend in Fig. 89, where the lowest energy consumption are reported between 0.1 W/m²K and 0.3 W/m²K and the highest consumptions are reported between 0.4 W/m²K and 0.8 W/m²K. the graph indicates a jump in energy demand after 0.3 W/m²K. However, unlike in Fig. 89, in Fig. 90 the results due to different thermal transmittance values are not constant; each thermal transmittance value gives a different energy demand consumption. The impact of different slabs on grade is high, according to Fig. 90, where the difference between the lowest and highest energy demand exceeds 30%. This behavior was not expected, because the roof's analysis in section 7.3.2 reported less impact on the total energy demand, with less than 5% difference between the lowest and highest energy demand. It was expected for the roof to show greater energy impact on the building, because the building is in hot and arid climate, which makes the roof constantly under direct solar radiation exposure. These phenomena can be linked to several factors, firstly, the roof has 2 different insulation layers, whereas the slab on grade has only one thermal insulation layer. Secondly, the roof is investigated for thermal transmittance values between 0.05 W/m²K and 0.3 W/m²K, whereas the slab on grade is investigated for thermal transmittance values between 0.1 W/m²K and 0.8 W/m²K, which means that the range of investigation to the slab on grade is much higher.

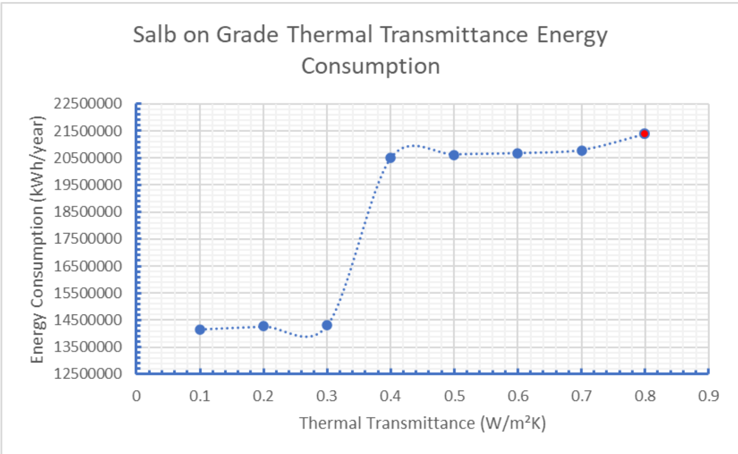

Figure 90 Energy consumption difference with slabs on grade different thermal transmittance values, Revit Built-in function, calibrated model

8.6 Optimizing Solar Heat Gain Coefficient

In this set of simulations, the effect of different values of solar heat gain coefficients is going to be analyzed. The analysis will be conducted on coefficients from 0.25% to 0.95%. In these simulations the building that was prepared in section 7.2 will be used, hence, properties of Tables 10, 11, 12 and Table 14 are respected. Properties of Table 13 are respected as well except solar heat gain coefficients that are changed according to the analysis. In section 7.2 the different WWR were examined. It is concluded to use WWR of 100% to conduct SHGC analysis. This is in order to increase the impact of solar radiation to its maximum, in order to closely analyze the behaviors of different solar coefficients. In section 7.2, the WWR was applied to each façade separately in each set of simulations, however, in these simulations the 100% WWR will be applied to all 4 facades.

8.6.1 Revit Insight

Fig. 91 demonstrates the energy consumption behavior for applying different solar heat gain coefficients to the model. The trend describes the progressive increase of energy consumption with the increase of solar heat gain coefficient values, which is the expected trend, because increased values of solar heat gain coefficients means that more solar radiation passes through the glazed components, which will affect the cooling loads greatly in a hot climate. Therefore, Fig. 91 shows that solar heat gain coefficients have considerable impact on the energy consumption, where the difference between the lowest and highest consumptions due to different coefficients reports more than 30%.

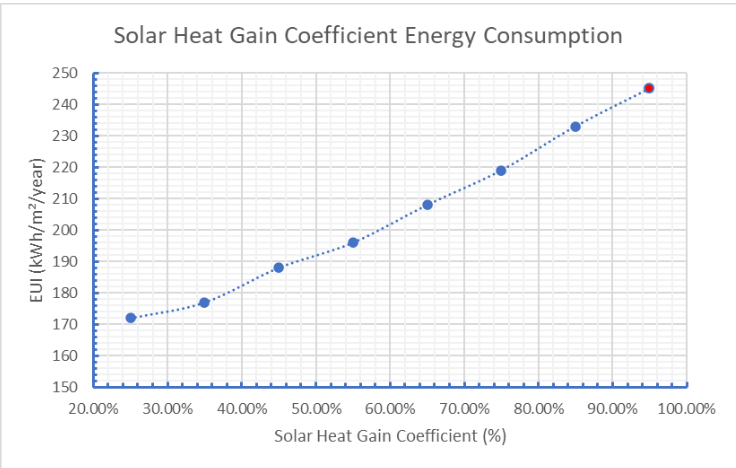

Figure 91 Energy consumption difference with glass panels different solar heat gain coefficient values, Revit Insight, calibrated model

8.6.2 Revit Built-in Function

Fig. 92 demonstrates the energy consumption for the building, with Revit Built-in function, when applying different solar heat gain coefficients to the glazed envelope. Similarly, to Fig. 91, Fig. 92 shows increase in energy consumption with higher values of solar heat gain coefficients. However, differently than Fig. 91, with Revit Built-in simulation function there is a decrease in energy consumption after 65% SHGC and then the consumption increases again. Furthermore, Fig. 92 shows that different values of solar heat gain coefficients have less impact on energy consumption compared to simulations conducted with Revit Insight, where Revit Built-in function records a merely 10% difference in energy consumption between the lowest and highest consumptions.

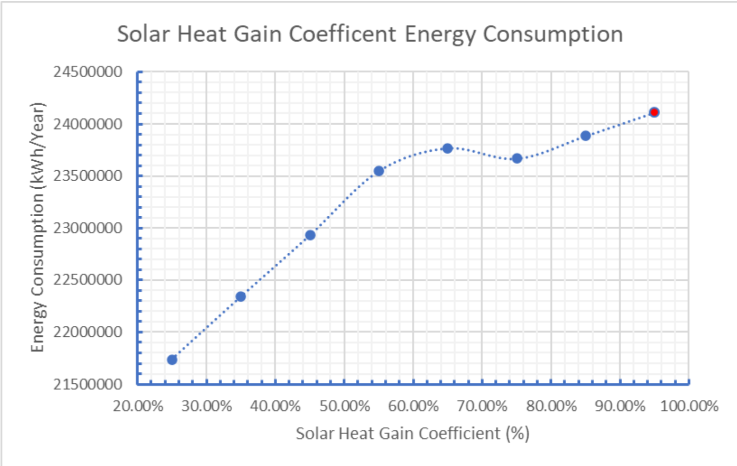

Figure 92 Energy consumption difference with glass panels different solar heat gain coefficient values, Revit Built-in function, calibrated model

8.7 Optimizing Thermal Transmittance for Glass Panels

In this set of simulations, the effect of different thermal transmittance for the glass panels are going to be analyzed. The same models in simulations in section 7.6 are used, except the difference of changing the values of thermal transmittance in Table 13 according to the required analysis and fixing the solar heat gain coefficient similar to the base case at 86%.

8.7.1 Revit Insight

Fig. 93 depicts the energy consumption behavior according to different thermal transmittance values. The graph does not represent the expected trend, because the highest consumption is recorded at the lowest thermal transmittance value, which is wrong, as stated before. Fig. 93 depicts the lowest energy consumption at the thermal transmittance value of 0.4 w/m²K, after this thermal transmittance value the consumption increases.

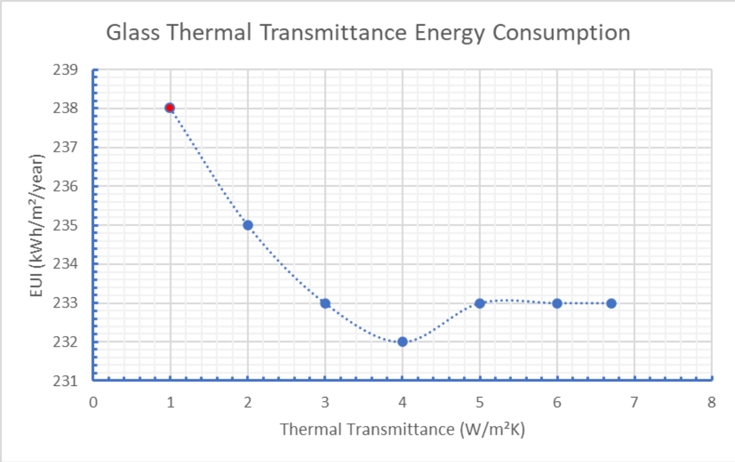

Figure 93 Energy consumption difference with glass panels different thermal transmittance values, Revit Insight, calibrated model

8.7.2 Revit Built-in Function

Fig. 94 demonstrates the energy consumption behavior, simulated with Revit Built-in function, according to different thermal transmittance values for the glass panels. The trend described in Fig. 94 is almost identical to the behavior depicted in Fig. 93, with the exception that the lowest energy consumption is recorded at 0.5 W/m²K. In this case as well the trend described is simply wrong, because the lower the thermal transmittance, the more efficient is the envelope in isolating the internal atmosphere from the external conditions, hence, the building should consume less energy.

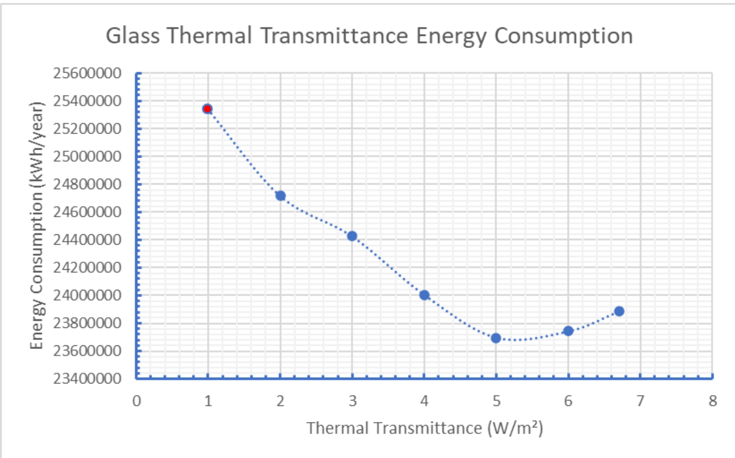

Figure 94 Energy consumption difference with glass panels different thermal transmittance values, Revit Built-in Function, calibrated model

8.8 Optimizing Shading

In these set of simulations, the effect of external shading is tested. The identical model in section 7.7 and section 7.6 is used to conduct these simulations, which means that properties in Tables 10, 11, 12, 13 and Table 14 are completely applied. Vertical and horizontal shading are tested for each façade separately, meaning, the model has 100% WWR in all facades and only has shading in one façade. The shading elements are applied every 2 m distance concerning the vertical shading, whereas shading is applied at floor level for the horizontal shading elements.

8.8.1 Revit Insight

Table 25 demonstrates the results obtained with Revit Insight for vertical shading. In these simulations the depth of the shading, namely 1/3 and 2/3, is related to the windows height, which is in this case the full height, because the model has 100% WWR. The values in this table are comparable with the same model in section 7.6 and 7.7 with solar heat gain coefficient of 86% and thermal transmittance value of 6.7 W/m²K, which reported 233 kWh/m²/year. According to Table 25, all the simulated vertical shadings report reduced energy consumption compared to 233 kWh/m²/year, which is expected, because external shading reduces the amount of direct solar radiation entering and heating the internal space.

However, the comparison made between different shading depths reveals that larger depth in the southern and northern façade are responsible for energy consumption increase compared to smaller shading depth, which is incorrect. The shading depth might have insignificant influence on energy consumption reduction, but it should not under any circumstances be responsible for energy consumption increase.

Vertical Shading			
Façade Orientation	Shading Depth		Energy Consumption Difference (%)
	1/3	2/3	
	EUI (kWh/m²/year)		
South	136	214	44.00%
North	142	219	42.00%
West	209	191	-4.50%
East	229	208	-4.80%

Table 25 Vertical shading, different depths energy consumption comparison, Revit Insight, calibrated model

Table 26 demonstrates the results obtained with Revit Insight for horizontal shading. In these simulations the depth of the shading is 1/3 and 2/3 as well. Unlike the results obtained for the vertical shading, most of increased depths of horizontal shading, report decrease in energy consumption. However, most of the consumption values are increased compared to 233 kWh/m²/year, which is the consumption of the reference model. This consumption increase is just unjustified, because the model that reported 233 kWh/m²/year in section 7.6 and section 7.7 is totally the same model simulated here in this section, with the difference of applying external shading. Therefore, if anything, the energy consumption should be decreased or in the worst-case scenario it should remain the same. Please note, that nothing has changed between these models except for the external shading incorporation, which means all the parameters and building components are identical.

Horizontal Shading			
Façade Orientation	Shading Depth		Energy Consumption Difference (%)
	1/3	2/3	
	EUI (kWh/m²/year)		
South	248	242	-1.20%
North	254	252	0.40%
West	246	210	-7.90%
East	250	220	-6.40%

Table 26 Horizontal shading, different depths energy consumption comparison, Revit Insight, calibrated model

Table 27 compares the energy consumptions obtained due to vertical and horizontal shading. It is concluded to compare shading depths of 2/3 in both cases because it is imperative that increased depth of shading should report the more effective scenario, regardless of the inconsistent results obtained in Tables 25 and 26.

Table 27 depicts that vertical shading is more effective in protecting against direct solar radiation in all façade orientations, which is not completely correct. The sun's path in the northern hemisphere, especially in Cairo, is relatively high in the sky, therefore horizontal shading elements should be more effective in blocking the high-angle sunlight during the hottest parts of the day at the southern facade.

The northern facade receives less direct sunlight in a hot climate. Therefore, shading elements on the northern facade may not be as critical. However, vertically oriented shading elements can still provide some benefits by diffusing glare and controlling daylight.

The eastern facade receives direct sunlight in the morning from a median solar angle according to Fig. 5, whereas the western façade receives direct solar radiation in the afternoon. Therefore, a combination of vertical and horizontal shading elements should be more effective in direct solar radiation protection for the eastern and western facade.

Vertical & Horizontal Shading Comparison			
Façade Orientation	***Vertical***	***Horizontal***	***Energy Consumption Difference (%)***
	Shading Depth		
	2/3	***2/3***	
	EUI (kWh/m²/year)		
South	214	242	3.07%
North	219	252	3.50%
West	191	210	2.37%
East	208	220	1.40%

Table 27 Vertical & horizontal shading energy consumption comparison, Revit Insight, calibrated model

8.8.2 Revit Built-in Function

In this set of simulations, the same identical procedures were applied as mentioned in section 7.8.1 with the difference that the simulations are conducted with Revit Built-in Function. Table 28 demonstrates the difference in energy consumption due to different vertical shading depths. It is remarkable that the same identical model reports different behaviors when simulated with different tools. In Table 26, an increase in vertical shading depth reports decrease in energy consumption in the western and eastern façade, whereas, in Table 28, energy consumption decrease is reported with vertical shading depth in the northern and western façade. Unlike in Table 26, all energy consumptions reported in Table 28 report an increase in energy consumption when compared to the consumption of the reference model, in section 7.6 and 7.7 with solar heat gain coefficient of 86% and thermal transmittance value of 6.7 W/m²K, which reports 23,884,591 kWh/year. Please note that this inconsistency in illogical energy consumption behavior was recognized in section 7.8.1 in the case of horizontal shading and not vertical shading.

Vertical Shading			
Façade Orientation	***Shading Depth***		***Energy Consumption Difference (%)***
	1/3	***2/3***	
	Energy Consumption (kWh/year)		
South	24,177,110.00	24,367,975.00	0.79%
North	24,348,411.00	23,990,722.00	-1.48%
West	25,917,038.00	23,885,389.00	-8.16%
East	25,015,244.00	25,092,772.00	0.31%

Table 28 Vertical shading, different depths energy consumption comparison, Revit Built-in function, calibrated model

Table 29 reports the different energy consumption due to different shading horizontal shading depths. All facades report a decrease in energy consumption with the increase of the shading element except for the eastern facades, which report an increase in energy consumption with the increase of the shading element. Similar to Table 27, almost all reported values indicate an increase in consumption when compared to the reference model in section 7.6 and 7.7 with the exception of the southern façade which reports a decrease in consumption with shading depth of 2/3.

Horizontal Shading			
Façade Orientation	Shading Depth		Energy Consumption Difference (%)
	1/3	2/3	
	Energy Consumption (kWh/year)		
South	24,078,194.00	23,108,136.00	-4.11%
North	24,130,094.00	24,075,369.00	-0.23%
West	24,086,302.00	23,964,910.00	-0.51%
East	24,054,644.00	24,292,213.00	0.98%

Table 29 Horizontal shading, different depths energy consumption comparison, Revit Built-in function, calibrated model

Table 30 depicts the degree of impact due to vertical and horizontal shading elements in energy consumption. In this case, unlike in Table 27, the southern façade indicates more effectiveness in protection against direct solar radiation with the incorporation of horizontal shading elements, compared to the vertical elements. As stated before, the northern façade should be better protected against low-angle solar radiation with the use of vertical shading elements, which is correctly reported in Table 30.

Vertical & horizontal Shading Comparison			
Façade Orientation	Vertical	Horizontal	Energy Consumption Difference (%)
	Shading Depth		
	2/3	2/3	
	Energy Consumption (kWh/year)		
South	24,367,975.00	23,108,136.00	-5.31%
North	23,990,722.00	24,075,369.00	0.35%
West	23,885,389.00	23,964,910.00	0.33%
East	25,092,772.00	24,292,213.00	-3.24%

Table 30 Vertical & horizontal shading energy consumption comparison, Revit Built-in function, calibrated model

9. Optimized Model

After conducting the energy optimization analysis, the following was concluded:

- Simulating with Revit Insight and Revit Built-in Function demonstrated many unexpected results, and in some cases, these results are considered incorrect.
- Revit Insight demonstrated many incorrect energy consumption trends with different optimization analysis, as stated in section 7, however, the overall energy consumption, which is between 150 kWh/m²/year and 250 kWh/m²/year can be referred to as reasonable outcome, which is extremely high energy demand, in a hot and arid climate.
- Furthermore, it is observed that the energy model that is created in Revit Insight is not always identical to the energy model created in Revit itself. As Fig. 95 demonstrates, the energy model in Revit Insight contains some errors in recognizing the external walls, where the external walls are totally absent in some parts of the building.

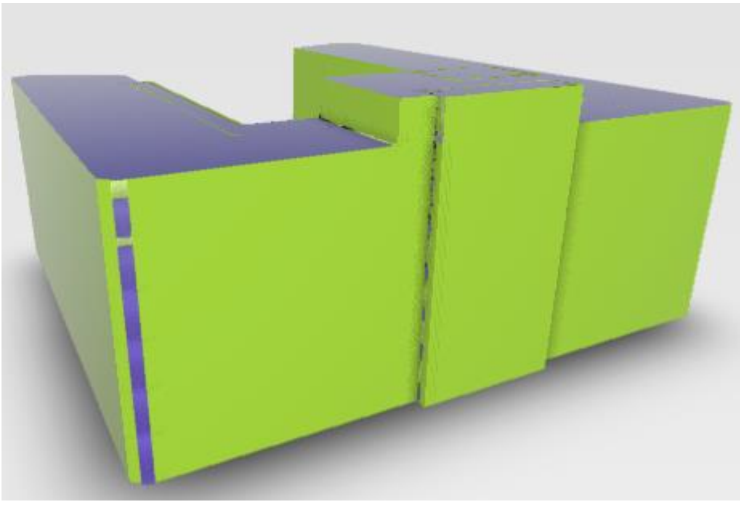

Figure 95 Parts of external walls are not recognized in Revit Insight energy model

- On the other hand, Revit Built-in Function demonstrated more reasonable energy consumption trends in the different simulations conducted in section 7, however, the overall energy consumption is extremely high, beyond reason. All energy consumption results are above 20,000,000 kWh/year. Converting this consumption into EUI values by dividing the consumption by the total building's area which is less than 9600 m², the result would be more than 2000 kWh/m²/year. This energy demand is just ridiculously high.

- Revit Built-in function, provides a breakdown for the energy consumption regarding the cooling and heating demand and internal lighting and internal equipment energy demand. The simulation values of internal lighting and equipment energy demand almost does not change throughout the simulations, which makes sense for the equipment demand, however, the constant value for internal lighting indicates that the simulation does not take into consideration the degree of natural light that enters into the internal spaces.

Therefore, it is concluded to construct 2 Optimized energy models. One model will respect the optimized results obtained by Revit Built-in simulation function, because the aim of the thesis project is to obtain guidelines for reducing energy demand for buildings in hot and arid climates, and the trends described by the Built-in function are more accurate regardless of the total energy consumption values. The second model will be constructed with values that are supposed to provide least energy consumptions for the building, even if the values of the parameters are not correlated to the trend described by the built-in function simulations. It should be noted that both optimized models have almost identical parameters, except for the optimum thermal transmittance for the glass panels. Optimum building 1 will have the properties indicated in Table 31, whereas optimum building 2 will have the properties indicated in Table 31 except for having glass thermal transmittance value of 5 W/m²K, as the optimum results reported by simulations conducted with Revit Built-in function.

Envelope's Optimum Characteristics	
Envelope Component	***Thermal Transmittance (W/m²K)***
External Walls	0.1
Roof	0.05
Internal Slabs	0.1
Slab on Grade	0.1
Glass Panel	1

Table 31 Optimum thermal transmittance for the simulated building

Furthermore, it is concluded for both optimized models to have the following additional properties:

- Northern Façade will have WWR of 60%, to allow for maximum utilization of the natural light entering the building without the effect of overheating the spaces inside. This façade will have 1/3 vertical shading as well.
- Southern, eastern, and western facades will have WWR of 30%, because according to Fig. 82, exceeding this threshold, the energy consumption would remarkably increase.
- The southern façade will have 2/3 horizontal external shading, to limit the direct solar radiation from entering the internal spaces due to the high sun angle.
- The western and eastern façade will have both, 2/3 horizontal vertical shading elements, to protect these facades from the medium sun angle that exposes these facades to direct solar radiation.
- All the glass panels will have 25% solar heat gain coefficient value.

9.1 Optimized Model 1

Fig. 96 depicts the energy model for the optimized models. As stated before, both models are identical except that model 2 has a glass thermal transmittance of 5 W/m²K. Even though it is concluded to use simulations conducted with Revit Built-in function as a basis to reach the optimized building, both simulation tools are used to simulate the optimized models.

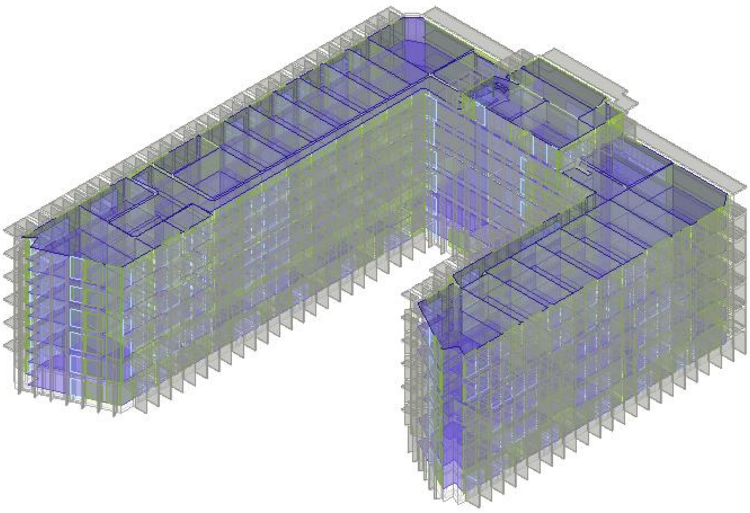

Figure 96 Optimized energy model

9.1.1 Revit Insight

Please note that after model calibration in in section 6.4, the model reported 198 kWh/m²/year. After uploading the model to conduct energy simulation with Revit Insight, the simulation failed because the wall thickness is too thick, as Fig. 97 demonstrates.

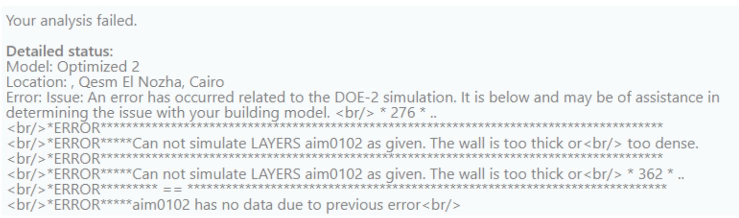

Your analysis failed.

Detailed status:
Model: Optimized 2
Location: , Qesm El Nozha, Cairo
Error: Issue: An error has occurred related to the DOE-2 simulation. It is below and may be of assistance in determining the issue with your building model.
 * 276 * ..

*ERROR**

*ERROR*****Can not simulate LAYERS aim0102 as given. The wall is too thick or
 too dense.

*ERROR**

*ERROR*****Can not simulate LAYERS aim0102 as given. The wall is too thick or
 * 362 * ..

*ERROR********* == ***

*ERROR*****aim0102 has no data due to previous error

Figure 97 Failed simulation attempt for simulating the optimized building

9.1.2 Revit Built-in Function

Please note that the calibrated base case model reported energy consumption of 26,311,424 kWh/year. Simulation with Revit Built-in function reports 12,413,845 kWh/year for Optimized model 1, which is more than 70% in total energy consumption reduction as Table 32. It is worth noting that according to Table 32, the cooling demand is greatly reduced with 73%, while the heating demand is increased by 28%. This is due to the fact that the optimized model is built to protect the building from the soar heat in Cairo, which should in return reduce the cooling loads, but at the same time, the absence of the heat entering the building, will increase the heating loads in the winter.

Base Case Comparison with Optimized Model 1			
Energy Breakdown	**Base Case Energy Consumption (kWh/year)**	**Optimized Model 1 Energy Consumption (kWh/Year)**	**Energy Consumption Difference**
Heating	30,908	41,247	28.66%
Cooling	25,937,533	12,018,531	-73.34%
Int. Light	166,789	179,561	7.38%
Int. Equipment	176,200	174,506	-0.97%
Total Energy Demand	26,311,430	12,413,845	-71.78%

Table 32 Energy consumption comparison between base case and optimized model 1, Revit Built-in Function

9.2 Optimized Model 2

As stated before, the only difference between optimized model 1 and optimized model 2 is the value of glass thermal transmittance, which is 5 W/m²K in model 2 according to the optimum value suggested by Revit Built-in function in section 7.7.2. Apart from this the thermal transmittance, all properties in Table 31 are respected, the same shading and WWR are applied as in optimized model 1.

9.2.1 Revit Insight

After uploading the model to conduct energy simulation in Revit Insight, the simulation failed as well due to the same reasons stated in section 8.1.1.

9.2.2 Revit Built-in Function

Tabel 33 demonstrates the comparison in energy consumption between the base case model and optimized model 2. As anticipated the total energy consumption is increased compared to the total energy consumption of optimized model 1. However, model 2 still reports a decrease in consumption of 57% compared to the base case model.

Base Case Comparison with Optimized Model 2			
Energy Breakdown	Base Case Energy Consumption (kWh/year)	Optimized Model 2 Energy Consumption (kWh/Year)	Energy Consumption Difference
Heating	30,908	53,381	53.32%
Cooling	25,937,533	14,169,575	-58.68%
Int. Light	166,789	179,561	7.38%
Int. Equipment	176,200	174,506	-0.97%
Total Energy Demand	26,311,430	14,577,023	-57.40%

Table 33 Energy consumption comparison between base case and optimized model 2, Revit Built-in Function

10. Conclusion

After conducting a thorough energy investigation to the case study building, it became evident that the building's performance needs to be improved. These improvements are simple measures to take into account while design g and building. For example, the external shading have demonstrated that it is a crucial parameter that needs to be integrated in the design to protect against the harsh hot and arid conditions in Cairo.

References

ASHRAE Handbook. “*Heating, Ventilating and Air-Conditioning Systems and Equipment.*”, edited by Heather E. Kennedy, 2020.

ASHRAE Standards Committee, ANSI/ASHRAE Standard 55-2010 “*Thermal Environmental Conditions for Human Occupancy*”, 2010

ASHRAE Standards Committee, ANSI/ASHRAE Standard 90.1-2007 “*Energy Standards for Buildings Except Low-Rise Residential Buildings*”, 2007

ASHRAE Standards Committee, ANSI/ASHRAE Standard 62.1-2019 “*Ventilation for Acceptable Indoor Air Quality*”, 2019

Average daily incident shortwave solar energy in Cairo, Weather Spark, https://weatherspark.com/y/96939/Average-Weather-in-Cairo-Egypt-Year-Round

Average monthly dry bub temperatures in Cairo, Weather Spark, https://weatherspark.com/y/96939/Average-Weather-in-Cairo-Egypt-Year-Round

Average monthly rainfall in Cairo, Weather Spark, https://weatherspark.com/y/96939/Average-Weather-in-Cairo-Egypt-Year-Round

Average Wind Speed in Cairo, Weather Spark, https://weatherspark.com/y/96939/Average-Weather-in-Cairo-Egypt-Year-Round

Britannica, The Editors of Encyclopaedia. "*Microclimate*". Encyclopedia Britannica, 17 Mar. 2022, https://www.britannica.com/science/microclimate. Accessed 20 November 2023.

“*Cairo, Egypt Metro Area Population 1950-2024.*” MacroTrends, https://www.macrotrends.net/cities/22812/cairo/population

“*Cairo Governorate Areas.*” Official Portal of Cairo Governorate, http://www.cairo.gov.eg/en/Maps/Pages/cairo-areas.aspx

Cerutti, Emiliano Adam. “*Parametric Facade Modelling for Visual Comfort Optimization and Overheating Mitigation.*” *Politesi, Politecnico di Milano*, 2020, www.politesi.polimi.it/.

Chang, Roger, and Dury B Crawley. “*Influence of Plug and Process Loads and Occupancy on Ultimate Energy Savings - a New Approach* .” Building Performance Analysis Conference and SimBuilt Co-Organized by ASHRAE and IBPSA, 2018.

Chua, Klan Jon, and Slaw Klang Chou. Tsinghua University Press and Springer-Verlag Berlin Heidelberg, 2010, *Evaluating the Performance of Shading Devices and Glazing Types to Promote Energy Efficiency of Residential Buildings*.

Cloud coverage in Cairo, Weather Spark, https://weatherspark.com/y/96939/Average-Weather-in-Cairo-Egypt-Year-Round

Daily chance of precipitation in Cairo, Weather Spark, https://weatherspark.com/y/96939/Average-Weather-in-Cairo-Egypt-Year-Round

Edme-François, Jomard M. "*Le Kaire. Plan Particulier de La Ville.*" The American University in Cairo, Rare Books and Special Collections Digital Library, Paris: Imprimerie Impériale, https://digitalcollections.aucegypt.edu/digital/collection/p15795coll6/id/213/rec/1

"*Egypt Built 935 Bridges, 7K New Main Roads in 9 Yrs: Minister of Transportation.*" State Information Service, https://www.sis.gov.eg/Story/187073/Egypt-built-935-bridges%2C-7K-new-main-roads-in-9-yrs-Minister-of-Transportation?lang=en-us#:~:text=Egypt%20has%20built%20new%2013,President%20Abdel%20Fattah%20El%20Sisi's

El Shamaa, Mohamed. "*This Town Ain't Big Enough for Both of Us: New Cairo Bridge 50cm* ..." Arab News, https://www.arabnews.com/node/1673876/middle-east

"*Energy Performance Testing, Certification, and Labelling*." U.S. Department of Energy, www.energy.gov/energysaver/energy-performance-ratings-windows-doors-and-skylights.

Geonetwork/Catalog/Components/Common/Map/, https://www.cedejcapmas.org/adws/app/4d5b52dc-669d-11e9-b6a6-975656a88994/index.html

Gowri, K, et al. U.S. Department of Energy, 2009, *Infiltration on Modelling Guidelines for Commercial Building Energy Analysis*.

Grand, Pierre Bey. "*Plan Général de La Ville Du Caire.*" The American University in Cairo, Rare Books and Special Collections Digital Library, Le Caire, Égypte : Ebner et Cie, https://digitalcollections.aucegypt.edu/digital/collection/p15795coll6/id/212/rec/1

Great Britain, War Office, Intelligence Division. "Great Britain War Office - Maps of Egypt." The American University in Cairo, Rare Books and Special Collections Digital Library, Intelligence Division, https://digitalcollections.aucegypt.edu/digital/collection/p15795coll6/id/136/rec/1

Hamed, Mohammed, et al. "*Climatic Zonation of Egypt Based on High-Resolution Dataset Using Image Clustering Technique.*" Progress in Earth and Planetary Science , 2022, doi:https://doi.org/10.1186/s40645-022-00494-3.

He, Qiong, et al. "*Energy-Efficiency Window Retrofit for High-Rise Residential Buildings in Different Climatic Zones of China.*" Sustainability, 2019.

Lane-Poole, Stanley, "*Maps from "The Story of Cairo".*" The American University in Cairo, Rare Books and Special Collections Digital Library, London : J.M. Dent, https://digitalcollections.aucegypt.edu/digital/collection/p15795coll6/id/245/rec/1

Mady, Mohamed. The Center for the Study of Architecture in Arab Region (CSAAR), 2010, *Traditional Ways of Dealing with Climate in Egypt*.

OECD et al. (2022), *"Policies and partnerships to achieve Egypt's potential"*, in Production Transformation Policy Review of Egypt: Embracing Change, Achieving Prosperity, OECD Publishing, Paris, https://doi.org/10.1787/3418e76a-en

Office building location in Cairo, Google Eart, https://earth.google.com/web/search/Cairo/@30.05948843,31.25846435,23.42793067a,16099.04478904d,35y,0h,0t,0r/data=CnAaRhJACiUweDE0NTgzZmE2MGIyMWJlZWI6MHg3OWRmYjI5NmU4NDIzYmJhGShNORVfCz5AIa9JbZhXPD9AKgVDYWlybxgCIAEiJgokCf_iWQtjUUBAEY8xbAsKODNAGQ6vu1bYRUhAIQTkmlWAaipAOgMKATA

Perez-Lombard, Luis, et al. "*A Review on Building Energy Consumption Information.*" *Science Direct*, 2007.

"*Population below the International Poverty Line.*" World Health Organization, https://www.who.int/data/nutrition/nlis/info/population-below-the-international-poverty-line

Sadineni, Suresh, et al. "*Passive Building Energy Savings: A Review of Building Envelope Components.*" Science Direct, 2011.

Satellite image for the map of Egypt, Google Eart, https://earth.google.com/web/search/egypt/@26.91098568,30.87770329,234.04753853a,2122801.83462582d,35y,0h,0.00041327t,0r/data=CnAaRhJACiUweDE0MzY4OTc2YzM1YzM2ZTk6MHgyYzQ1YTAwOTI1YzRjNDQ0GXui68IP0jpAIfwaSYJwzT5AKgVlZ3lwdBgCIAEiJgokCRJlfVO9BT5AEQ5-2g_rBD5AGc2Pra3Mbj9AIS3oUie9bD9AOgMKATA

Shahdan, et al. "*External Shading Devices for Energy Efficient Buildings*." Earth and Environmental Science, 2018, doi:doi :10.1088/1755-1315/117/1/012034.

Solar elevation and azimuth angle in Cairo, Weather Spark, https://weatherspark.com/y/96939/Average-Weather-in-Cairo-Egypt-Year-Round

Staff, MEO. "*Egypt: Trees and Green Spaces Are Almost Systematically Destroyed*." Middle East Observer, 6 Oct. 2021, https://middleeastobserver.org/2021/10/04/egypt-trees-and-green-spaces-are-almost-systematically-destroyed/

Temperature profile depicting heat transfer behaviour through a wall, Transfer rate in terms of bulk fluid properties, https://www.sciencedirect.com/topics/mathematics/heat-transfer-rate.

"*Urbanization in Egypt: Building Inclusive and Sustainable Cities.*" Urbanization in Egypt: Building Inclusive & Sustainable Cities, UN Habitat, 2020, 7 July, https://unhabitat.org/egypt

Wand, Julian, et al. "*Selection of Energy Efficient Windows for Hot Climates Using Genetic Algorithms Optimization.*" PLEA 32nd International Conference on Passive and Low Energy Architecture, vol. 1, 2016.

William, Micheal, et al. "Techno-Economic Evaluation of Building Envelope Solutions in Hot Arid Climate: A Case Study of Educational Building." Science Direct, 2021.

"*World Urbanization Prospects - Population Division*." United Nations, https://population.un.org/wup/DataQuery/

Yang, Liu, et al. "*Energy Performance of Building Envelopes in Different Climate Zones in China.*" Science Direct, 2008.

خريطة مشروعات مصر | *Egypt's Projects Map*, https://egy-map.com/governorates

خريطة مشروعات مصر / المحافظات / محافظة | *Egypt's Projects Map | Governorates | Alexandria Governorate*, https://egy-map.com/governorate/%D9%85%D8%AD%D8%A7%D9%81%D8%B8%D8%A9-%D8%A7%D9%84%D8%A3%D8%B3%D9%83%D9%86%D8%AF%D8%B1%D9%8A%D8%A9

"المخطط الاستراتيجى القومى للتنمية العمرانية" | "National Strategic Plan for Urban Development", Ministry of Housing, Utilities and Urban Communities, General Authority for Urban Planning Division, 2017

الجهاز المركزي للتعبئة العامة والإحصاء | CAPMAS, Statistics, https://www.capmas.gov.eg/Pages/StaticPages.aspx?page_id=5035

"تحديث مشروع الهيكلة العمرانية لمدينة القاهرة في ضوء المتغيرات الاقليمية" | *"Updating the Urban Structuring Project for Cairo in Light of Regional Changes"*, Ministry of Housing, Utilities and Urban Communities, General Authority for Urban Planning Division, 2022

الهيئة المصرية العامة *للمساحة* | *Egyptian General Authority for Survey. "Cairo City."* The American University in Cairo, Rare Books and Special Collections Digital Library, Egyptian General Authority for Survey, https://digitalcollections.aucegypt.edu/digital/collection/p15795coll6/id/763/rec/1

الجهاز المركزي للتعبئة العامة والإحصاء | CAPMAS, https://www.capmas.gov.eg/?lang=2

"الهيكلة العمرانية للقطاعات مدينة القاهرة" | *"Urban structuring of Cairo city sectors*", Ministry of Housing, Utilities and Urban Communities, General Authority for Urban Planning Division, 2021

"مستشار المركزي للإحصاء: 33.3% من سكان مصر تحت خط الفقر خلال 2023." | "CAPMAS Advisor: 33.3% of Egypt's population will be below the poverty line during 2023"*Cairo 24*, 16 Oct. 2023, https://www.cairo24.com/1885018#:~:text=%D9%88%D8%A3%D8%B6%D8%A7%D9%81%D8%AA%20%D8%A7%D9%84%D9%85%D9%87%D8%AF%D9%8A%20%D8%A3%D9%86%20%D9%86%D8%B3%D8%A8%D8%A9%20%D8%A7%D9%84%D9%81%D9%82%D8%B1,%D8%AD%D8%A7%D9%84%D8%A9%20%D9%81%D9%82%D8%B1%20%D9%81%D9%8A%20%D8%B9%D8%A7%D9%85%202023.

Egypt's Governorate's Population History Compared to Total Population															
Governorate	**1882**	**1897**	**1907**	**1917**	**1927**	**1937**	**1947**	**1960**	**1966**	**1976**	**1986**	**1996**	**2006**	**2017**	**2023**
Cairo	5.72%	5.86%	5.85%	6.22%	7.59%	8.34%	11.19%	12.89%	14.35%	13.84%	12.61%	11.47%	10.85%	10.06%	9.77%
Domiat	0.67%	0.45%	NR	0.24%	0.25%	0.26%	0.29%	1.49%	1.47%	1.57%	1.54%	1.54%	1.51%	1.58%	1.54%
Rashid	0.30%	NR	NR	NR	NR	NR	NR	NR	NR	NR	NR	NR	NR	NR	NR
Port Said	0.33%	NR	NR	NR	NR	NR	NR	0.94%	0.96%	0.72%	0.83%	0.80%	0.78%	0.79%	0.76%
Arish	0.04%	0.17%	0.05%	NR	NR	NR	NR	NR	NR	NR	NR	NR	NR	NR	NR
Quşayr	0.04%	NR	NR	NR	NR	NR	NR	NR	NR	NR	NR	NR	NR	NR	NR
Beherah	5.69%	6.48%	7.13%	7.01%	6.97%	6.75%	6.66%	6.49%	6.73%	6.72%	6.94%	6.73%	6.52%	6.51%	6.54%
Daqahleya	8.87%	7.57%	8.15%	7.76%	7.71%	7.75%	7.56%	7.75%	7.77%	7.46%	6.78%	7.12%	6.85%	6.85%	6.71%
Sharqeya	6.69%	7.69%	7.86%	7.51%	7.25%	7.12%	7.20%	7.00%	7.17%	7.14%	7.10%	7.22%	7.35%	7.56%	7.52%
Qalyubeya	3.89%	3.82%	3.88%	4.16%	3.98%	3.88%	3.71%	3.80%	4.12%	4.58%	5.23%	5.57%	5.84%	5.94%	5.84%
Gharbeya	14.04%	13.33%	13.27%	13.04%	12.78%	12.51%	12.45%	6.60%	6.47%	6.25%	6.00%	5.74%	5.51%	5.27%	5.18%
Asyut	8.40%	8.04%	8.07%	7.71%	7.69%	7.66%	7.35%	5.12%	4.82%	4.63%	4.61%	4.72%	4.73%	4.62%	4.80%
Banisweif	2.98%	3.23%	3.33%	3.56%	3.62%	3.57%	3.27%	3.31%	3.16%	3.03%	3.00%	3.13%	3.15%	3.33%	3.41%
Fayoum	3.08%	3.81%	3.95%	3.99%	3.95%	3.83%	3.58%	3.23%	3.18%	3.11%	3.22%	3.35%	3.45%	3.79%	3.87%
Giza	4.20%	4.13%	4.11%	4.12%	4.22%	4.36%	4.38%	5.14%	5.61%	6.59%	7.74%	8.07%	8.65%	9.11%	9.05%
Ilmenia	4.51%	5.63%	5.90%	6.01%	5.99%	5.90%	5.59%	6.00%	5.80%	5.60%	5.49%	5.58%	5.72%	5.80%	6.01%
Isna	3.43%	NR	NR	NR	NR	NR	NR	NR	NR	NR	NR	NR	NR	NR	NR
Jirja	7.88%	7.07%	7.09%	6.79%	6.90%	7.11%	6.87%	NR	NR	NR	NR	NR	NR	NR	NR
Qina	5.86%	7.31%	6.90%	6.61%	6.43%	6.47%	5.92%	5.20%	5.00%	4.66%	4.70%	4.12%	4.12%	3.34%	3.45%

Table 34 Egypt's Governorates' Population Compared to Total Population, Part 1

Egypt's Governorate's Population History Compared to Total Population															
Governorate	***1882***	***1897***	***1907***	***1917***	***1927***	***1937***	***1947***	***1960***	***1966***	***1976***	***1986***	***1996***	***2006***	***2017***	***2023***
Monofeya	9.83%	8.88%	8.67%	8.43%	7.88%	7.37%	6.23%	5.19%	4.96%	4.67%	4.62%	4.65%	4.49%	4.54%	4.51%
Alexandria	3.53%	3.28%	2.97%	3.50%	4.09%	4.36%	4.92%	5.83%	6.13%	6.44%	6.08%	5.63%	5.66%	5.45%	5.29%
Qanâl al-Suways	NR	0.52%	0.55%	0.72%	NR	NR	NR	NR	NR	NR	NR	NR	NR	NR	NR
Suweis	NR	0.26%	0.16%	0.24%	0.29%	0.32%	0.57%	0.78%	0.90%	0.53%	0.69%	0.70%	0.70%	0.77%	0.75%
Nuba	NR	2.47%	NR	NR	NR	NR	NR	NR	NR	NR	NR	NR	NR	NR	NR
Tur Sinai	NR	NR	0.01%	NR	NR	NR	NR	NR	NR	NR	NR	NR	NR	NR	NR
Aswan	NR	NR	2.08%	1.99%	1.91%	1.94%	1.56%	1.48%	1.77%	1.69%	1.68%	1.64%	1.63%	1.55%	1.57%
Asaharaa Al Gharbeya	NR	NR	NR	0.04%	0.35%	0.33%	0.40%	NR	NR	NR	NR	NR	NR	NR	NR
Asaharaa Asharqeya	NR	NR	NR	0.29%	NR	NR	NR	NR	NR	NR	NR	NR	NR	NR	NR
Sinai	NR	NR	NR	0.04%	0.11%	0.11%	0.20%	0.19%	0.22%	0.03%	NR	NR	NR	NR	NR
Red Sea	NR	NR	NR	NR	0.04%	0.06%	0.09%	0.10%	0.05%	0.15%	0.18%	0.27%	0.40%	0.38%	0.38%
Kafresheikh	NR	NR	NR	NR	NR	NR	NR	3.74%	2.11%	3.84%	3.76%	3.75%	3.60%	3.55%	3.54%
Suhaj	NR	NR	NR	NR	NR	NR	NR	6.08%	5.75%	5.25%	5.09%	5.27%	5.15%	5.24%	5.43%
Ismaeleya	NR	NR	NR	NR	NR	NR	NR	1.09%	1.17%	0.97%	1.13%	1.21%	1.31%	1.38%	1.38%
Al Wadi Al Jadid	NR	NR	NR	NR	NR	NR	NR	0.13%	0.10%	0.23%	0.24%	0.24%	0.26%	0.25%	0.25%
Matrouh	NR	NR	NR	NR	NR	NR	NR	0.40%	0.21%	0.31%	0.33%	0.36%	0.44%	0.45%	0.52%
North Sinai	NR	NR	NR	NR	NR	NR	NR	NR	NR	NR	0.36%	0.43%	0.47%	0.48%	0.48%
South Sinai	NR	NR	NR	NR	NR	NR	NR	NR	NR	NR	0.06%	0.09%	0.21%	0.11%	0.11%
Luxor	NR	NR	NR	NR	NR	NR	NR	NR	NR	NR	NR	0.61%	0.63%	1.32%	1.33%

Table 35 Egypt's governorates' Population Compared to Total Population, Part 2

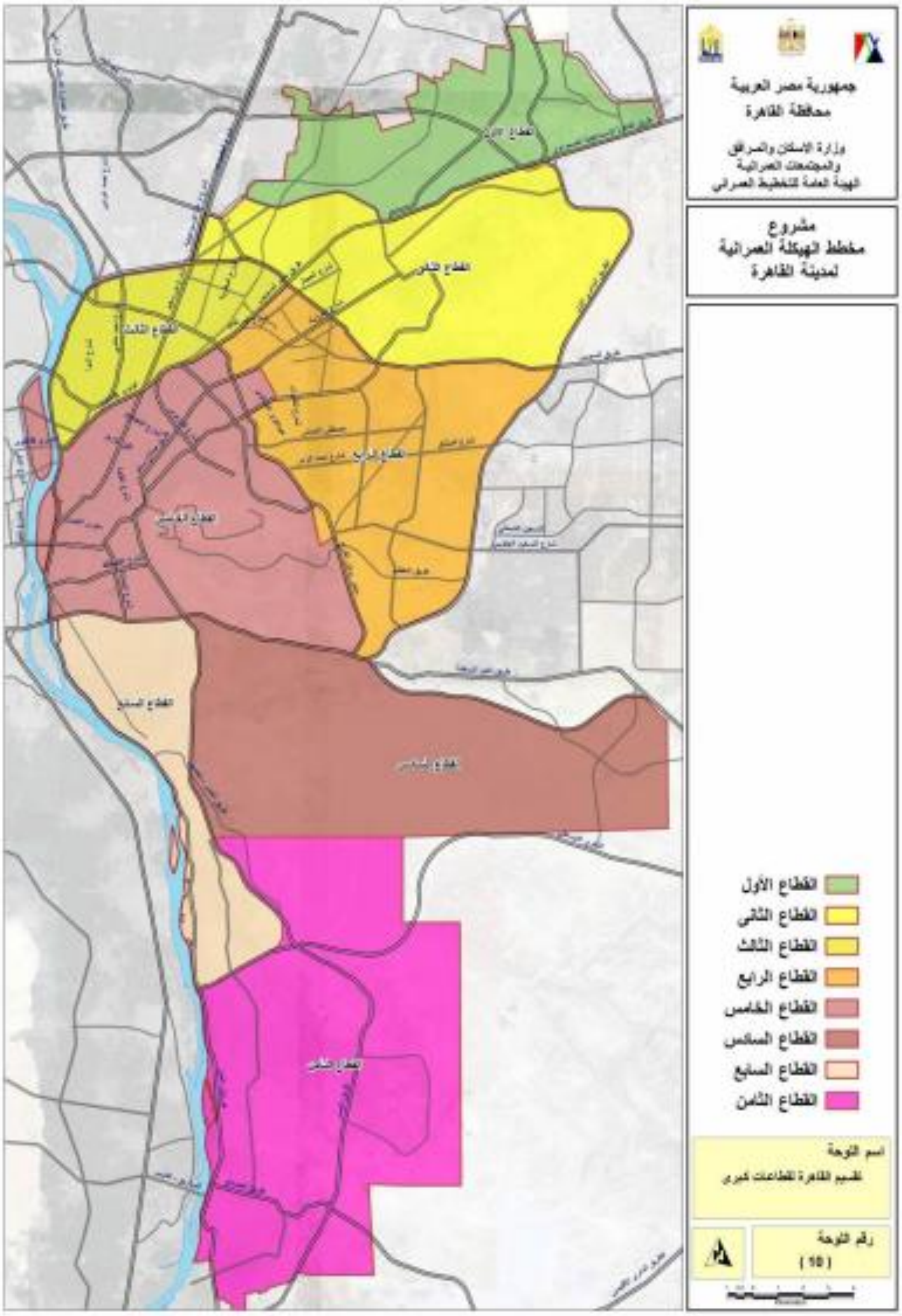

Figure 98 Cairo's Map Governmental 1

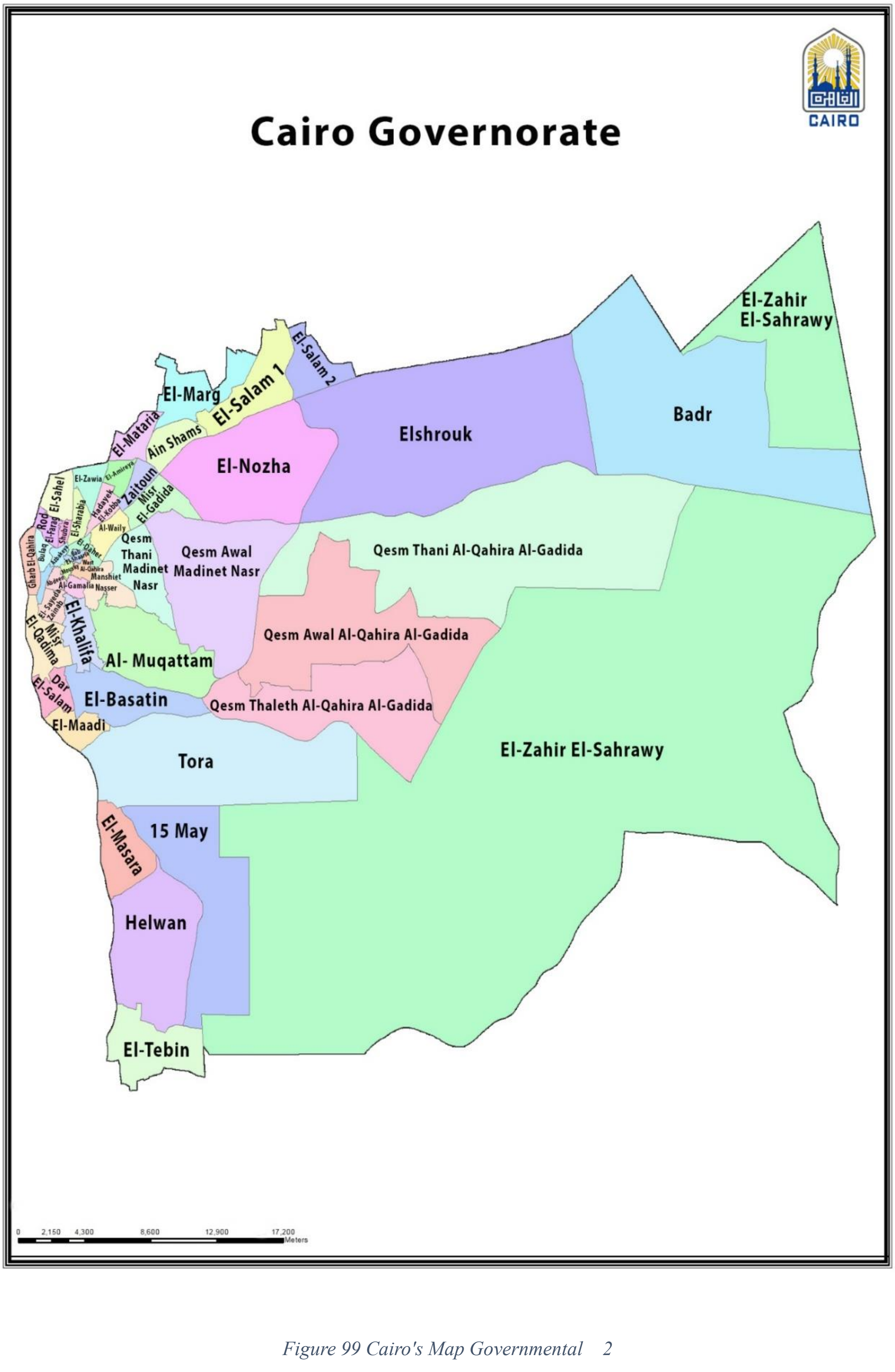

Figure 99 Cairo's Map Governmental 2

Investigated Element		Non-residential		Residential	
Opaque Elements		***Assembly Maximum***	***Insulation Min. R-Value***	***Assembly Maximum***	***Insulation Min. R-Value***
Roof	Insulation Entirely above Deck	U-0.273 (W/m²K)	R-3.5 (m²K/W)	U-0.273 (W/m²K)	R-3.5 (m²K/W)
	Metal Building	U-0.369 (W/m²K)	R-3.3 (m²K/W)	U-0.369 (W/m²K)	R-3.3 (m²K/W)
	Attic and Other	U-0.153 (W/m²K)	R-6.7 (m²K/W)	U-0.153 (W/m²K)	R-6.7 (m²K/W)
Walls (above Grade)	Mass	U-0.857	R-1.0 (m²K/W)	U-0.701 (W/m²K)	R-1.3 (m²K/W)
	Metal Building	U-0.642 (W/m²K)	R-2.3 (m²K/W)	U-0.642 (W/m²K)	R-2.3 (m²K/W)
	Steel-Framed	U-0.705 (W/m²K)	R-2.3 (m²K/W)	U-0.365 (W/m²K)	R-2.3 (m²K/W)
	Wood-Framed and Other	U-0.504 (W/m²K)	R-2.3 (m²K/W)	U-0.504 (W/m²K)	R-2.3 (m²K/W)
Walls (below Grade)	Below Grade Wall	C-6.473 (W/m²K)	NR	C-6.473 (W/m²K)	NR
Floors	Mass	U-0.606 (W/m²K)	R-1.1 (m²K/W)	U-0.496 (W/m²K)	R-1.5 (m²K/W)
	Steel-Joist	U-0.296 (W/m²K)	R-3.3 (m²K/W)	U-0.296 (W/m²K)	R-3.3 (m²K/W)
	Wood-Framed and Other	U-0.288 (W/m²K)	R-3.3 (m²K/W)	U-0.188 (W/m²K)	R-5.3 (m²K/W)
Slab-On-Grade Floors	Unheated	F-1.264 (W/mK)	NR	F-1.264 (W/mK)	NR
	Heated	F-1.766 (W/mK)	R-1.3 (m²K/W)	F-1.766 (W/mK)	R-1.3 (m²K/W)
Opaque Doors	Swinging	U-3.975 (W/m²K)	-	U-3.975 (W/m²K)	-
	Nonswinging	U-8.233 (W/m²K)	-	U-2.839 (W/m²K)	-
Fenestration		***Assembly Max. U***	***Assembly Max. SHGC***	***Assembly Max. U***	***Assembly Max. SHGC***
Vertical Glazing, 0%–40% of Wall	Nonmetal framing	U-4.26 (W/m²K)	SHGC-0.25	U-4.26 (W/m²K)	SHGC-0.25
	Metal framing (curtainwall/storefront)	U-3.97 (W/m²K)		U-3.97 (W/m²K)	
	Metal framing (entrance door)	U-6.25 (W/m²K)		U-6.25 (W/m²K)	
	Metal framing (all other)	U-4.26 (W/m²K)		U-4.26 (W/m²K)	
Skylight with Curb, Glass, % of Roof	0%–2.0%	U-11.24 (W/m²K)	SHGC-0.36	U-11.24 (W/m²K)	SHGC-0.19
	2.1%–5.0%	U-11.24 (W/m²K)	SHGC-0.19	U-11.24 (W/m²K)	SHGC-0.19
Skylight with Curb, Plastic, % of Roof	0%–2.0%	U-10.79 (W/m²K)	SHGC-0.39	U-10.79 (W/m²K)	SHGC-0.27
	2.1%–5.0%	U-10.79 (W/m²K)	SHGC-0.34	U-10.79 (W/m²K)	SHGC-0.27
Skylight without Curb, All, % of Roof	0%–2.0%	U-7.72 (W/m²K)	SHGC-0.36	U-7.72 (W/m²K)	SHGC-0.19
	2.1%–5.0%	U-7.72 (W/m²K)	SHGC-0.19	U-7.72 (W/m²K)	SHGC-0.19

C-factor = Thermal Conductance, F-factor = the perimeter heat loss factor for slab-on-grade floors, NR = Not Reported, SHGC = Solar Heat Gain Coefficient, R-factor = Thermal Resistance, U-factor = Thermal Transmittance

Table 36 ANSI/ASHRAE Standard 90.1-2007, building envelope requirements zone 2B

The Building Area Method	
Building Area Type	***Lighting Power Density (W/m²)***
Automotive Facility	10
Convention Centre	13
Courthouse	13
Dining: Bar Lounge/Leisure	14
Dining: Cafeteria/Fast Food	15
Dining: Family	17
Dormitory	11
Exercise Centre	11
Gymnasium	12
Health-Care Clinic	11
Hospital	13
Hotel	11
Library	14
Manufacturing Facility	14
Motel	11
Motion Picture Theatre	13
Multifamily	8
Museum	12
Office	11
Parking Garage	3
Penitentiary	11
Performing Arts Theatre	17
Police/Fire Station	11
Post Office	12
Religious Building	14
Retail	16
School/University	13
Sports Arena	12
Town Hall	12
Transportation	11
Warehouse	9
Workshop	15

Table 37 ANSI/ASHRAE Standard 90.1-2007, lighting power density using the building area classification

Occupancy Category	*People Outdoor Air Rate (L/s· person)*	*Area Outdoor Air Rate (L/s·m2)*	*Default Values for Occupant Density (#/100 m2)*
Educational Facilities (continued)			
University/college laboratories	5.00	0.90	25
Wood/metal shop	5.00	0.90	20
Food and Beverage Service			
Bars, cocktail lounges	3.80	0.90	100
Cafeteria/fast-food dining	3.80	0.90	100
Kitchen (cooking)	3.80	0.60	20
Restaurant dining rooms	3.80	0.90	70
Food and Beverage Service, General			
Break rooms	2.50	0.30	25
Coffee stations	2.50	0.30	20
Conference/meeting	2.50	0.30	50
Corridors	—	0.30	—
Occupiable storage rooms for liquids or gels	2.50	0.60	2
Hotels, Motels, Resorts, Dormitories			
Barracks sleeping areas	2.50	0.30	20
Bedroom/living room	2.50	0.30	10
Laundry rooms, central	2.50	0.60	10
Laundry rooms within dwelling units	2.50	0.60	10
Lobbies/prefunction	3.80	0.30	30
Multipurpose assembly	2.50	0.30	120
Miscellaneous Spaces			
Banks or bank lobbies	3.80	0.30	15
Bank vaults/safe deposit	2.50	0.30	5
Computer (not printing)	2.50	0.30	4
Freezer and refrigerated spaces (<50°F [10°C])	5.00	0.00	0
Manufacturing where hazardous materials are not used	5.00	0.90	7
Manufacturing where hazardous materials are used (excludes heavy industrial and chemical processes)	5.00	0.90	7
Pharmacy (prep. area)	2.50	0.90	10
Photo studios	2.50	0.60	10
Shipping/receiving	5.00	0.60	2
Transient Residential			
Common Corridors	-	0.30	-
Dwelling Units	2.50	0.30	-

Table 38 ANSI/ASHRAE Standard 62.1-2019, minimum ventilation rates in breathing zones

Activity	***MetUnits***	***Metabolic Rate (W/m²)***
	Resting	
Sleeping	0.70	40
Reclining	0.80	45
Seated, quiet	1.00	60
Standing, relaxed	1.20	70
	Walking (on level surface)	
0.9 m/s, 3.2 km/h	2.00	115
1.2 m/s, 4.3 km/h	2.60	150
1.8 m/s, 6.8 km/h	3.80	220
	Office Activities	
Reading, seated	1.00	55
Writing	1.00	60
Typing	1.10	65
Filing, seated	1.20	70
Filing, standing	1.40	80
Walking about	1.70	100
Lifting/packing	2.10	120
	Driving/Flying	
Automobile	1.00–2.00	60–115
Aircraft, routine	1.20	70
Aircraft, instrument landing	1.80	105
Aircraft, combat	2.40	140
Heavy vehicle	3.20	185
	Miscellaneous Occupational Activities	
Cooking	1.60–2.00	95–115
Housecleaning	2.00–3.40	115–200
Seated, heavy limb movement	2.20	130
	Machine work	
Sawing (table saw)	1.80	105
Light (electrical industry)	2.00–2.40	115–140
heavy	4.00	235
Handling50kg(100lb) bags	4.00	235
Pick and shovel work	4.00–4.80	235–280
	Miscellaneous Leisure Activities	
Dancing, social	2.40–4.40	140–255
Calisthenics/exercise	3.00–4.00	175–235
Tennis, single	3.60–4.00	210–270
Basketball	5.00–7.60	290–440
Wrestling, competitive	7.00–8.70	410–505

Table 39 ANSI/ASHRAE Standard 55-2010 , metabolic rates for typical tasks

Facility	Area (m²)	Occupant Density (-)	Total Occupants	People Outdoor Air Rate/Person (L/(s*person))	Total People Outdoor Air Rate (L/s) due Occupants	Area Outdoor Air Rate/Area (L/(s*m²))	Total Area Outdoor Air Rate (L/s) due Area	Total Area Outdoor Rate (L/s)
Café1	93.00	0.70	65	3.80	247.38	0.90	83.70	331.08
Cafe2	102.00	0.70	71	3.80	271.32	0.90	91.80	363.12
Cafe3	99.00	0.70	69	3.80	263.34	0.90	89.10	352.44
Café4	73.00	0.70	51	3.80	194.18	0.90	65.70	259.88
Cafe5	140.00	0.70	98	3.80	372.40	0.90	126.00	498.40
Cafe6	142.00	0.70	99	3.80	377.72	0.90	127.80	505.52
Cafe7	73.00	0.70	51	3.80	194.18	0.90	65.70	259.88
Cafe8	99.00	0.70	69	3.80	263.34	0.90	89.10	352.44
Cafe9	101.00	0.70	71	3.80	268.66	0.90	90.90	359.56
Corridor1	25.00	-	-	-	-	0.30	7.50	7.50
Corridor2	25.00	-	-	-	-	0.30	7.50	7.50
Stairs1	30.00	-	-	-	-	0.30	6.30	6.30
Stairs18	30.00	-	-	-	-	0.30	6.30	6.30
Stairs19	30.00	-	-	-	-	0.30	6.30	6.30
WC1	54.00	-	-	-	-	0.30	16.20	16.20
WC2	76.00	-	-	-	-	0.30	22.80	22.80
WC3	5.00	-	-	-	-	0.30	1.50	1.50
WC4	24.00	-	-	-	-	0.30	7.20	7.20
Lobby1	259.00	0.10	26	2.50	64.75	0.30	77.70	142.45
Lobby2	114.00	0.10	11	2.50	28.50	0.30	34.20	62.70
Meeting Room1	13.00	0.25	3	2.50	8.13	0.30	3.90	12.03
Meeting Room2	11.00	0.25	3	2.50	6.88	0.30	3.30	10.18
Meeting Room3	20.00	0.25	5	2.50	12.50	0.30	6.00	18.50

Table 40 Calculated total outdoor air flow rate, Ground floor

Facility	Area (m^2)	Occupant Density (-)	Total Occupants	People Outdoor Air Rate/Person (L/(s*person))	Total People Outdoor Air Rate (L/s) due Occupants	Area Outdoor Air Rate/Area (L/(s*m²))	Total Area Outdoor Air Rate (L/s) due Area	Total Area Outdoor Rate (L/s)
Common Area1	95.30	0.50	48	2.50	119.13	0.60	57.18	176.31
Meeting R.4	35.50	0.25	9	2.50	22.19	0.30	10.65	32.84
Meeting R.5	14.00	0.25	4	2.50	8.75	0.30	4.20	12.95
Meeting R.6	14.00	0.25	4	2.50	8.75	0.30	4.20	12.95
Corridor 3	268.00	-	-	-	-	0.30	80.40	80.40
Eating Area 1	52.00	0.70	36	3.80	138.32	0.60	31.20	169.52
Kitchenette 1	25.00	0.20	5	3.80	19.00	0.60	15.00	34.00
Office 1	84.00	0.05	4	2.50	10.50	0.30	25.20	35.70
Office 2	83.00	0.05	4	2.50	10.38	0.30	24.90	35.28
Office 3	83.00	0.05	4	2.50	10.38	0.30	24.90	35.28
Office 4	83.00	0.05	4	2.50	10.38	0.30	24.90	35.28
Office 5	81.00	0.05	4	2.50	10.13	0.30	24.30	34.43
Office 6	82.00	0.05	4	2.50	10.25	0.30	24.60	34.85
Office 7	82.00	0.05	4	2.50	10.25	0.30	24.60	34.85
Office 8	195.00	0.05	10	2.50	24.38	0.30	58.50	82.88
Stairs 2	30.00	-	-	-	-	0.30	9.00	9.00
Stairs 3	30.00	-	-	-	-	0.30	9.00	9.00
Stairs 13	30.00	-	-	-	-	0.30	9.00	9.00
WC 5	74.00	-	-	-	-	0.30	22.20	22.20
WC 6	74.00	-	-	-	-	0.30	22.20	22.20
Reception1	55.00	0.30	17	2.50	41.25	0.30	16.50	57.75

Table 41 Calculated total outdoor air flow rate, first floor

Facility	*Area (m^2)*	*Occupant Density (-)*	*Total Occupants*	*People Outdoor Air Rate/Person (L/(s*person))*	*Total People Outdoor Air Rate (L/s) due Occupants*	*Area Outdoor Air Rate/Area (L/(s*m^2))*	*Total Area Outdoor Air Rate (L/s) due Area*	*Total Area Outdoor Rate (L/s)*
Common Area2	95.30	0.50	48	2.50	119.13	0.60	57.18	176.31
Meeting R.7	35.50	0.25	9	2.50	22.19	0.30	10.65	32.84
Meeting R.8	14.00	0.25	4	2.50	8.75	0.30	4.20	12.95
Meeting R.9	14.00	0.25	4	2.50	8.75	0.30	4.20	12.95
Corridor 4	268.00	-	-	-	-	0.30	80.40	80.40
Eating Area 2	52.00	0.70	36	3.80	138.32	0.60	31.20	169.52
Kitchenette 2	25.00	0.20	5	3.80	19.00	0.60	15.00	34.00
Office 9	84.00	0.05	4	2.50	10.50	0.30	25.20	35.70
Office 10	83.00	0.05	4	2.50	10.38	0.30	24.90	35.28
Office 11	83.00	0.05	4	2.50	10.38	0.30	24.90	35.28
Office 12	83.00	0.05	4	2.50	10.38	0.30	24.90	35.28
Office 13	81.00	0.05	4	2.50	10.13	0.30	24.30	34.43
Office 14	82.00	0.05	4	2.50	10.25	0.30	24.60	34.85
Office 15	82.00	0.05	4	2.50	10.25	0.30	24.60	34.85
Office 16	195.00	0.05	10	2.50	24.38	0.30	58.50	82.88
Stairs 4	30.00	-	-	-	-	0.30	9.00	9.00
Stairs 5	30.00	-	-	-	-	0.30	9.00	9.00
Stairs 14	30.00	-	-	-	-	0.30	9.00	9.00
WC 7	74.00	-	-	-	-	0.30	22.20	22.20
WC 8	74.00	-	-	-	-	0.30	22.20	22.20
Reception2	55.00	0.30	17	2.50	41.25	0.30	16.50	57.75

Table 42 Calculated total outdoor air flow rate, second floor

Facility	Area (m^2)	Occupant Density (-)	Total Occupants	People Outdoor Air Rate/Person (L/(s*person))	Total People Outdoor Air Rate (L/s) due Occupants	Area Outdoor Air Rate/Area (L/(s*m²))	Total Area Outdoor Air Rate (L/s) due Area	Total Area Outdoor Rate (L/s)
Common Area3	95.30	0.50	48	2.50	119.13	0.60	57.18	176.31
Meeting R.10	35.50	0.25	9	2.50	22.19	0.30	10.65	32.84
Meeting R.11	14.00	0.25	4	2.50	8.75	0.30	4.20	12.95
Meeting R.12	14.00	0.25	4	2.50	8.75	0.30	4.20	12.95
Corridor 5	268.00	-	-	-	-	0.30	80.40	80.40
Eating Area 3	52.00	0.70	36	3.80	138.32	0.60	31.20	169.52
Kitchenette 3	25.00	0.20	5	3.80	19.00	0.60	15.00	34.00
Office 17	84.00	0.05	4	2.50	10.50	0.30	25.20	35.70
Office 18	83.00	0.05	4	2.50	10.38	0.30	24.90	35.28
Office 19	83.00	0.05	4	2.50	10.38	0.30	24.90	35.28
Office 20	83.00	0.05	4	2.50	10.38	0.30	24.90	35.28
Office 21	81.00	0.05	4	2.50	10.13	0.30	24.30	34.43
Office 22	82.00	0.05	4	2.50	10.25	0.30	24.60	34.85
Office 23	82.00	0.05	4	2.50	10.25	0.30	24.60	34.85
Office 24	195.00	0.05	10	2.50	24.38	0.30	58.50	82.88
Stairs 6	30.00	-	-	-	-	0.30	9.00	9.00
Stairs 7	30.00	-	-	-	-	0.30	9.00	9.00
Stairs 15	30.00	-	-	-	-	0.30	9.00	9.00
WC 9	74.00	-	-	-	-	0.30	22.20	22.20
WC 10	74.00	-	-	-	-	0.30	22.20	22.20
Reception3	55.00	0.30	17	2.50	41.25	0.30	16.50	57.75

Table 43 Calculated total outdoor air flow rate, third floor

Facility	Area (m²)	Occupant Density (-)	Total Occupants	People Outdoor Air Rate/Person (L/(s*person))	Total People Outdoor Air Rate (L/s) due Occupants	Area Outdoor Air Rate/Area (L/(s*m²))	Total Area Outdoor Air Rate (L/s) due Area	Total Area Outdoor Rate (L/s)
Common Area4	95.30	0.50	48	2.50	119.13	0.60	57.18	176.31
Meeting R.13	35.50	0.25	9	2.50	22.19	0.30	10.65	32.84
Meeting R.14	14.00	0.25	4	2.50	8.75	0.30	4.20	12.95
Meeting R.15	14.00	0.25	4	2.50	8.75	0.30	4.20	12.95
Corridor 6	286.00	-	-	-	-	0.30	85.80	85.80
Eating Area 4	52.00	0.70	36	3.80	138.32	0.60	31.20	169.52
Kitchenette 4	25.00	0.20	5	3.80	19.00	0.60	15.00	34.00
Office 25	42.00	0.05	2	2.50	5.25	0.30	12.60	17.85
Office 26	41.00	0.05	2	2.50	5.13	0.30	12.30	17.43
Office 27	41.00	0.05	2	2.50	5.13	0.30	12.30	17.43
Office 28	41.00	0.05	2	2.50	5.13	0.30	12.30	17.43
Office 29	41.00	0.05	2	2.50	5.13	0.30	12.30	17.43
Office 30	41.00	0.05	2	2.50	5.13	0.30	12.30	17.43
Office 31	83.00	0.05	4	2.50	10.38	0.30	24.90	35.28
Office 32	81.00	0.05	4	2.50	10.13	0.30	24.30	34.43
Office 33	41.00	0.05	2	2.50	5.13	0.30	12.30	17.43
Office 34	41.00	0.05	2	2.50	5.13	0.30	12.30	17.43
Office 35	41.00	0.05	2	2.50	5.13	0.30	12.30	17.43
Office 36	41.00	0.05	2	2.50	5.13	0.30	12.30	17.43
Office 37	41.00	0.05	2	2.50	5.13	0.30	12.30	17.43
Office 38	41.00	0.05	2	2.50	5.13	0.30	12.30	17.43
Office 39	92.00	0.05	5	2.50	11.50	0.30	27.60	39.10
Stairs 8	30.00	-	-	-	-	0.30	9.00	9.00
Stairs 9	30.00	-	-	-	-	0.30	9.00	9.00
Stairs 16	30.00	-	-	-	-	0.30	9.00	9.00
WC 11	74.00	-	-	-	-	0.30	22.20	22.20
WC 12	74.00	-	-	-	-	0.30	22.20	22.20
Reception4	55.00	0.30	17	2.50	41.25	0.30	16.50	57.75

Table 44 Calculated total outdoor air flow rate, fourth floor

Facility	Area (m²)	Occupant Density (-)	Total Occupants	People Outdoor Air Rate/Person (L/(s*person))	Total People Outdoor Air Rate (L/s) due Occupants	Area Outdoor Air Rate/Area (L/(s*m²))	Total Area Outdoor Air Rate (L/s) due Area	Total Area Outdoor Rate (L/s)
Common Area5	95.30	0.50	48	2.50	119.13	0.60	57.18	176.31
Meeting R.16	35.50	0.25	9	2.50	22.19	0.30	10.65	32.84
Meeting R.17	14.00	0.25	4	2.50	8.75	0.30	4.20	12.95
Meeting R.18	14.00	0.25	4	2.50	8.75	0.30	4.20	12.95
Corridor 7	286.00	-	-	-	-	0.30	85.80	85.80
Eating Area 5	52.00	0.70	36	3.80	138.32	0.60	31.20	169.52
Kitchenette 5	25.00	0.20	5	3.80	19.00	0.60	15.00	34.00
Office 40	42.00	0.05	2	2.50	5.25	0.30	12.60	17.85
Office 41	41.00	0.05	2	2.50	5.13	0.30	12.30	17.43
Office 42	41.00	0.05	2	2.50	5.13	0.30	12.30	17.43
Office 43	41.00	0.05	2	2.50	5.13	0.30	12.30	17.43
Office 44	41.00	0.05	2	2.50	5.13	0.30	12.30	17.43
Office 45	41.00	0.05	2	2.50	5.13	0.30	12.30	17.43
Office 46	83.00	0.05	4	2.50	10.38	0.30	24.90	35.28
Office 47	81.00	0.05	4	2.50	10.13	0.30	24.30	34.43
Office 48	41.00	0.05	2	2.50	5.13	0.30	12.30	17.43
Office 49	41.00	0.05	2	2.50	5.13	0.30	12.30	17.43
Office 50	41.00	0.05	2	2.50	5.13	0.30	12.30	17.43
Office 51	41.00	0.05	2	2.50	5.13	0.30	12.30	17.43
Office 52	41.00	0.05	2	2.50	5.13	0.30	12.30	17.43
Office 53	41.00	0.05	2	2.50	5.13	0.30	12.30	17.43
Office 54	92.00	0.05	5	2.50	11.50	0.30	27.60	39.10
Stairs 10	30.00	-	-	-	-	0.30	9.00	9.00
Stairs 11	30.00	-	-	-	-	0.30	9.00	9.00
Stairs 17	30.00	-	-	-	-	0.30	9.00	9.00
WC 13	74.00	-	-	-	-	0.30	22.20	22.20
WC 14	74.00	-	-	-	-	0.30	22.20	22.20
Reception5	55.00	0.30	17	2.50	41.25	0.30	16.50	57.75

Table 45 Calculated total outdoor air flow rate, fifth floor